γ.

CR-98243

FINAL REPORT

SOUND WAVE SHEAR WAVE INTERACTION
WITH OBLIQUE SHOCK FRONTS

Report Covering Period September 1, 1967 to August 31, 1968

PRF No. 5115

Contract No. NGR 15-005-056

Report Submitted

by

Kenneth R. Purdy
Principal Investigator
Associate Professor
Mechanical Engineering

Purdue University
Lafayette, Indiana

160

FOREWARD

This final report was prepared by the staff of Purdue University, Lafayette, Indiana on Contract NGR 15-005-056 for National Aeronautics and Space Administration. The report presents the results of three studies 1) Analytical investigation of sound wave-shock front interaction by Lynn E Snyder and K. R. Purdy; 2) Analytical investigation of shear wave-shock front interaction by K. R. Purdy; and 3) Experimental investigation of sound wave-shock front interaction by David W. McKinley and K. R. Purdy. The research was administered under the technical cognizance of Mr. Gilbert A. Wilhold, Aero-Astrodynamics Laboartory, George C. Marshall Space Flight Center. Mr. Wilhold's interest in this work is deeply appreciated.

TABLE OF CONTENTS

ABSTRACT

This report treats the flow field downstream of an oblique shock front that is perturbed by either plane sound waves or plane shear waves.

The sound wave analysis predicts that under certain conditions there exists an angle of incidence which produces shock wave resonance. This results in a large amplification of the sound pressure and in large amplitude motion of the shock front itself.

Experimental studies of sound wave-shock front interaction showed that the shock front is definitely excited by an impressed acoustic field. The shock front motion is periodic and at the same frequency as the impressed sound field. Natural pressure fluctuations in the upstream flow also excited the shock front and amplifications at the shock front of 22 to 30 dB were found for frequencies from 20 to 2000 Hz.

The shear wave analysis contains some anomalies that have not been reconciled. Therefore it requires critical review and, if necessary, revision before being used.

NOMENCLATURE

Sound Wave-Shock Front Interaction

Symbol	
A_i	as defined in text
a_i	isentropic speed of sound in Region i
B_i	as defined in text
C_i	as defined in text
c_p	constant pressure specific heat
c_v	constant volume specific heat
D_i	as defined in text
E_1	amplitude of shock front displacement
F_1	as defined in equation (41)
G_1	as defined in equation (42)
H_1	as defined in equation (43)
h	specific enthalpy of gas
L	as defined in text
M_o	acoustic Mach number, $U_o/\overline{a}$
M_i	Mach number in Region i, W_i/a_i
p	pressure of gas
R	gas constant
r	U_1/U_2
s	specific entropy of gas
T	absolute temperature of gas
t	time
U_i	unperturbed velocity component in i-direction, or velocity component normal to shock front in Region i

$\overline{U}_i$	normal Mach number in Region i, U_i/a_i
U_{oi}	amplitude of sound particle velocity in Region i
u_i	velocity component in i-direction
u_{ij}	velocity component in i-direction in Region j
V_i	velocity component tangent to shock front in Region i
W_i	unperturbed velocity component in Region i
x	Cartesian coordinate normal to shock front
x_i	Cartesian coordinates
y	Cartesian coordinate tangent to shock front
z_i	as defined in text

Greek Symbols

α	shock front displacement
α_y	$\frac{\partial\alpha}{\partial y}$
α_t	$\frac{\partial\alpha}{\partial t}$
β	entropy-vorticity wave angle
γ	ratio of specific heats, c_p/c_v
δ	number much smaller than one
η_i	Cartesian coordinate in Region i
θ	sound wave incidence angle
λ	wavelength
ξ_i	Cartesian coordinate in Region i
ρ	density of gas
σ	shock wave angle
ϕ	streamline direction (flow angle) in Region 2
ϕ'	refracted-sound wave angle
ω	circular frequency

Script Symbol

$\mathcal{O}$	order of magnitude of

Subscripts

evw	entropy-vorticity wave
p	perturbed
sw	shock wave

Superscripts

'	perturbed component
—	unperturbed component
~	dimensionless form

Shear Wave-Shock Front Interaction

Symbol

A	function defined in equations (124), (150)
a	isentropic speed of sound
a_A	isentropic speed of sound in region A
$\tilde{a}$	function defined in equations (120), (148)
B	function defined in equation (125)
$\tilde{b}$	function defined in equation (121)
C	function defined in equation (114)
C'	function defined in equation (142)
$\tilde{c}$	function defined in equations (122), (149)
D	function defined in equation (115)
D'	function defined in equations (116), (143)
$\tilde{d}$	function defined in equation (123)

E	function defined in equation (117)
E'	function defined in equation (144)
F	function defined in equation (118)
F'	function defined in equations (119), (145)
f	frequency
G'	function defined in equation (146)
k	wave number of shear wave in region A
k_{sur}	surface wave number of pressure wave
$\tilde{M}_A$	stream Mach number ($\tilde{W}_A/a_A$)
m	velocity ratio across normal shock (U_A/U)
N_s	nodal point on shock front (Figure 10)
P	period
p	pressure of gas
p_{ref}	reference pressure (0.290×10^{-8} psi.)
S*	coefficient defined in equation (129)
S**	coefficient defined in equation (152)
SPL	sound pressure level
T	absolute temperature of gas
T_A	absolute temperature of gas in region A
t	time
U	stream velocity component in x-direction (Figure 13)
$\bar{U}$	Mach number associated with U (U/a)
U_A	stream velocity component in x-direction (Figure 13)
$\bar{U}_A$	Mach number associated with U_A (U_A/a_A)
V	stream velocity component in y-direction (Figure 13)
V_{N_s}	nodal point speed

$V_{p_{sur}}$	surface pressure wave speed
W	stream velocity in ξ-direction (Figure 13)
$\overline{W}$	Mach number associated with W (W/a)
W_A	stream velocity in ξ_A-direction (Figure 13)
$\tilde{W}_A$	stream velocity before oblique shock (Figure 10)
w	perturbation velocity component in ξ-direction
$\tilde{w}$	perturbation velocity component in $\tilde{\xi}$-direction
w'	perturbation velocity component in η-direction
$\tilde{w}'$	perturbation velocity component in $\tilde{\eta}$-direction
w_A	perturbation velocity (Figure 10)
$\tilde{w}_A$	perturbation velocity as defined in text
w_p	pressure wave velocity component in ξ-direction
w_p'	pressure wave velocity component in η-direction
w_s	refracted shear wave velocity component in ξ-direction
w_s'	refracted shear wave velocity component in η-direction
x	rectangular coordinate (Figure 13)
$\tilde{x}$	rectangular coordinate (Figure 14)
y	rectangular coordinate (Figure 13)
$\tilde{y}$	rectangular coordinate (Figure 14)

Greek Symbols

β	function defined in equation (109)
β_w	function defined in equations (112), (141)
γ	specific heat ratio
δ	turning angle across shock
δ_p	shear wave phase angle
δ_s	shear wave phase angle

δ_{shock}	shock deflection phase angle
δp	perturbation pressure
δx	local shock deflection
ε	measure of strength of incident shear wave (equation (79))
η, $\tilde{\eta}$, η_A	rectangular coordinate (Figures 13, 14)
θ	shear wave incidence angle (Figure 10)
$\tilde{\theta}$	shear wave incidence angle (Figure 14)
θ_{cr}	critical value of θ (equation (80))
λ	wavelength of incident shear waves
λ_{sur}	wavelength of pressure waves
μ	Mach angle ($\tan^{-1}$ $(1/\beta_w)$)
ξ, $\tilde{\xi}$, ξ_A	rectangular coordinate (Figures 13, 14)
Π	as defined in text
Π^*	coefficient defined in equation (130)
Π^{**}	coefficient defined in equation (153)
σ	angle of shock to incoming flow (Figure 10)
ϕ	refracted shear wave angle (Figure 14)
$\tilde{\phi}$	refracted shear wave angle (Figure 14)
ϕ'	pressure wave angle (Figure 14)
$\tilde{\phi}'$	pressure wave angle (Figure 14)

Subscripts

A	region A (upstream of shock)
o	evaluated at shock ($\tilde{x} = 0$)
rms	root-mean-square

CHAPTER I

INTRODUCTION

Statement of Intent

The intent of this investigation is to conduct an analytical and an experimental investigation of the flow field produced by the interaction of sound waves and shear waves with an oblique shock front.

The analytical phase of this work deals with an extension of the normal shock analyses to the oblique shock case; the experimental phase entails a pilot study of the pressure field associated with the sound wave shock front interaction phenomenon.

Historical Background

Although there have been analytical studies of sound wave and shear wave interactions with normal shocks, there has been no investigation of their interactions with stationary oblique shock fronts. Consequently this discussion will be devoted to the previous research efforts involving normal shocks that are most germane to the proposed research. The classic work in this area has been done by H. S. Ribner, F. K. Moore and W. R. Johnson.

Ribner's initial study [1]* was concerned with the

*Numbers in brackets refer to similarly numbered references in the Literature Cited.

convection of a pattern of vorticity through a normal shock. It treated the simple case of a plane sinusoidal shear wave of any orientation and wavelength. The interaction of such a wave with a normal shock front produced: (i) a refracted shear wave of altered wavelength and amplitude (the intensity of the shear wave is increased), (ii) an entropy wave which moves with the flow downstream of the shock, (iii) either a "pressure" wave or a sound wave depending on the orientation of the initial shear wave (the pressure wave is quite intense just behind the shock, but it is exponentially damped with distance downstream from the shock front), and (iv) a distorted shock front. A relatively weak initial shear wave was found to produce a surprisingly intense pressure wave or sound field downstream of the shock.

Later studies by Ribner [2] and Ram and Ribner [3] extended the plane shear wave case to those of the passage of (i) both isotropic and strongly axisymmetrical initial turbulence and (ii) a columnar vortex through a normal shock front.

Moore [4], in his investigations, considered the unsteady oblique interaction of a normal shock wave with a plane disturbance. His analyses treated a normal shock wave traveling into a perfect gas which is at "rest". Solutions were given for three cases of interaction: (i) plane sound waves propagating in the "rest gas" into which the shock moves, (ii) plane sound waves overtaking the shock front from behind, and (iii) stationary incompressible vorticity waves in the gas ahead of the shock. In the first case the sound waves were refracted either as simple isentropic sound waves or as attenuating isentropic pressure waves depending on the orientation of the initial sound waves. A stationary vorticity wave was also produced behind the shock. In the second case the sound waves were reflected as sound waves and a stationary vorticity wave was produced. The third case was the same as Ribner's initial study [1]. However, Moore treated it as a completely unsteady problem whereas Ribner transformed it into a steady flow problem.

Johnson [5], in his Ph.D. dissertation, considered the interaction of plane and cylindrical sound waves with a stationary normal shock. His plane wave case was the same as the first two cases of Moore's study except that the shock front was stationary in Johnson's analysis and it was moving in the analyses of Moore. Johnson's analysis, however, strengthened the mathematical foundation for the plane wave case in that it was not necessary to appeal to physical reasoning for the form of certain functions.

Purdy [6] considered the convection of a plane sound wave of arbitrary orientation and wavelength through a stationary oblique shock front. While this appears to be a simple extension of the studies by Moore and Johnson, it was found that the shock front oscillations appear to be unstable for certain combinations of initial Mach number, shock front angle and sound wave incidence angle. This investigation formed the basis for the research program reported herein.

The most recent work appearing in the literature is that of Lowson [7]. It contains computations based on the methods of Ribner [2] and Moore [4] for shear wave and sound wave interactions with normal shock fronts. The computations are compared with experimental data.

Significance and Scope

The study of plane shear wave and plane sound wave interaction with oblique shock fronts is an abstraction of at least two very significant physical phenomena, namely, the pressure field associated with the oscillating oblique shock front produced by an axisymmetric step, and the pressure field associated with a supersonic fluid jet.

The first phenomenon is currently a problem area for large launch vehicles since sizeable pressure fluctuations have been found to exist at interstage flares. It is quite possible that these fluctuations are due to the interaction of turbulent wakes, from the launch escape tower and vehicle protuberences, with the oblique shocks at the flares. It is also possible that in wind tunnel tests the tunnel sound field interaction with these shocks also contributes to the measured pressure fluctuations. When oblique shocks occur in series as they do for many current configurations the problem is compounded. If, for example, shear waves interact with the first shock then the intensified shear waves and the concomitant sound waves and/or pressure waves will all/both interact with the next shock. It is clear that each interaction could yield a fluctuating pressure field which would be stronger than the previous one. For the case of a flare the reattachment shock should oscillate with a larger amplitude and produce more intense pressure waves and/or sound waves than the separation shock.

The second phenomenon is characterized by multiple shocks and therefore the reasoning given above should be applicable here as well.

Although the models that are to be analyzed are much simplier than the actual phenomena, they should portray the characteristic behavior of such processes and they should also predict typical orders of magnitude for the pressure fluctuations.

The research reported herein is specifically concerned with the following problems:

1. The analytical prediction of the flow field downstream of a stationary oblique shock front when plane sound waves are present in the flow. The sound waves are to be of arbitrary orientation and wavelength and they have their origin upstream of the shock front.
2. The analytical prediction of the flow field downstream of a stationary oblique shock front for the convection of a plane sinusoidal shear wave of arbitrary orientation and wavelength through the shock.

3. The experimental investigation of the sound pressure field upstream and downstream of a stationary oblique shock front when sound waves interact with the shock.

In the two analytical studies the medium will be assumed to be an inviscid perfect gas. The experimental study will utilize atmospheric air as the working fluid. The specific objectives of this research are:

1. To obtain mathematical expressions for the velocity field, the pressure field, the density field, the shock front displacement, and the shock front velocity as functions of the upstream Mach number, the shock front angle, and the angle of incidence and wavelength of (i) plane sound waves and (ii) plane sinusoidal shear waves interacting with a stationary oblique shock front.
2. To obtain experimental data for the acoustic pressure field associated with the interaction of sound waves and a stationary oblique shock front, and
3. To compare the experimental data for sound pressure amplification across the shock front with the values predicted by the mathematical model for sound wave shock front interaction..

CHAPTER II

ANALYTICAL INVESTIGATIONS*

A. Sound Wave Shock Front Interaction

The perturbed flow field downstream of a stationary oblique shock front produced by the convection-propagation of plane sound waves through the shock front is to be determined. This analysis represents an extension of the earlier analyses of Ribner [1] and Moore [4]; its main objective is to provide a simple means for computing the change in the acoustic properties across a specific oblique shock front.

Mathematical Formulation of the Problem

To formulate a mathematically tractable problem, it is assumed that the acoustic pressure is sufficiently small for the pressure waves to travel at the isentropic speed in the undisturbed uniform flow. This wave speed is relative to an observer moving with the flow.

Unsteady-Flow Problem. The flow field shown in Figure 1 is unsteady as viewed by an observer on the shock front since, in general, the nodal lines will either move up or down the shock front. The nodal speed along the shock is given by

*The analysis presented for this case is a revised extended version of that contained in reference [6].

(see Figure 2)

$$V_{swy_1} = [M_1 \cos \sigma + \sin \theta] \, a_1 \; . \tag{1}$$

There seems to be no advantage to changing the point of view to one in which the nodal lines are stationary since the resulting problem would still be unsteady. Thus the governing equations will be obtained for the Cartesian coordinate system shown in Figure 1.

Governing Equations. The assumptions upon which the governing equations will be based are

Assumptions

1. Two-dimensional flow
2. Inviscid flow
3. Adiabatic flow
4. No body forces
5. Perfect gas
6. Small perturbation of a uniform flow; that is, for Cartesian coordinates x_i, with corresponding velocity components u_i, we have

   $u_1 = U_1 + u_1'$, $u_2 = u_2'$ (Figure 3);

   $p = \bar{p} + p'$, $\rho = \bar{\rho} + \rho'$, $T = \bar{T} + T'$, and

   $s = \bar{s} + s'$

   with

   u_1'/U_1, u_2'/U_1, $p'/\bar{p}$, $\rho'/\bar{\rho}$, $T'/\bar{T}$

   and $s'/\bar{s}$ much less than one.

The governing equations are

1. Continuity

$$\frac{1}{\rho}\frac{D\rho}{Dt} + \frac{\partial u_i}{\partial x_i} = 0$$

The continuity equation has a simpler form for the flow under consideration, since, for this flow,

$$u_1 = U_1 + u_1', \ u_2 = u_2', \ u_3 = 0 \text{ and } U_1 = \text{constant}.$$

Therefore, the continuity equation is

$$\frac{1}{\rho}\frac{D\rho}{Dt} + \frac{\partial u_1'}{\partial x_1} + \frac{\partial u_2'}{\partial x_2} = 0 \qquad (2)$$

2. Momentum

$$\frac{\partial u_i}{\partial t} + u_j \frac{\partial u_i}{\partial x_j} = -\frac{1}{\rho}\frac{\partial p}{\partial x_i} \quad ,$$

or if the momentum equations are written in terms of the perturbation quantities

$$[1 + \rho'/\bar{\rho}]\frac{\partial u_1'}{\partial t} + U_1 \frac{\partial u_1'}{\partial x_1} + u_1' \frac{\partial u_1'}{\partial x_1} + u_2' \frac{\partial u_1'}{\partial x_2} = -\frac{1}{\bar{\rho}}\frac{\partial p'}{\partial x_1}$$

$$[1 + \rho'/\bar{\rho}]\frac{\partial u_2'}{\partial t} + U_1 \frac{\partial u_2'}{\partial x_1} + u_1' \frac{\partial u_2'}{\partial x_1} + u_2' \frac{\partial u_2'}{\partial x_2} = -\frac{1}{\bar{\rho}}\frac{\partial p'}{\partial x_2}$$

Since the sound field characterizes the perturbations and it is assumed to be composed of simple sinusoidal waves, the foregoing equations will be nondimensionalized in terms of the wavelength λ and the circular frequency ω of these waves. The following dimensionless variables are chosen such that derivatives with respect to dimensionless position and time will be of the order of magnitude of one and the dimensionless velocity components, pressure and density will be of the order of magnitude of one:

$$x_1 = \tilde{x}_1 \frac{\lambda}{2\pi}$$

$$x_2 = \tilde{x}_2 \frac{\lambda}{2\pi}$$

$$t = \tilde{t}/\omega = \tilde{t} \frac{\lambda}{2\pi\bar{a}}$$

$$U_1 = \tilde{U}_1 U_1$$

$$u_1' = \tilde{u}_1' U_{01}$$

$$u_2' = \tilde{u}_2' U_{02}$$

$$\bar{\rho} = \tilde{\bar{\rho}} \bar{\rho}$$

$$\rho' = \tilde{\rho}' \bar{\rho} \frac{U_0}{\bar{a}}$$

$$\bar{p} = \tilde{\bar{p}} \bar{p}$$

$$p' = \tilde{p}' \gamma\bar{p} \frac{U_0}{\bar{a}}$$

where

$$U_0^2 = U_{01}^2 + U_{02}^2$$

$$\bar{a}^2 = \gamma\bar{p}/\bar{\rho}$$

The momentum equations in dimensionless form are

$$[1 + M_0\tilde{\rho}'/\tilde{\bar{\rho}}] \frac{U_{01}}{U_0} \frac{\partial \tilde{u}_i}{\partial \tilde{t}} + \frac{U_{01}}{U_0} \frac{U_1}{\bar{a}} \tilde{U}_1 \frac{\partial \tilde{u}_i}{\partial \tilde{x}_1} +$$

1* δ 1/1 1 1 1 1 1 1

$$\frac{U_{01}}{U_0} \frac{U_{01}}{\bar{a}} \tilde{u}' \frac{\partial \tilde{u}_i}{\partial \tilde{x}_1} + \frac{U_{01}}{U_0} \frac{U_{02}}{\bar{a}} \tilde{u}_2' \frac{\partial \tilde{u}_i}{\partial \tilde{x}_2} = -\frac{1}{\tilde{\bar{\rho}}} \frac{\partial p'}{\partial \tilde{x}_1}$$

1 δ 1 1 1 δ 1 1 1/1 1

*Represents the order of magnitude of the term or quantity in the equation directly above.

and

$$[1 + M_0 \tilde{\rho}' / \tilde{\bar{\rho}}] \frac{U_{02}}{U_0} \frac{\partial \tilde{u}_2'}{\partial \tilde{t}} + \frac{U_{02}}{U_0} \frac{U_1}{\bar{a}} \tilde{U}_1 \frac{\partial \tilde{u}_2'}{\partial \tilde{x}_1} +$$

1 δ 1/1 1 1 1 1 1 1

$$\frac{U_{01}}{U_0} \frac{U_{02}}{\bar{a}} \tilde{u}_1' \frac{\partial \tilde{u}_2'}{\partial \tilde{x}_1} + \frac{U_{02}}{U_0} \frac{U_{02}}{\bar{a}} \tilde{u}_2' \frac{\partial \tilde{u}_2'}{\partial \tilde{x}_2} = -\frac{1}{\tilde{\bar{\rho}}} \frac{\partial \tilde{p}'}{\partial \tilde{x}_2}$$

1 δ 1 1 1 δ 1 1 1/1 1

where

U_0 = amplitude of the sound particle velocity,

$U_{01} = U_0 \cos\theta$,

$U_{02} = U_0 \sin\theta$,

θ = angle between the sound wave propagation direction and the x_1 axis,

and where the following order of magnitudes are assumed:

$$\text{ORDER } (U_1/\bar{a}) = 1 \quad \text{and} \quad \text{ORDER } (U_0/\bar{a}) = \delta << 1.$$

These assumptions are consistent with supersonic flow and linear acoustics.

Retaining only those terms that are of the order of magnitude of one we have, in dimensional form,

$$\frac{\partial u_1'}{\partial t} + U_1 \frac{\partial u_1'}{\partial x_1} = -\frac{1}{\bar{\rho}} \frac{\partial p'}{\partial x_1} \tag{3a}$$

and

$$\frac{\partial u_2'}{\partial t} + U_1 \frac{\partial u_2'}{\partial x_1} = -\frac{1}{\bar{\rho}} \frac{\partial p'}{\partial x_2} \tag{3b}$$

3. Equation of State

For the assumed perfect gas we have

$$p = \rho RT$$

$$h = C_p T$$

$$Tds = dh - \frac{dp}{\rho}$$

$$a^2 = \gamma RT$$

The combination of these equations yields

$$\frac{d\rho}{\rho} = \frac{dp}{\rho a^2} - \frac{ds}{C_p}$$

Integration between the unperturbed state and the perturbed state gives the following approximate relation*

$$\frac{\rho'}{\bar{\rho}} = \frac{p'}{\bar{\rho}\bar{a}^2} - \frac{s'}{C_p} \tag{4}$$

4. Energy

It was assumed that there is no heat transfer between a fluid particle and its surroundings; thus changes of state are adiabatic. If the shock front is excluded from the flow field (the shock front will serve as a boundary condition for the flow field), the changes of state of a fluid particle are

---

*This assumes that $\int \frac{d\rho}{\rho} \approx \frac{1}{\bar{\rho}} \int d\rho$ and that $\int \frac{dp}{\rho a^2} \approx \frac{1}{\bar{\rho}\bar{a}^2} \int dp$.

also reversible. Thus

$$\frac{Ds}{Dt} = 0. \tag{5}$$

Reduction of the Governing Equations

The momentum equations have already been reduced to a linear form by an order of magnitude analysis. In order to further simplify the governing equations the density will now be eliminated from the continuity equation.

Since the density, pressure and entropy are Eulerian variables,

$$d\rho = \frac{\partial \rho}{\partial t}\, dt + \frac{\partial \rho}{\partial x_i}\, dx_i,$$

$$dp = \frac{\partial p}{\partial t}\, dt + \frac{\partial p}{\partial x_i}\, dx_i \text{ and}$$

$$ds = \frac{\partial s}{\partial t}\, dt + \frac{\partial s}{\partial x_i}\, dx_i.$$

Substituting the foregoing equations into the differential form of equation (4), dividing by dt and taking the limit as dt approaches zero results in the following expression for a fluid particle

$$\frac{1}{\bar{\rho}} \frac{D\rho}{Dt} = \frac{1}{\bar{\rho}\bar{a}^2} \frac{Dp}{Dt} - \frac{1}{C_p} \frac{Ds}{Dt} \quad .$$

However, from equation (5), $\frac{Ds}{Dt} = 0$, and therefore

$$\frac{1}{\bar{\rho}} \frac{D\rho}{Dt} = \frac{1}{\bar{\rho}\bar{a}^2} \frac{Dp}{Dt} \equiv \frac{1}{\bar{\rho}\bar{a}^2} \left[\frac{\partial p}{\partial t} + u_1 \frac{\partial p}{\partial x_1} + u_2 \frac{\partial p}{\partial x_2} \right] \, .$$

We have expressed the static pressure, p, as the sum of a time-mean component, $\bar{p}$, and a time-dependent component, p'. Since the unperturbed flow field is uniform, $\bar{p}$ is constant. Thus $p = \bar{p} + p'$ and consequently $\frac{\partial p}{\partial t} = \frac{\partial p'}{\partial t}$, $\frac{\partial p}{\partial x_1} = \frac{\partial p'}{\partial x_1}$ and $\frac{\partial p}{\partial x_2} = \frac{\partial p'}{\partial x_2}$. Introducing dimensionless variables, as previously defined, the substantial derivative of the density becomes

$$\frac{1}{\bar{\rho}} \frac{D\rho^{*}}{Dt} = \frac{2\pi\bar{a}}{\lambda} \frac{U_0}{\bar{a}} \left[\frac{1}{\tilde{\bar{\rho}}\,\tilde{\bar{a}}^2} \left[\frac{\partial \tilde{p}'}{\partial \tilde{t}} + \frac{U_1}{\bar{a}} \tilde{U}_1 \frac{\partial \tilde{p}'}{\partial \tilde{x}_1} + \right. \right.$$

1/1·1 1 1 1 1

$$\left. \left. \frac{U_{01}}{\bar{a}} \tilde{u}_1' \frac{\partial \tilde{p}'}{\partial \tilde{x}_1} + \frac{U_{02}}{\bar{a}} \tilde{u}_2' \frac{\partial \tilde{p}'}{\partial \tilde{x}_2} \right] \right]$$

δ 1 1 δ 1 1

If only those terms in the bracket that are of the order of magnitude of one are retained, then, in dimensional form, we have

$$\frac{1}{\bar{\rho}} \frac{D\rho}{Dt} = \frac{1}{\bar{\rho}\,\bar{a}^2} \left[\frac{\partial p'}{\partial t} + U_1 \frac{\partial p'}{\partial x_1} \right]$$

Substituting the foregoing equation and equation (3a) into equation (2) we obtain

$$\frac{1}{\bar{\rho}\bar{a}^2} \frac{\partial p'}{\partial t} - \frac{U_1}{\bar{a}^2} \frac{\partial u_1'}{\partial t} + \left[1 - \frac{U_1^2}{\bar{a}^2} \right] \frac{\partial u_1'}{\partial x_1} + \frac{\partial u_2'}{\partial x_2} = 0 \qquad (6)$$

---

*This term appears in dimensional form.

Finally, the governing equations have been reduced to a set of partial differential equations that express the acoustic pressure field in terms of the velocity; that is, equations (3a), (3b) and (6), rewritten as

$$\frac{\partial p'}{\partial x_1} = -\bar{\rho}\left[\frac{\partial u_1'}{\partial t} + U_1 \frac{\partial u_1'}{\partial x_1}\right] , \tag{7a}$$

$$\frac{\partial p'}{\partial x_2} = -\bar{\rho}\left[\frac{\partial u_2'}{\partial t} + U_1 \frac{\partial u_2'}{\partial x_1}\right] , \tag{7b}$$

$$\frac{\partial p'}{\partial t} = \bar{\rho}\left[U_1 \frac{\partial u_1'}{\partial t} - \bar{a}^2\left[1-\frac{U_1^2}{\bar{a}^2}\right]\frac{\partial u_1'}{\partial x_1} - \bar{a}^2 \frac{\partial u_2'}{\partial x_2}\right] , \tag{7c}$$

with

$$dp' = \frac{\partial p'}{\partial t}\, dt + \frac{\partial p'}{\partial x_1}\, dx_1 + \frac{\partial p'}{\partial x_2}\, dx_2 \; . \tag{7d}$$

Solution of the Governing Equations

The solutions to equations (7) in the regions upstream and downstream of the shock front are linked to one another through the oblique shock front relations. These boundary conditions will be presented at this point in the analysis.

Boundary Conditions. The unperturbed and perturbed oblique shock system is shown in Figure 4. From Figure 4 it follows that

$$V_1 = W_1 \cos \sigma , \tag{8a}$$

$$U_1 = W_1 \sin \sigma , \tag{8b}$$

$$V_{1p} = V_1 \cos \alpha_y + U_1 \sin \alpha_y + u_{11}' \cos (\sigma-\alpha_y) + u_{21}' \sin (\sigma-\alpha_y) \tag{8c}$$

and

$$U_{1p} = U_1 \cos \alpha_y - V_1 \sin \alpha_y + u'_{11} \sin (\sigma-\alpha_y) - u'_{21} \cos (\sigma-\alpha_y) - \alpha_t . \qquad (8d)$$

Since only small perturbations are being considered it is assumed that $\cos \alpha_y \approx 1$, $\sin \alpha_y \approx \alpha_y$ and products of perturbations are negligible in comparison to perturbation quantities alone. Under these assumptions equations (8) reduce to

$$V_{1p} \approx [W_1 + u'_{11}] \cos \sigma + [W_1\alpha_y + u'_{21}] \sin \sigma \qquad (9a)$$

and

$$U_{1p} \approx [W_1 + u'_{11}] \sin \sigma - [W_1\alpha_y + u'_{21}] \cos \sigma - \alpha_t . \qquad (9b)$$

For an oblique shock the tangential velocity component is unaltered by the shock whereas the normal velocity component experiences a normal shock. The normal shock relation is (reference 8)

$$\frac{U_1}{U_2} = \frac{\rho_2}{\rho_1} = \frac{\frac{\gamma+1}{2} \bar{U}_1^2}{1 + \frac{\gamma-1}{2} \bar{U}_1^2} \equiv r , \qquad (10)$$

or, in differential form

$$\frac{dU_2}{U_2} = \frac{dU_1}{U_1} + 2\left[r \frac{\gamma-1}{\gamma+1} - 1\right] \frac{d\bar{U}_1}{\bar{U}_1} . \qquad (11)$$

Now, by definition, $\bar{U}_1 \equiv U_1/a_1$ and therefore

$$\frac{d\bar{U}_1}{\bar{U}_1} = \frac{dU_1}{U_1} - \frac{da_1}{a_1} .$$

Substituting this relation into equation (11) gives

$$\frac{dU_2}{U_2} = \left[2r\,\frac{\gamma-1}{\gamma+1} - 1\right]\frac{dU_1}{U_1} - \left[2r\,\frac{\gamma-1}{\gamma+1} - 2\right]\frac{da_1}{a_1} \qquad (12)$$

Assuming that

$$dU_1 \simeq U_{1p} - U_1$$

and

$$dU_2 \simeq U_{2p} - U_2 = U_{2p} - \frac{1}{r}\,U_1$$

we have

$$U_{2p} \simeq U_2 + dU_2 = \frac{1}{r}\,U_1\left[1 + \frac{dU_2}{U_2}\right]$$

or

$$U_{2p} \simeq \frac{1}{r}\,U_1\left[1 + \left[2r\,\frac{\gamma-1}{\gamma+1} - 1\right]\frac{dU_1}{U_1} - \left[2r\,\frac{\gamma-1}{\gamma+1} - 2\right]\frac{da_1}{a_1}\right]. \qquad (13a)$$

Again, for an oblique shock

$$V_{2p} = V_{1p} \qquad (13b)$$

Solving for $\frac{dU_1}{U_1}$ we obtain

$$\frac{dU_1}{U_1} \simeq \frac{U_{1p}}{U_1} - 1$$

or

$$\frac{dU_1}{U_1} \simeq \frac{u'_{11}}{W_1} - \cot\sigma\,\frac{u'_{21}}{W_1} - \cot\sigma\,\alpha_y - \csc\sigma\,\frac{\alpha t}{W_1} \qquad (14)$$

Solving for $\frac{da_1}{a_1}$, from first order acoustics we have

$$\frac{p'_1}{\bar{p}_1} = \gamma\,\frac{u'_1}{\bar{a}_1}$$

and

$$\frac{T_1'}{\bar{T}_1} = \frac{\gamma-1}{\gamma} \frac{p_1'}{\bar{p}_1} = (\gamma-1) \frac{u_1'}{\bar{a}_1}$$

For the assumed perfect gas

$$a_1^2 = \gamma R T_1$$

and therefore

$$\frac{da_1}{a_1} = \frac{1}{2} \frac{dT_1}{T_1} \quad .$$

If it is assumed that $\frac{dT_1}{T_1} \simeq \frac{T_1'}{\bar{T}_1}$, then

$$\frac{da_1}{a_1} \simeq \frac{\gamma-1}{2} \frac{u_1'}{\bar{a}_1} \quad .$$

Now the acoustic particle velocity in Region 1 (upstream of the shock front), u_1', is related to the perturbation velocity components in Region 1 in the following way (see Figure 5)

$$u_{11}' = u_1' \sin (\sigma+\theta) \tag{15a}$$

and

$$u_{21}' = -u_1' \cos (\sigma+\theta). \tag{15b}$$

Substituting equations (15) into equation (14) yields

$$\frac{dU_1}{U_1} = \frac{u_1'}{W_1} \csc \sigma \cos \theta - \alpha_y \cot \sigma - \frac{\alpha t}{W_1} \csc \sigma. \tag{16}$$

The perturbation velocity components in Region 2 at the shock front are given by (see Figure 4)

$$u_{12}' = U_{2p} \cos (\phi+\alpha_y) + V_{2p} \sin (\phi+\alpha_y) - W_2$$

and

$$u'_{22} = V_{2p} \cos(\phi+\alpha_y) - U_{2p} \sin(\phi+\alpha_y) .$$

Noting that α_y is small (by assumption) and that

$$W_2 = W_1 \cos\sigma \csc\phi$$

we have

$$u'_{12} = U_{2p} [\cos\phi - \alpha_y \sin\phi] +$$

$$V_{2p} [\sin\phi + \alpha_y \cos\phi] -$$

$$W_1' \cos\sigma \csc\phi$$

and

$$u'_{22} = V_{2p} [\cos\phi - \alpha_y \sin\phi] -$$

$$U_{2p} [\sin\phi + \alpha_y \cos\phi] .$$

Written in terms of the perturbation quantities in Region 1 and neglecting products of perturbations, these become

$$u'_{12} = A_2 u'_1 + B_2 W_1 \alpha_y + C_2 \alpha_t \tag{17a}$$

and

$$u'_{22} = A_3 u'_1 + B_3 W_1 \alpha_y + C_3 \alpha_t , \tag{17b}$$

where, by definition,

$$A_1 = \left[2r \frac{\gamma-1}{\gamma+1} - 1\right] \csc\sigma \cos\theta + \left[\gamma - 1 - r \frac{(\gamma-1)^2}{\gamma+1} M_1\right]$$

$$B_1 = -\left[2r \frac{\gamma-1}{\gamma+1} - 1\right] \cot\sigma$$

$$C_1 = -\left[2r \frac{\gamma-1}{\gamma+1} - 1\right] \csc\sigma$$

$$A_2 = \sin\theta \sin\phi + \frac{A_1}{r} \sin\sigma \cos\phi$$

$$B_2 = \sin\sigma \sin\phi + \frac{B_1}{r} \sin\sigma \cos\phi .$$

$$C_2 = \frac{C_1}{r} \sin\sigma \cos\phi$$

$$A_3 = \sin\theta \cos\phi - A_1 \cos\sigma \cos\phi$$

$$B_3 = \sin\sigma \cos\phi - \cos\sigma \csc\phi - B_1 \cos\sigma \cos\phi$$

$$C_3 = - C_1 \cos\sigma \cos\phi$$

To relate the perturbed pressure in Region 2 at the shock to the perturbation properties u_1', α_y and α_t, the pressure rise across an oblique shock front, as given by reference 8, namely

$$\frac{p_2}{p_1} = \frac{2\gamma}{\gamma+1} \bar{U}_1^2 - \frac{\gamma-1}{r+1} , \tag{18}$$

will be used. In differential form, equation (18) becomes

$$\frac{dp_2}{p_2} = \frac{dp_1}{p_1} + \frac{4\gamma \bar{U}_1^2}{2\gamma\bar{U}_1^2-(\gamma-1)} \frac{d\bar{U}_1}{\bar{U}_1}$$

As before it is assumed that $\frac{dp_1}{p_1} \approx \frac{p_1'}{\bar{p}_1}$ and $\frac{dp_2}{p_2} \approx \frac{p_2'}{\bar{p}_2}$ and, therefore,

$$\frac{p_2'}{\bar{p}_2} = \frac{A_4}{\bar{a}_1} u_1' + B_4 \alpha_y + \frac{C_4}{\bar{W}_1} \alpha_t \tag{19}$$

where

$$A_4 = \frac{2\gamma\bar{U}_1^2 - \gamma(\gamma-1)}{2\gamma\bar{U}_1^2 - (\gamma-1)} + \frac{4\gamma \bar{U}_1^2}{2\gamma\bar{U}^2 - (\gamma-1)} \cos\theta ,$$

$$B_4 = -\frac{4\gamma\,\bar{U}_1^2}{2\gamma\bar{U}_1^2 - (\gamma-1)}\cot\sigma,$$

and

$$C_4 = -\frac{4\gamma\,\bar{U}_1^2}{2\gamma\bar{U}_1^2 - (\gamma-1)}\csc\sigma$$

To relate the perturbed density in Region 2 at the shock to the perturbation properties u_1', α_y and α_t the density ratio across the shock, as given by reference 8, namely

$$\frac{\rho_2}{\rho_1} = \frac{U_1}{U_2} \qquad (20)$$

or

$$\frac{\bar{\rho}_2 + \rho_2'}{\bar{\rho}_1 + \rho_1'} = \frac{U_1 + dU_1}{U_2 + dU_2}$$

will be used. Neglecting products of perturbation quantities, it can be shown that

$$\frac{\rho_2'}{\bar{\rho}_2} = \frac{\rho_1'}{\bar{\rho}_1} + \frac{dU_1}{U_1} - \frac{dU_2}{U_2}$$

or, substituting for $\rho_1'/\bar{\rho}_1$, dU_1/U_1 and dU_2/U_2 previously derived expressions in terms of u_1', α_y and α_t,

$$\frac{\rho_2'}{\bar{\rho}_2} = \frac{A_5}{\bar{a}_1}\,u_1' + B_5\,\alpha_y + \frac{C_5}{\bar{W}_1}\,\alpha_t \qquad (21)$$

where

$$A_5 = 1 - 2\left[\frac{\csc\sigma\,\cos\theta}{M_1} + \frac{\gamma-1}{2}\right]\left[r\,\frac{\gamma-1}{\gamma+1} - 1\right],$$

$$B_5 = -\,2\left[r\,\frac{\gamma-1}{\gamma+1} - 1\right],$$

and

$$C_5 = -2\left[r^{\frac{\gamma-1}{\gamma+1}} - 1\right] \csc \sigma .$$

With the boundary conditions given by equations (17), (19) and (21) it is now possible to solve for the perturbation properties in Region 2 in terms of those for Region 1.

<u>Sound Field in Region 1</u>. For the plane sound field shown in Figure 1 the acoustic particle velocity and acoustic pressure are, respectively,

$$u_1' = U_{0_1} \cos\left[\frac{\omega_1 z_1}{\bar{a}_1} - \omega_1 t\right] \tag{22}$$

and

$$p_1' = \gamma \frac{U_{0_1}}{\bar{a}_1} \bar{p}_1 \cos\left[\frac{\omega_1 z_1}{\bar{a}_1} - \omega_1 t\right] . \tag{23}$$

From Figure 5 it is seen that the z_1-axis is in rectilinear motion in the ξ_1-direction and it lies at an angle of $(\sigma + \theta - \pi/2)$ with respect to the ξ_1-axis. Thus, since the z_1-axis moves with speed W_1,

$$z_1 = [\xi_1 - W_1 t] \sin(\sigma+\theta) - \eta_1 \cos(\sigma+\theta) \tag{24}$$

and, therefore, equations (22) and (23) may be written as

$$u_1' = U_{0_1} \cos\left[\frac{\omega_1}{\bar{a}_1}\Big[[\xi_1 - W_1 t] \sin(\sigma+\theta) - \eta_1 \cos(\sigma+\theta)\Big] - \omega_1 t\right] \tag{25}$$

and

$$p_1' = \gamma \frac{U_{0_1}}{\bar{a}_1} \bar{p}_1 \cos\left[\frac{\omega_1}{\bar{a}_1}\Big[[\xi_1 - W_1 t] \sin(\sigma+\theta) - \eta_1 \cos(\sigma+\theta)\Big] - \omega_1 t\right] \tag{26}$$

If the transformation $x_1 = \xi_1$, $x_2 = \eta_1$ and $U_1 = W_1$ is made, then equations (25) and (26) exactly satisfy equation (6). Thus equations (3a), (3b) and (6) are consistent with linear acoustic theory.

Sound Field in Region 2. For a restricted range of sound wave incidence angles the pressure perturbation downstream of the shock front will be entirely due to acoustic waves. This range of angles will now be determined.

Consider a fluid particle at the point P_1 in Figure 6 at time t. At this same point and time a sound wave interacts with the shock front and a cylindrical sound wave is assumed to be generated. At time $t + \delta t$ the plane sound wave front in Region 1 intersects (interacts with) the shock front at point P_2 and the cylindrical wave has spread a radial distance $a_2\delta t$ from an origin tied to the fluid particle that has moved from P_1 to P_1', a distance $W_2\delta t$.

If P_2 lies outside the cylindrical wave front, a refracted sound wave is generated; if not, a pressure wave is formed and the original assumption is invalid. Two limiting cases exist for θ for the existence of acoustic waves in Region 2; namely the two values of θ, say θ_c, for which P_2 lies at the intersection of the cylindrical wave front and the shock front. This is shown in Figure 7 for one of the critical angles.

From Figure 7 it can be shown that

$$L = [1 + M_1 \sin (\sigma+\theta_c)] \csc \theta_c \, \bar{a}_1 \, \delta t$$

and

$$L = \left[M_2 \sin \phi \pm \left[1 - M_2^2 \cos^2 \phi \right]^{1/2} \right] \bar{a}_2 \, \delta t$$

where, in the second equation for L, the (+) is used if $0<\theta_c<\pi$ and the (-) is used if $-\pi<\theta_c<0$. Equating these expressions results in

$$[1 + M_1 \sin (\sigma+\theta_c)] \csc \theta_c = \left[M_2 \sin \phi \pm \left[1 - M_2^2 \cos^2 \phi \right]^{1/2} \right] \frac{\bar{a}_2}{\bar{a}_1} \quad (27)$$

Assuming that θ is such that acoustic waves do exist in Region 2, expressions for the acoustic velocity and pressure will now be determined. A typical wave front pattern is shown in Figure 8. Letting the z_2-axis be in rectilinear motion in the ξ_2-direction with the speed W_2, the acoustic waves are given by

$$u_2' = U_{0_2} \cos \left[\frac{\omega_2}{\bar{a}_2} z_2 - \omega_2 t \right] \quad (28)$$

and

$$p_2' = \gamma \frac{U_{0_2}}{\bar{a}_2} \bar{p}_2 \cos \left[\frac{\omega_2}{\bar{a}_2} z_2 - \omega_2 t \right] . \quad (29)$$

Now z_2 may be written in terms of ξ_2, η_2, t and W_2 as

$$z_2 = [\xi_2 - W_2 t] \cos (\phi-\phi') - \eta_2 \sin (\phi-\phi'). \quad (30)$$

At the shock front the arguments in Regions 1 and 2 must match since the functional form of the acoustic waves was assumed to be the same in both of these regions. Thus

$$\frac{\omega_2}{\bar{a}_2}\left[\left[\xi_2 - W_2 t\right] \cos\,(\phi-\phi') - \eta_2 \sin\,(\phi-\phi')\right] - \omega_2 t =$$

$$\frac{\omega_1}{\bar{a}_1}\left[\left[\xi_1 - W_1 t\right] \sin\,(\sigma+\theta) - \eta_1 \cos\,(\sigma+\theta)\right] - \omega_1 t$$

and along the shock front

$$\eta_1 = \xi_1 \tan\sigma,$$

$$\eta_2 = \xi_2 \cot\phi,$$

and

$$\xi_2 = \xi_1 \sin\phi \sec\sigma.$$

Solving these equations for ω_2 and ϕ' yields

$$\frac{\omega_2}{\omega_1} = \frac{1 + M_1 \sin\,(\sigma+\theta)}{1 + M_2 \cos\,(\phi-\phi')} \quad ,$$

$$\frac{\omega_2}{\omega_1} = \frac{\bar{a}_2}{\bar{a}_1}\,\frac{\sin\theta}{\sin\phi'} \quad , \tag{31}$$

and combining these last two equations to eliminate ω_2/ω_1 gives

$$\frac{\bar{a}_2 \sin\theta}{\bar{a}_1 \sin\phi'} = \frac{1 + M_1 \sin\,(\sigma+\theta)}{1 + M_2 \cos\,(\phi-\phi')} \tag{32}$$

In summary, the angle of the refracted sound wave, the shift in frequency, and the angles of incidence that yield refracted sound waves have been determined. The only remaining quantity of interest is U_{0_2}, the amplitude of the acoustic particle velocity. This can be found only after the shock front displacement is determined.

Shock Front Displacement, $\alpha(y,t)$. The shock front displacement should be a periodic function of distance along the shock front, y, and time, t. From equation (31) the wavelength is

$$\lambda_{sf} = \frac{\lambda_1}{\sin\theta} = \frac{\lambda_2}{\sin\phi'} \quad . \tag{33}$$

When acoustic waves exist in Region 2 it is assumed that the shock front perturbation velocity, α_t, and the sound particle velocity, u_1', have the same functional form. Thus

$$\alpha(y,t) = E_1 \sin\left[\frac{\omega_1}{\bar{a}_1}\sin\theta\, y - \left[1 + M_1\sin(\sigma+\theta)\right]\omega_1 t\right], \tag{34}$$

$$\alpha_t = -E_1[1 + M_1\sin(\sigma+\theta)]\,\omega_1\cos\left[\frac{\omega_1}{\bar{a}_1}\sin\theta\, y - \left[1 + M_1\sin(\sigma+\theta)\right]\omega_1 t\right] \tag{35}$$

and

$$\alpha_y = E_1\frac{\omega_1}{\bar{a}_1}\sin\theta\cos\left[\frac{\omega_1}{\bar{a}_1}\sin\theta\, y - \left[1 + M_1\sin(\sigma+\theta)\right]\omega_1 t\right]. \tag{36}$$

Entropy-Vorticity Waves in Region 2. Since the entropy in Region 1 is constant (by assumption) and the strength of the shock front is variable, the entropy in Region 2 will be variable. Thus entropy-vorticity waves are convected downstream with the velocity $\vec{W}_2$. To an observer moving with the flow in Region 2, the entropy is a function of position alone since the acoustic compression-rarefaction process has been assumed to be isentropic.

The entropy-vorticity wave front in Region 2 generated by a plane sound wave in Region 1 is shown in Figure 9. The E-V wave front ray angle, β, is given by

$$\beta = \tan^{-1}\left[\frac{M_1 \cos\sigma \cot\phi \sin\theta}{1 + M_1 \sin\sigma \cos\theta}\right] \tag{37}$$

The E-V wavelength is

$$\lambda_{evw} = \lambda_1 \frac{\sin\beta}{\sin\theta} \tag{38}$$

and since the z_3-axis moves rectilinearly in the ξ_2-direction

$$z_3 = [\xi_2 - W_2 t]\cos(\varphi-\beta) - \eta_2 \sin(\phi-\beta)\ . \tag{39}$$

Thus the argument of the entropy-vorticity wave, $2\pi z_3/\lambda_{evw}$, can be shown to be

$$\frac{2\pi z_3}{\lambda_{evw}} = \frac{2\pi\sin\theta\Big[\left[\xi_2 - W_2 t\right]\cos(\phi-\beta) - \eta_2\sin(\phi-\beta)\Big]}{\lambda \sin\beta} \tag{40}$$

<u>Perturbation Velocity Components in Region 2</u>. The perturbation velocity components in Region 2 consist of two parts: one due to the sound field and one due to the vorticity waves. Assuming the vorticity waves to be of the same functional form as the sound waves, the perturbation velocity components may be written as

$$u'_{12} = U_{0_2} \cos\left[\frac{\omega_2}{\bar{a}_2} z_2 - \omega_2 t\right] \cos(\phi-\phi') + F_1 \cos\left[\frac{2\pi\ z_3}{\lambda_{evw}}\right] \tag{41}$$

and

$$u_{22}' = -U_{0_2} \cos\left[\frac{\omega_2}{\bar{a}_2} z_2 - \omega_2 t\right] \sin(\phi - \phi') + G_1 \cos\left[\frac{2\pi z_3}{\lambda_{evw}}\right] \tag{42}$$

Perturbation Pressure in Region 2. From equations (3a) and (3b) it can be shown that the perturbation pressure in Region 2 is only that associated with the sound field; that is

$$\frac{p_2'}{\bar{p}_2} = \gamma \frac{U_{0_2}}{\bar{a}_2} \cos\left[\frac{\omega_2}{\bar{a}_2} z_2 - \omega_2 t\right] . \tag{29}$$

Perturbation Density in Region 2. With only an acoustic pressure perturbation in Region 2 the perturbation density is composed of an acoustic part and an entropy-vorticity part; that is

$$\frac{\rho_2'}{\bar{\rho}_2} = \frac{U_{0_2}}{\bar{a}_2} \cos\left[\frac{\omega_2}{\bar{a}_2} z_2 - \omega_2 t\right] + H_1 \cos\left[\frac{2\pi z_3}{\lambda_{evw}}\right]. \tag{43}$$

In review, there are now five unknown quantities in Region 2; namely, E_1, F_1, G_1, H_1 and U_{0_2}. There are only four equations relating these to known quantities at this point in the analysis and, therefore, an additional relation, the continuity equation in Region 2, will now be derived.

Continuity Equation in Region 2. Consider a change in variables in Region 2 such that

$$\xi_3 = \xi_2 - W_2 t$$

and

$$\eta_3 = \eta_2 \; ;$$

that is, a change to a coordinate system that moves with the unperturbed flow. Now, in terms of ξ_3 and η_3,

$$z_2 = \xi_3 \cos(\phi - \phi') - \eta_3 \sin(\phi - \phi')$$

and

$$z_3 = \xi_3 \cos(\phi - \beta) - \eta_3 \sin(\phi - \beta).$$

Equation (2), written in dimensionless form for the ξ_3, η_3 coordinate system, is

$$\underset{1}{\frac{\partial \tilde{\rho}_2'}{\partial \tilde{t}}} + \underset{\delta}{\frac{U_{0_2}}{\bar{a}_2}} \underset{1}{\cos(\phi - \phi')} \underset{1}{\frac{\partial \tilde{\rho}_2'}{\partial \tilde{\xi}_3}} - \underset{\delta}{\frac{U_{0_2}}{\bar{a}_2}} \underset{1}{\sin(\phi - \phi')} \underset{1}{\frac{\partial \tilde{\rho}_2'}{\partial \tilde{\eta}_3}} +$$

$$\left[\underset{1}{\tilde{\bar{\rho}}_2} + \underset{\delta}{\frac{U_{0_2}}{\bar{a}_2}} \underset{1}{\tilde{\rho}_2'}\right] \left[\underset{1}{\cos(\phi - \phi')} \underset{1}{\frac{\partial \tilde{u}_{12}'}{\partial \tilde{\xi}_3}} - \underset{1}{\sin(\phi - \phi')} \underset{1}{\frac{\partial \tilde{u}_{22}'}{\partial \tilde{\eta}_3}}\right] = 0.$$

Retaining only those terms that are of the order of magnitude of one, this becomes, in dimensional form,

$$\frac{\partial \rho_2'}{\partial t} + \bar{\rho}_2 \left[\frac{\partial u_{12}'}{\partial \xi_3} + \frac{\partial u_{22}'}{\partial \eta_3}\right] = 0. \tag{44}$$

Substituting the expressions for ρ_2', u_{12}' and u_{22}' into equation (44) yields

$$G_1 = F_1 \cot(\phi - \beta). \tag{45}$$

There are now four unknown quantities in Region 2 and four equations thereby forming a determinable system. The unknowns will now be determined.

Evaluation of E_1, F_1, H_1 and U_{0_2}. The following equations are to be solved simultaneously at the shock front:

$$A_2\, u_1' + B_2\, W_1\, \alpha_y + C_2\, \alpha_t = u_{12}' \,, \qquad (17a)$$

$$A_3\, u_1' + B_3\, W_1\, \alpha_y + C_3\, \alpha_t = u_{22}' \,, \qquad (17b)$$

$$\frac{A_4}{\bar{a}_1}\, u_1' + B_4\, \alpha_y + \frac{C_4}{W_1}\, \alpha_t = \frac{p_2'}{\bar{p}_2} \qquad (19)$$

and

$$\frac{A_5}{\bar{a}_1}\, u_1' + B_5\, \alpha_y + \frac{C_5}{W_1}\, \alpha_t = \frac{\rho_2'}{\bar{\rho}_2} \,. \qquad (21)$$

It is also known that

$$u_{12}' = U_{0_2} \cos\left[\frac{\omega_2}{\bar{a}_2} z_2 - \omega_2 t\right] \cos\,(\phi - \phi') + F_1 \cos\left[\frac{2\pi\ z_3}{\lambda_{evw}}\right], \qquad (41)$$

$$u_{22}' = -\,U_{0_2} \cos\left[\frac{\omega_2}{\bar{a}_2} z_2 - \omega_2 t\right] \sin\,(\phi - \phi') + G_1 \cos\left[\frac{2\pi\ z_3}{\lambda_{evw}}\right], \qquad (42)$$

$$\frac{p_2'}{\bar{p}_2} = \gamma\, \frac{U_{0_2}}{\bar{a}_2} \cos\left[\frac{\omega_2}{\bar{a}_2} z_2 - \omega_2 t\right], \qquad (29)$$

$$\frac{\rho_2'}{\bar{\rho}_2} = \frac{U_{0_2}}{\bar{a}_2} \cos\left[\frac{\omega_2}{\bar{a}_2} z_2 - \omega_2 t\right] + H_1 \cos\left[\frac{2\pi z_3}{\lambda_{evw}}\right], \tag{43}$$

$$u_1' = U_{0_2} \cos\left[\frac{\omega_1}{\bar{a}_1} z_1 - \omega_1 t\right], \tag{22}$$

$$\alpha_y = E_1 \frac{\omega_1}{\bar{a}_1} \sin\theta \cos\left[\frac{\omega_1}{\bar{a}_1} \sin\theta\, y - \left[1 + M_1 \sin(\sigma+\theta)\right] \omega_1 t\right], \tag{36}$$

$$\alpha_t = - E_1 [1 + M_1 \sin(\sigma+\theta)]\, \omega_1 \cos\left[\frac{\omega_1}{\bar{a}_1} \sin\theta\, y - \left[1 + M_1 \sin(\sigma+\theta)\right] \omega_1 t\right], \tag{35}$$

and

$$G_1 = F_1 \cot(\phi-\beta). \tag{45}$$

It can be shown that the arguments of the cosine terms in equations (22), (29), (35), (36), (41), (42) and (43) are all equal at the shock front. Thus equations (17a), (17b), (19) and (21) may be written as

$$A_2 U_{0_1} + B_2 W_1 E_1 \frac{\omega_1}{\bar{a}_1} \sin\theta - C_2 \omega_1 E_1 [1 + M_1 \sin(\sigma+\theta)] = U_{0_2} \cos(\phi-\phi') + F_1, \tag{46}$$

$$A_3 U_{0_1} + B_3 W_1 E_1 \frac{\omega_1}{\bar{a}_1} \sin\theta - C_3 \omega_1 E_1 [1 + M_1 \sin(\sigma+\theta)] = - U_{0_2} \sin(\phi-\phi') + F_1 \cot(\phi-\beta), \tag{47}$$

$$A_4 \frac{U_{0_1}}{\bar{a}_1} + B_4 E_1 \frac{\omega_1}{\bar{a}_1} \sin\theta - \frac{C_4}{W_1}\omega_1 E_1 [1 + M_1 \sin(\sigma+\theta)] = \gamma \frac{U_{0_2}}{\bar{a}_2} , \qquad (48)$$

and

$$A_5 \frac{U_{0_1}}{\bar{a}_1} + B_5 E_1 \frac{\omega_1}{\bar{a}_1} \sin\theta - \frac{C_5}{W_1}\omega_1 E_1 [1 + M_1 \sin(\sigma+\theta)] = \frac{U_{0_2}}{\bar{a}_2} + H_1 . \qquad (49)$$

These four equations can be arranged to give

$$\begin{aligned} A_{11} E_1 + A_{12} F_1 + A_{13} U_{0_2} + A_{14} H_1 &= D_1 \\ A_{21} E_1 + A_{22} F_1 + A_{23} U_{0_2} + A_{24} H_1 &= D_2 \\ A_{31} E_1 + A_{32} F_1 + A_{33} U_{0_2} + A_{34} H_1 &= D_3 \\ A_{41} E_1 + A_{42} F_1 + A_{43} U_{0_2} + A_{44} H_1 &= D_4 \end{aligned} \qquad (50)$$

where

$$A_{11} = \left[\left[1 + M_1 \sin(\sigma+\theta)\right] C_2 - M_1 \sin\theta\, B_2 \right] \omega_1$$

$$A_{12} = 1$$

$$A_{13} = \cos(\phi-\phi')$$

$$A_{14} = 0$$

$$A_{21} = \left[\left[1 + M_1 \sin(\sigma+\theta)\right] C_3 - M_1 \sin\theta\, B_3 \right] \omega_1$$

$$A_{22} = \cot(\phi-\beta)$$

$$A_{23} = - \sin (\phi - \phi')$$

$$A_{24} = 0$$

$$A_{31} = \left[\left[1 + M_1 \sin (\sigma + \theta) \right] C_4 - M_1 \sin \theta \; B_4 \right] \omega_1$$

$$A_{32} = 0$$

$$A_{33} = \gamma \frac{\bar{a}_1}{\bar{a}_2} M_1$$

$$A_{34} = 0$$

$$A_{41} = \left[\left[1 + M_1 \sin (\sigma + \theta) \right] C_5 - M_1 \sin \theta \; B_5 \right] \omega_1$$

$$A_{42} = 0$$

$$A_{43} = \frac{\bar{a}_1}{\bar{a}_2} M_1$$

$$A_{44} = 1$$

$$D_1 = A_2 \; U_{0_1}$$

$$D_2 = A_3 \; U_{0_1}$$

$$D_3 = A_4 \; M_1 \; U_{0_1}$$

$$D_4 = A_5 \; M_1 \; U_{0_1}$$

Computations. To compute the perturbed flow field in Region 2 due to the interaction of plane sound waves from Region 1 with an oblique shock front, values for the following quantities must be known:

$\bar{a}_1, \gamma, M_1, \sigma, \delta, r, \bar{a}_2, \phi, \theta, U_{0_1}, \omega_1, \phi'$ and β.

To illustrate the computational method, γ, $\overline{a}_1$ (or $\overline{T}_1$), M_1, σ, θ, U_{0_1} and ω_1 will be treated as independent variables. The step-by-step procedure is as follows

1. Select a temperature T_1.
2. Select a working fluid, i.e. γ; e.g., air with $\gamma = 1.4$.
3. Select a Mach number M_1.
4. Select an oblique shock angle σ.
5. Select a sound wave incidence angle θ (if possible, i.e. must first consider θ_c's).
6. Select a sound wave particle velocity U_{0_1}.
7. Select a sound wave circular frequency ω_1.
8. Compute r as follows (reference 8)

$$r = \frac{U_1}{U_2} = \frac{\rho_2}{\rho_1} = \frac{(\gamma+1)\, M_1^2 \sin^2 \sigma}{2\left[1 + \frac{\gamma-1}{2}\, M_1^2 \sin^2 \sigma\right]} \tag{51}$$

9. Compute δ as follows (reference 8).

$$\delta = \sigma - \tan^{-1}\left[\frac{1}{r} \tan \sigma\right] \tag{52}$$

10. Compute $\overline{a}_2$ as follows (reference 8):

$$\overline{a}_2 = \sqrt{\gamma R\overline{T}} = \overline{a}_1 \sqrt{\overline{T}_2/\overline{T}_1} \tag{53}$$

and

$$\overline{T}_2/\overline{T}_1 = \frac{\left[1 + \frac{\gamma-1}{2}\, \overline{U}_1^2\right]\left[\frac{2\gamma}{\gamma-1}\, \overline{U}_1^2 - 1\right]}{\frac{(\gamma+1)^2}{2(\gamma-1)}\, \overline{U}_1^2} \tag{54}$$

where

$$\bar{U}_1 \equiv M_1 \sin \sigma \tag{55}$$

11. Compute ϕ by noting from Figure 1 that

$$\phi = \frac{\pi}{2} + \delta - \sigma \tag{56}$$

12. Compute θ_c from equation (27), i.e.

$$[1 + M_1 \sin (\sigma+\theta_c)] \csc \theta_c =$$

$$M_1 \cos \sigma \pm \left[\frac{\bar{a}_2^2}{\bar{a}_1^2} - \frac{M_1^2 \sin^2 \sigma}{r^2} \right]^{1/2}$$

where (+) is used if $0 < \theta < \pi$ is being considered or (-) if $0 > \theta > -\pi$ is being considered. (This is a transcendental equation for θ_c and an iterative method of solution is required.)

13. Check to see if the chosen value for θ is permissible, i.e. $|\theta| < |\theta_c|$.

14. Compute β from equation (37), i.e.

$$\beta = \tan^{-1} \left[\frac{M_1 \cos \sigma \cot \phi \sin \theta}{1 + M_1 \sin \sigma \cos \theta} \right] .$$

15. Compute ϕ' from equation (32), i.e.

$$\frac{\bar{a}_2 \sin \theta}{\bar{a}_1 \sin \phi'} = \frac{1 + M_1 \sin (\sigma+\theta)}{1 + M_2 \cos (\phi-\phi')}$$

where

$$M_2 = M_1 \frac{\cos \sigma}{\sin \phi} \frac{\bar{a}_1}{\bar{a}_2} . \tag{57}$$

(This is a transcendental equation for ϕ' and an iterative method of solution is required.)

16. Compute A_{ij} and D_i. (At this point the A_{ij}'s and D_i's can be computed using their defining equations.)

17. Compute E_1 as follows:

 a. Note that each D_i contains U_{0_1} and that ω_1 will be a factor of the coefficient determinant (solution by Cramer's rule). Therefore it is convenient to define new D_i's and concomitantly a new E_1; i.e.

$$D_i = D_i^* U_{0_1}$$

 and

$$E_1 = E_1^* U_{0_1}/\omega_1 .$$

 b. Using Cramer's rule the solution of equations (50) for E_1^* is

$$E_1^* = [D_1^* A_{22}A_{33} + D_2^* A_{32}A_{13} + D_3^* A_{23}A_{12} - D_1^* A_{23}A_{32} - D_2^* A_{12}A_{33} - D_3^* A_{22}A_{13}]/\text{DET}\,[A_{ij}] \quad (58)$$

 where

$$\text{DET}\,[A_{ij}] = A_{11}A_{22}A_{33} + A_{21}A_{32}A_{13} + A_{31}A_{23}A_{12} - A_{31}A_{22}A_{13} - A_{21}A_{12}A_{33} - A_{11}A_{23}A_{32} \quad (59)$$

 and finally

$$E_1 = E_1^* U_{0_1}/\omega_1 .$$

18. Compute F_1 as follows:

 a. Define a new F_1 as

$$F_1 = F_1^* U_{0_1} .$$

b. Using Cramer's rule the solution of equations (50) for F_1^* is

$$F_1^* = [D_1^* A_{23} A_{31} + D_2^* A_{11} A_{33} + D_3^* A_{13} A_{21} - D_1^* A_{21} A_{33} - D_2^* A_{31} A_{13} - D_3^* A_{11} A_{23}]/\mathrm{DET}\,[A_{ij}]. \tag{60}$$

Therefore

$$F_1 = F_1^* \, U_{0_1} \, .$$

(It should be noted that ω_1 is a factor of both the numerator and denominator and, therefore, F_1 is independent of frequency.)

19. Compute U_{0_2} as follows:

a. Define a new U_{0_2} as

$$U_{0_2} = U_{0_2}^* \, U_{0_1} \, .$$

b. Using Cramer's rule the solution of equations (50) for $U_{0_2}^*$ is

$$U_{0_2}^* = [D_1^* A_{32} A_{21} + D_2^* A_{12} A_{31} + D_3^* A_{11} A_{22} - D_1^* A_{31} A_{22} - D_2^* A_{11} A_{32} - D_3^* A_{21} A_{12}]/\mathrm{DET}\,[A_{ij}] \tag{61}$$

and finally

$$U_{0_2} = U_{0_2}^* \, U_{0_1} \, .$$

(Note that U_{0_2} is also independent of frequency.)

20. Compute H_1 as follows:

a. Define a new H_1 as

$$H_1 = H_1^* \, U_{0_1} \, .$$

b. Using Cramer's rule the solution of equations (50) for H_1^* is

$$H_1^* = \Big[-D_1^*[A_{21}A_{32}A_{43} + A_{31}A_{42}A_{23} + A_{41}A_{33}A_{22} - A_{41}A_{32}A_{23} - A_{31}A_{22}A_{43} - A_{21}A_{33}A_{42}] + D_2^*[A_{11}A_{32}A_{43} + A_{12}A_{33}A_{41} + A_{13}A_{42}A_{31} - A_{41}A_{32}A_{13} - A_{31}A_{12}A_{43} - A_{11}A_{33}A_{42}] - D_3^*[A_{11}A_{22}A_{43} + A_{12}A_{23}A_{41} + A_{31}A_{42}A_{21} - A_{41}A_{22}A_{13} - A_{21}A_{12}A_{43} - A_{11}A_{23}A_{42}] + D_4^* \text{ DET } [A_{ij}]\Big] / \text{DET } [A_{ij}] \quad (62)$$

and, therefore,

$H_1 = H_1^* \, U_{0_1}$.

(Note that H_1 is independent of frequency.)

21. Compute the acoustic pressure ratio p_2'/p_1' as follows:

a. From equations (23) and (29)

$$\frac{p_2'}{p_1'} = \frac{U_{0_2} \, \bar{p}_2 \, \bar{a}_1 \cos\left[\frac{\omega_2}{\bar{a}_2} z_2 - \omega_2 t\right]}{U_{0_1} \, \bar{p}_1 \, \bar{a}_2 \cos\left[\frac{\omega_1}{\bar{a}_1} z_1 - \omega_1 t\right]}$$

or upon taking the root-time-mean-square of p_2' and p_1'

$$\frac{[p_2']_{rms}}{[p_1']_{rms}} = \frac{U_{0_2}}{U_{0_1}} \frac{\bar{p}_2}{\bar{p}_1} \frac{\bar{a}_1}{\bar{a}_2} \quad (63)$$

where

$$\frac{U_{0_2}}{U_{0_1}} = U^*_{0_2} ,$$

$$\frac{\bar{p}_2}{\bar{p}_1} = \frac{2\gamma}{\gamma+1} M_1^2 \sin^2 \sigma - \frac{\gamma-1}{\gamma+1} \text{ (reference 8)}, \tag{64}$$

and

$\frac{\bar{a}_1}{\bar{a}_2}$ is as given in Step 10.

b. From the definition of sound pressure level, the change in SPL across the shock is

$$SPL_2 - SPL_1 = 20 \log_{10} \frac{[p'_2]_{rms}}{[p'_1]_{rms}}$$

and therefore

$$SPL_2 - SPL_1 = 20 \log_{10} \left[\frac{U_{0_2}}{U_{0_1}} \frac{\bar{p}_2}{\bar{p}_1} \frac{\bar{a}_1}{\bar{a}_2} \right] \tag{65}$$

22. Compute the ratio of the acoustic particle velocities u'_2/u'_1 from equations (22) and (28); i.e.

$$\frac{u'_2}{u'_1} = \frac{U_{0_2} \cos\left[\frac{\omega_2}{\bar{a}_2} z_2 - \omega_2 t\right]}{U_{0_1} \cos\left[\frac{\omega_1}{\bar{a}_1} z_1 - \omega_1 t\right]}$$

or upon taking the root-mean-square of u'_1 and u'_2

$$\frac{[u'_2]_{rms}}{[u'_1]_{rms}} = \left|\frac{U_{0_2}}{U_{0_1}}\right| = \left|U^*_{0_2}\right| \tag{66}$$

23. Compute the intensity of the vorticity (shear) wave, $[u'_{evw}]_{rms}/W_2$, as follows:

a. From equations (41) and (42), the velocity perturbation due to the E-V wave is

$$u'_{evw} = [F_1^2 + G_1^2]^{1/2} \cos\left[\frac{2\pi\, z_3}{\lambda_{evw}}\right]$$

or taking the root-mean-square of u'_{evw}

$$[u'_{evw}]_{rms} = \left[\frac{F_1^2 + G_1^2}{2}\right]^{1/2}$$

b. Now $G_1^2 = F_1^2 \cot^2 (\phi-\beta)$ and therefore

$$F_1^2 + G_1^2 = F_1^2\,[1 + \cot^2 (\phi-\beta)]$$

or

$$[u'_{evw}]_{rms} = F_1 \csc (\sigma-\beta)/\sqrt{2}$$

$$= F_1^* \csc (\sigma-\beta)\, \frac{U_{0_1}}{\sqrt{2}}$$

c. From equation (57)

$$W_2 = M_1\, \bar{a}_1\, \frac{\cos \sigma}{\sin \phi}$$

and therefore

$$\frac{[u'_{evw}]_{rms}}{W_2} = \frac{M_{0_1}}{\sqrt{2}\, M_1}\; \frac{\csc (\sigma-\beta) \sin \phi}{\cos \sigma}\, F_1^* \qquad (67)$$

24. Compute the perturbation entropy in Region 2 as follows:

a. For a perfect gas

$$ds = c_v \frac{dp}{p} - c_p \frac{d\rho}{\rho} .$$

Replacing differential quantities by perturbations, this becomes

$$s_2' \simeq c_v \frac{p_2'}{\bar{p}_2} - c_p \frac{\rho_2'}{\bar{\rho}_2} \tag{68}$$

b. Substituting equations (29) and (43) for $p_2'/\bar{p}_2$ and $\rho_2'/\bar{\rho}_2$, respectively, yields

$$s_2' \simeq \gamma\, c_v \frac{U_{0_2}}{\bar{a}_2} \cos\left[\frac{\omega_2}{\bar{a}_2} z_2 - \omega_2 t\right] - c_p \frac{U_{0_2}}{\bar{a}_2} \cos\left[\frac{\omega_2}{\bar{a}_2} z_2 - \omega_2 t\right] - c_p H_1 \cos\left[\frac{2\pi\ z_3}{\lambda_{evw}}\right]$$

or after noting that $\gamma\, c_v = c_p$

$$\frac{s_2'}{c_p} = - H_1^* U_{0_1} \cos\left[\frac{2\pi\ z_3}{\lambda_{evw}}\right] \tag{69}$$

25. Compute the perturbation density in Region 2 from equation (43); i.e.

$$\frac{\rho_2'}{\bar{\rho}_2} = \left[\frac{U_{0_2}^*}{\bar{a}_2} \cos\left[\frac{\omega_2}{\bar{a}_2} z_2 - \omega_2 t\right] + H_1^* \cos\left[\frac{2\pi\ z_3}{\lambda_{evw}}\right]\right] U_{0_1} \tag{70}$$

26. Compute the shock front perturbation velocity, α_t, from equation (35); i.e.

$$\frac{\alpha_t}{U_{0_1}} = - E_1^*[1 + M_1 \sin(\sigma+\theta)] \cos\left[\frac{\omega_1}{\bar{a}_1} \sin\theta\ y - \left[1 + M_1 \sin(\sigma+\theta)\right]\omega_1 t\right] \tag{71}$$

or in terms of the ratio of the root-mean-squares of α_t and u_1'

$$\frac{[\alpha_t]_{rms}}{[u_1']_{rms}} = |E_1^*| \; |1 + M_1 \sin (\sigma + \theta)| \tag{72}$$

27. Compute the peak-to-peak amplitude of the shock front displacement, $|2\alpha|$, from equation (34), i.e.

$$|2\alpha| = 2E_1 = 2E_1^* \, U_{0_1}/\omega_1$$

or

$$\frac{|2\alpha|\omega_1}{U_{0_1}} = 2E_1^* \tag{73}$$

A FORTRAN IV program to make these computations is given in Appendix A.

Results

Rather than making computations for arbitrary shock fronts, it was decided to illustrate the sound wave - shock front interaction process for two Saturn V interstage flare angles, namely, $\delta = 8° \, 58'$, corresponding to the flare between the Service Module and the S-IVB stage, and $\delta = 16° \, 44'$, corresponding to the flare between the S-IVB and the S-II stage.

Appendix B contains computed data for the following cases

M_1	1.50	2.00	2.50	3.00	1.75	2.00	2.50	3.00
δ	8.98	8.96	8.97	8.98	16.74	16.73	16.74	16.75

The data column headings are defined as·

THETA - θ, the sound wave incidence angle, in degrees

BETA - β, the entropy-vorticity wave angle, in degrees

PHIP - ϕ, the refracted sound wave angle, in degrees

PP2/PP1 - p_2'/p_1', the ratio of the acoustic pressure in Region 2 to that in Region 1 evaluated at the shock front

SPL2/1 - $SPL_2 - SPL_1$, the change in sound pressure level across the shock, in dB

UO2/UO1 - U_{0_2}/U_{0_1}

UEVW2 - $[u'_{evw}]_{rms}/(M_{0_1}W_2)$, vorticity wave intensity

SPRCU - $[s_2']_{shock}/c_p U_{0_1}$

AT/UP1 - $[\alpha_t/u_1']_{shock}$, the ratio of the shock front velocity to the sound particle velocity in Region 1, evaluated at the shock front

PPAMPL - $[2\alpha\omega_1/u_1']_{shock}$, the ratio of the product of twice the shock front displacement and the circular frequency in Region 1 to the sound particle velocity in Region 1, evaluated at the shock front.

It should be noted that shock front resonance is predicted for all but one of the cases considered, namely, $M_1 = 1.50$ and $\delta = 8.98$: The data are not displayed graphically.

B. Shear Wave — Shock Front Interaction

Since shear waves (vorticity waves) are generated when plane sound waves interact with an oblique shock front and since a given flow often interacts with more than one oblique shock, a method to determine the flow field produced by shear wave — shock front interaction is required. Rather than develop a solution for an oblique shock, a coordinate transformation will be performed so that Ribner's [1] analysis of the shear wave — normal shock front interaction can be used.

Mathematical Formulation of the Problem

Unsteady-Flow Problem. Consider a uniform velocity field $\tilde{W}_A$ perturbed by the addition of a sinusoidal shear wave of arbitrary amplitude, wavelength and orientation. This flow undergoes an oblique shock as shown in Figure 10 . Since, in general the perturbation velocity w_A is not parallel to $\tilde{W}_A$. and since the shear wave pattern is frozen in the uniform flow, the perturbed flow will be unsteady from the viewpoint of a stationary observer on the shock front. For example, the nodal lines N-N_s will be convected into the front and the nodal points N_s will move up the front for the case depicted in Figure 10.

Equivalent Steady-Flow Problem. If an observer moves up the shock front with the speed of the nodal points, V_{N_s} , the flow will appear to be steady. To determine this speed consider the nodal line N_1-N_{s_1} at time t as shown in Figure 11. This line is convected into the shock front by the uniform flow $\tilde{W}_A$. At time t + δt the point N_1 has reached the shock and now represents the nodal point N_{s_1} or N'_{s_1} to distinguish it from the nodal point at time t.

From Figure 11 it can be shown that

$$\overline{N_1 N'_{s_1}} = \overline{N_1 N_{s_1}} \cos [90-(\theta+\sigma)] + \overline{N_{s_1} N'_{s_1}} \cos \sigma,$$

$$\overline{N_1 N_{s_1}} \sin [90-(\theta+\sigma)] = \overline{N_{s_1} N'_{s_1}} \sin \sigma,$$

$$\overline{N_1 N'_{s_1}} = \tilde{W}_A \,\delta t \quad \text{and} \quad \overline{N_{s_1} N'_{s_1}} = V_{N_s} \,\delta t.$$

Solving these equations for V_{N_s} yields

$$V_{N_s} = \tilde{W}_A \cos \sigma - \tilde{W}_A \sin \sigma \tan \theta. \tag{74}$$

Moving up the shock front with the speed V_{N_s} the flow appears to be steady and the unperturbed flow appears to have the velocity W_A as shown in Figure 12. The angle that W_A makes with the normal to the shock front is

$$\theta_A = \tan^{-1}\left[\frac{\tilde{W}_A \sin \sigma \tan \theta}{\tilde{W}_A \sin \sigma}\right]$$

or

$$\theta_A = \theta.$$

Thus from this viewpoint the unperturbed uniform flow is aligned with the perturbation velocity component w_A. The magnitude of W_A is given by

$$W_A = \tilde{W}_A \sin \sigma \sec \theta \tag{75}$$

and therefore it gets very large as θ approaches 90 degrees.

The flow field is now in Ribner's equivalent steady-flow form. His solution will be stated next and it will then be transformed back to the original oblique shock form.

Ribner's Solution

Ribner's coordinate systems and velocity components are shown in Figure 13. In terms of the oblique shock properties, his velocity components before the shock front are

$$W_A = \tilde{W}_A \sin \sigma \sec \theta, \tag{76}$$

$$U_A = \tilde{W}_A \sin \sigma \tag{77}$$

and

$$V = \tilde{W}_A \sin \sigma \tan \theta. \tag{78}$$

His perturbation velocity component w_A is

$$w_A' = \varepsilon W_A \cos (k\eta_A)$$

or in terms of oblique shock quantities

$$w_A' = \varepsilon \tilde{W}_A \sin \sigma \sec \theta \tag{79}$$

From this last relation it should be noted that the assumed amplitude of the perturbation is strongly dependent on θ; i.e. it goes as $\sec \theta$. Thus for a given $\tilde{W}_A$, σ and ε

(to be taken as a number less than about 0.1) the strength of the perturbation varies with θ and it is unbounded at $\theta = 90$ degrees. This point will be discussed further when the flow field is transformed back to its original unsteady form.

The Critical Incidence Angle. Two forms of the solution for all flow quantities appear, one for $\bar{W}^{*} < 1$ and the other for $\bar{W} > 1$. $\bar{W} = 1$ forms the dividing line and, since $\bar{W}$ depends on both $\bar{U}_A$ and the inclination θ, the sonic conditions gives a critical value of θ in terms of $\bar{U}_A$. From Ribner [1]

$$\theta_{cr} = \pm \tan^{-1}\sqrt{\frac{(\gamma+1)\ (m-1)^2}{2m}} \tag{80}$$

where

$$m = \frac{U_A}{U} = \frac{\frac{\gamma+1}{2}\ \bar{U}_A^2}{1 + \frac{\gamma-1}{2}\ \bar{U}_A^2}$$

$$\bar{U}_A = \frac{U_A}{a_A} = \frac{\tilde{W}_A}{a_A} \sin \sigma .$$

Thus for a given $\tilde{W}_A$ and σ there exists a θ_{cr}.

Velocity Perturbation Field, $\bar{W} < 1$. From Ribner [1]

$$\frac{w}{|w_A|^*} = S^* \cos [k \cos \theta\ (y - x \tan \phi) + \delta_s] +$$

$$\Pi^* \cos [k \cos \theta\ (y - x \tan \phi') + \delta_p] \tag{81a}$$

---

*The bar superscript denotes the Mach number formed by the ratio of the velocity component and the local speed of sound; e.g. $\bar{W} = W/a$, $\bar{U}_A = U_A/a_A$.

$$\frac{w'}{|w_A|^*} = \beta_w \, \Pi^* \sin [k \cos \theta \, (y - x \tan \phi') + \delta_p] \qquad (81b)$$

where

$$|w_A|^* \equiv W_A \, \varepsilon \cos \theta = \varepsilon \, \tilde{W}_A \sin \sigma$$

$$S^* \equiv \frac{1}{m} \sqrt{A^2 + B^2}$$

$$\Pi^* \equiv \frac{1}{m} \frac{\sqrt{\tilde{c}^2 + \tilde{d}^2}}{\beta} \exp \left[- x k \cos \theta \, \beta_w / \beta^2\right]$$

$$\delta_s = \tan^{-1} \left[\frac{-B}{A} \right]$$

$$\phi = \tan^{-1} [m \tan \theta]$$

$$\phi' = - \tan^{-1} \left[\frac{\bar{U}^2 \tan \phi}{\beta^2} \right]$$

$$\delta_p = \tan^{-1} \left[\frac{\tilde{c} \, \beta_w - \tilde{d} \tan \phi}{\tilde{d} \, \beta_w + \tilde{c} \tan \phi} \right]^+$$

$$\beta^2 \equiv 1 - \bar{U}^2$$

$$\beta_w^2 \equiv 1 - \bar{W}^2$$

$$A \equiv \sec \phi + 2 (m-1) \cos \phi + \tilde{a} \frac{(m-1)^2}{m} \sin \phi$$

$$B \equiv \tilde{b} \frac{(m-1)^2}{m} \sin \phi$$

$$\tilde{a} \equiv m \frac{CE + DF}{C^2 + D^2}$$

$$\tilde{b} \equiv m \frac{CF - DE}{C^2 + D^2}$$

+Ribner gives the denominator as $d\beta_w - c \tan \phi$ but a positive sign was obtained by this author.

$$\tilde{c} \equiv \frac{\tilde{a}}{m} D' - F'$$

$$\tilde{d} \equiv \frac{\tilde{b}}{m} D'$$

$$C \equiv \left[\frac{\gamma-1}{\gamma+1} + \frac{3-\gamma}{\gamma+1} m \right] \tan\phi - \left[(m-1)^2 + \frac{2(m-1)}{\gamma+1} \right] \sin\phi \cos\phi$$

$$D \equiv \frac{\beta_w}{\beta^2} (m-1) [1 + (m-1) \cos^2\phi] \equiv \frac{\beta_w}{\beta^2} D'$$

$$E \equiv 2\left[1 - \frac{\gamma-1}{\gamma+1} m \right] + 2 (m-1) \frac{\beta_w^2 \cos^2\phi}{\beta^2}$$

$$F \equiv \frac{\beta_w}{\beta^2} [2 (m-1) \sin\phi \cos\phi] \equiv \frac{\beta_w}{\beta^2} F'$$

<u>Velocity Perturbation Field, $\bar{W} > 1$.</u> From Ribner [1]

$$\frac{w}{|w_A|^*} = S^{**} \cos[k \cos\theta (y - x \tan\phi)] + \Pi^{**} \cos[k \cos\theta (y - x \tan\phi')] \qquad (82a)$$

$$\frac{w'}{|w_A|^*} = \beta_w \Pi^{**} \cos[k \cos\theta (y - x \tan\phi')] \qquad (82b)$$

where

$$|w_A|^* \equiv W_A \, \varepsilon \cos\theta = \varepsilon \tilde{W}_A \sin\sigma$$

$$S^{**} \equiv A/m$$

$$\Pi^{**} \equiv \frac{\tilde{c}}{m} \frac{\sin \mu}{\cos (\phi - \mu)^{+}}$$

$$\phi' \equiv |[|\phi| - \mu]| \quad \text{with sign of } \phi$$

$$\mu \equiv \cot^{-1} \beta_w \left[\beta_w \equiv \sqrt{\bar{W}^2 - 1}\right]$$

$$A = A \text{ for } \bar{W} < 1$$

$$\tilde{a} = m \frac{C' + GF'}{E' + GD'}$$

$$\tilde{b} = 0$$

$$\tilde{c} = \frac{\tilde{a}}{m} D' - F'$$

$$C' \equiv 2 \frac{\gamma-1}{\gamma+1} m - 2 [1 + (m-1) \cos^2 \phi]$$

$$D' \equiv (m-1) [1 + (m-1) \cos^2 \phi]$$

$$E' \equiv (m-1)^2 \sin \phi \cos \phi - \left[1 + \frac{3-\gamma}{\gamma+1} m\right] \tan \phi$$

$$F' \equiv 2 (m-1) \sin \phi \cos \phi$$

$$G \equiv \frac{1 - \beta_w \tan \phi}{\beta_w + \tan \phi} = \tan (\mu - \phi)$$

<u>Pressure Perturbation Field, $\bar{W} < 1$</u>. From Ribner [1] it can be shown that

$$\frac{\delta p}{p} = \varepsilon \frac{2 \gamma m \sec \phi}{(\gamma-1)-(\gamma+1) m} \Pi^{*} \cos [k \cos \theta (y - x \tan \phi') + \delta_p] \tag{83}$$

+Instead of cos $(\phi-\mu)$ Ribner has sin $(\phi+\mu)$. This is in error since the cos $(\phi-\mu)$ follows directly from his equations (32) and $\mu \equiv \cot^{-1} \beta_w$.

where Π^{*}, ϕ' and δ_p are the same as those defined for the "subsonic" velocity perturbation case.

Perturbation Pressure Field, $\bar{W} > 1$. From Ribner [1]

$$\frac{\delta p}{p} = \varepsilon \frac{2\ \gamma\ m\ \sec\ \phi}{(\gamma-1)-(\gamma+1)\ m}\ \Pi^{**} \cos\ [k\ \cos\ \theta\ (y-x\ \tan\ \phi')] \tag{84}$$

where Π^{**} and ϕ' are the same as those defined for the "supersonic" velocity perturbation case.

Shock - Wave Perturbation, $\bar{W} < 1$. From Ribner [1], the local deflection δx from the plane x=0 is given by

$$\delta x = \frac{\varepsilon}{k\ \cos\ \theta} \sqrt{\tilde{a}^2 + \tilde{b}^2}\ \cos\ [k\ \cos\ \theta\ y + \delta_{shock}] \tag{85}$$

where $\tilde{a}$, $\tilde{b}$ are the same as those defined for the "subsonic" velocity perturbation case and

where

$$\delta_{shock} \equiv \tan^{-1} (\tilde{a}/\tilde{b}).$$

Shock - Wave Perturbation, $\bar{W} > 1$. From Ribner [1]

$$\delta x = \frac{\varepsilon\ \tilde{a}}{k\ \cos\ \theta}\ \sin\ [k\ \cos\ \theta\ y] \tag{86}$$

where $\tilde{a}$ is the same as that defined for the "supersonic" velocity perturbation case.

Oblique Shock Solution

The following simple coordinate transformation will take the flow from Ribner's equivalent steady flow to that of an unsteady flow as viewed by an observer fixed to the shock front

$$\tilde{x} \equiv x \tag{87a}$$

and

$$\tilde{y} = y + V_{N_s} t \tag{87b}$$

or

$$x = \tilde{x}$$

and

$$y = \tilde{y} - V_{N_s} t.$$

where, from equation (74),

$$V_{N_s} = \tilde{W}_A [\cos\sigma - \sin\sigma \tan\theta]. \tag{74}$$

Thus $\tilde{x}$ is position measured normal to the unperturbed shock front with $\tilde{x} = 0$ representing the rest position of the shock and $\tilde{y}$ is position measured parallel to the shock front rest position; $\tilde{y} = 0$ is an arbitrary position.

The solution, in terms of the oblique shock properties, will now be given.

The Critical Incidence Angle. For the oblique shock, equation (80) is

$$\theta_{cr} = \pm \tan^{-1}\sqrt{\frac{(\gamma+1)(m-1)}{2m^2}} \tag{80}$$

where

$$m \equiv \frac{\frac{\gamma+1}{2} \tilde{M}_A^2 \sin^2\sigma}{1 + \frac{\gamma-1}{2} \tilde{M}_A^2 \sin^2\sigma} ,$$

$$\tilde{M}_A \equiv \frac{\tilde{W}_A}{a_A}$$

and

θ_{cr} is measured from the negative $\tilde{x}$-axis.

If the critical incidence angle is to be measured from the horizontal, then from Figure 14 ,

$$\tilde{\theta}_{cr} = 90 - \sigma - \theta_{cr} \quad . \tag{88}$$

<u>The Shear - Wave Incidence Angle</u>. If θ is measured from the horizontal instead of the negative $\tilde{x}$-axis then, as shown in Figure 14, θ becomes

$$\tilde{\theta} = 90 - \sigma - \theta \quad . \tag{89}$$

<u>Velocity Perturbation Field, $\tilde{\theta}_{cr_\ell} < \tilde{\theta} < \tilde{\theta}_{cr_u}$.</u>[+] Upon transforming to $\tilde{x}$ and $\tilde{y}$ and expressing the velocity perturbations in terms of streamline coordinates $\tilde{\xi}$ and $\tilde{\eta}$ (see Figure 14), equations (81) become

$$\frac{\tilde{w}}{|\tilde{w}_A|} = S^* \sin\sigma \cos(\tilde{\phi}-\delta) \cos[k \cos\theta(\tilde{y}-\tilde{x}\tan\phi - V_{N_s} t) + \delta_s] + \Pi^* \sin\sigma \cos[k\cos\theta(\tilde{y}-\tilde{x}\tan\phi' - V_{N_s} t) + \delta_p + \tilde{\phi} - \delta] \tag{90a}$$

[+] $\tilde{\theta}_{cr_\ell} = 90 - \sigma - |\theta_{cr}|$ and $\tilde{\theta}_{cr_u} = 90 - \sigma + |\theta_{cr}|$ where $|\theta_{cr}| = \tan^{-1}\sqrt{\frac{(\gamma+1)(m-1)}{2m^2}}$.

and

$$\frac{\tilde{w}'}{|\tilde{w}_A|} = S^* \sin\sigma \sin(\tilde{\phi}-\delta) \cos [k \cos\theta(\tilde{y}-\tilde{x} \tan\phi - V_{N_s} t) + \delta_s] + \Pi^* \sin\sigma \sin [k \cos\theta(\tilde{y}-\tilde{x} \tan\phi' - V_{N_s} t) + \delta_p + \tilde{\phi} - \delta] \quad (90b)$$

where

$$|\tilde{w}_A| \equiv \varepsilon\, W_A$$

$$\tilde{\phi} \equiv \phi + \sigma - 90$$

and where the other quantities are as previously defined for this case; i.e. $\bar{W} < 1$.

Velocity Perturbation Field, $\tilde{\theta} < \tilde{\theta}_{cr_\ell}$ or $\tilde{\theta} > \tilde{\theta}_{cr_u}$.

Performing these transformations for the "supersonic" case, equations (82) become

$$\frac{\tilde{w}}{|\tilde{w}_A|} = S^{**} \sin\sigma \cos(\tilde{\phi}-\delta) \cos [k \cos\theta(\tilde{y}-\tilde{x} \tan\phi - V_{N_s} t) + \delta_s] + \Pi^{**} \sin\sigma \cos [k \cos\theta(\tilde{y}-\tilde{x} \tan\phi' - V_{N_s} t) + \delta_p + \tilde{\phi} - \delta] \quad (91a)$$

and

$$\frac{\tilde{w}'}{|\tilde{w}_A|} = S^{**} \sin\sigma \sin(\tilde{\phi}-\delta) \cos [k \cos\theta(\tilde{y}-\tilde{x} \tan\phi - V_{N_s} t) + \delta_s] + \Pi^{**} \sin\sigma \sin [k \cos\theta(\tilde{y}-\tilde{x} \tan\phi' - V_{N_s} t) + \delta_p + \tilde{\phi} - \delta] \quad (91b)$$

where

$$|\tilde{w}_A| = \varepsilon\ W_A$$

$$\tilde{\phi} = \phi + \sigma - 90$$

and where the other quantities are as previously defined for this case; i.e. $\bar{W} > 1$.

<u>Pressure Perturbation Field, $\tilde{\theta}_{cr_\ell} < \tilde{\theta} < \tilde{\theta}_{cr_u}$.</u> Upon transforming to $\tilde{x}$ and $\tilde{y}$, equation (83) becomes

$$\frac{\delta p}{p} = \varepsilon \frac{2\ \gamma\ m\ \sec\ \phi}{(\gamma-1)-(\gamma+1)\ m}\ \Pi^{*}\ \cos\ [k\ \cos\ \theta(\tilde{y}-\tilde{x}\ \tan\ \phi' - V_{N_s} t) + \delta_p] \tag{92}$$

where Π^*, ϕ' and δ_p are the same as those defined for the "subsonic" velocity perturbation case.

<u>Pressure Perturbation Field, $\tilde{\theta} < \tilde{\theta}_{cr_\ell}$ or $\tilde{\theta} > \tilde{\theta}_{cr_u}$.</u>

After transforming to $\tilde{x}$ and $\tilde{y}$, equation (84) becomes

$$\frac{\delta p}{p} = \varepsilon \frac{2\ \gamma\ m\ \sec\ \varphi}{(\gamma-1)-(\gamma+1)\ m}\ \Pi^{**}\ \cos\ [k\ \cos\ \theta(\tilde{y}-\tilde{x}\ \tan\ \phi' - V_{N_s} t)] \tag{93}$$

where Π^{**} and ϕ' are the same as those defined for the "supersonic" velocity perturbation case.

<u>Shock - Wave Perturbation, $\tilde{\theta}_{cr_\ell} < \tilde{\theta} < \tilde{\theta}_{cr_u}$.</u> Transforming x to $\tilde{x}$, δx to $\delta\tilde{x}$ and y to $\tilde{y} - V_{N_s} t$, equation (85) becomes

$$\delta\tilde{x} = \frac{\varepsilon}{k \cos \theta} \sqrt{\tilde{a}^2 + \tilde{b}^2} \quad \cos [k \cos \theta(\tilde{y}-V_{N_s} t) + \delta_{shock}] \tag{94}$$

where $\tilde{a}$, $\tilde{b}$ and δ_{shock} are those defined for equation (85).

<u>Shock - Wave Perturbation, $\tilde{\theta} < \tilde{\theta}_{cr_\ell}$ or $\tilde{\theta} > \tilde{\theta}_{cr_u}$</u>. Upon transforming to $\tilde{x}$ and $\tilde{y}$, equation (86) becomes

$$\delta\tilde{x} = \frac{\varepsilon\, \tilde{a}}{k \cos \theta} \sin [k \cos \theta(\tilde{y} - V_{N_s} t)] \tag{95}$$

where $\tilde{a}$ is the same as that defined for equation (86).

The most important properties of the perturbed flow field downstream of the oblique shock front have been presented. However, there remains one property of interest that is normally viewed by a stationary observer on a surface inclined at the angle δ - the property is pressure and the observer is usually a small transducer which is taken herein to be much smaller than the shortest wavelength to be considered. Thus, in the next section the pressure at the transducer will be related to the shear-wave w_A.

<u>Perturbed Pressure at a Stationary Transducer</u>. The system to be treated is shown in Figure 15. It can be shown that the surface wave number k_{sur} is related to the shear - wave wave number k by

$$k_{sur} = \frac{\cos (\sigma+\phi' -\delta) \cos \theta}{\cos \phi'} \; k \tag{96}$$

or since the wavelength and wave number are simply related ($k\lambda = 2\pi = k_{sur}\lambda_{sur}$)

$$\lambda_{sur} = \frac{\cos \phi'}{\cos (\sigma+\phi'-\delta) \cos \theta} \lambda \tag{97}$$

where λ is the shear - wave wavelength.

The period of oscillation is

$$P = \frac{2\pi}{k \cos \theta \, V_{N_s}} \tag{98}$$

and therefore the frequency is

$$f = 1/P = \frac{k \cos \theta}{2\pi} V_{N_s}$$

or substituting for V_{N_s} from equation (74)

$$f = \frac{\tilde{W}_A}{\lambda} \cos (\sigma+\theta) \tag{99}$$

It should be noted that $f = 0$ when $\theta = 90 - \sigma$; i.e. the pressure wave fronts are stationary.

The surface pressure wave speed, $V_{p_{sur}}$, is

$$V_{p_{sur}} = \frac{\lambda_{sur}}{P}$$

or

$$V_{p_{sur}} = \frac{\cos \phi' \cos (\sigma+\theta)}{\cos \theta \cos (\sigma+\phi'-\delta)} \tilde{W}_A \tag{100}$$

or, if $V_{p_{sur}}$ is expressed in terms of the local isentropic speed of sound,

$$\frac{V_{p_{sur}}}{a} = \frac{\cos \phi' \cos (\sigma+\theta)}{\cos \theta \cos (\sigma+\phi'-\delta)} \tilde{M}_A \frac{a_A}{a} \tag{101}$$

where

$$\tilde{M}_A \equiv \frac{\tilde{W}_A}{a_A} \quad ,$$

$$\frac{a_A}{a} = \sqrt{\frac{T_A}{T}}$$

and

$\frac{T_A}{T}$ is given by equation (54) with $T = T_2$, $T_A = T_1$ and $\tilde{M}_A \sin\sigma = \overline{U}_1$.

Only the root-mean-square of the pressure remains to be evaluated. Taking the rms of equations (92) and (93) yields

$$(\delta p)_{rms} = \frac{2\ \gamma\ m \sec\phi}{(\gamma+1)m-(\gamma-1)}\ \Pi p \tag{102}$$

where Π is either Π^* or Π^{**} depending on the value of $\tilde{\theta}$; i.e. whether $\overline{W} < 1$ or $\overline{W} > 1$.

The "sound" pressure level is, by definition,

$$SPL = 20 \log_{10} \frac{(\delta p)_{rms}}{p_{ref}}\ \text{dB} \tag{103}$$

where $p_{ref} = 2 \times 10^{-4}\ \mu$ bar $\approx 0.290 \times 10^{-8}$psi.

<u>Computations</u>. To illustrate a computational method, γ, a_A (or T_A), $\tilde{M}_A$, σ, θ, ε and k will be treated as independent variables. Numerical computations using the following steps are given in Appendix D.

1. Select a temperature T_A.
2. Select a working fluid, i.e. γ.
3. Select a Mach number $\tilde{M}_A$.

4. Select an oblique shock angle σ.

5. Select a shear wave incidence angle θ.

6. Select a shear wave amplitude ε.

7. Select a wave number k.

8. Compute m as follows (reference 8)

$$m = \frac{U_A}{U} = \frac{\rho}{\rho_A} = \frac{(\gamma+1)\ \overline{U}_A^2}{2 + (\gamma-1)\ \overline{U}_A^2} \tag{104}$$

where

$$\overline{U}_A \equiv \tilde{M}_A \sin \sigma$$

9. Compute a as follows (reference 8)

$$a = a_A \sqrt{T/T_A}$$

$$\frac{T}{T_A} = \frac{\left[2 + (\gamma-1)\ \overline{U}_A^2 \right] \left[\frac{2\gamma}{\gamma-1}\ \overline{U}_A^2 - 1 \right]}{\frac{(\gamma+1)^2}{(\gamma-1)}\ \overline{U}_A^{\ 2}} \tag{105}$$

10. Compute δ as follows (reference 8)

$$\delta = \sigma - \tan^{-1}\left[\frac{1}{m} \tan \sigma \right] \tag{106}$$

11. Compute ϕ as follows (definition of terms following equations (81))

$$\phi = \tan^{-1}\ [m \tan \theta] \tag{107}$$

12. Compute θ_{cr} from equation (80), i.e.

$$|\theta_{cr}| = \tan^{-1}\sqrt{\frac{(\gamma+1)(m-1)}{2m^2}} \tag{108}$$

13. Test for type of solution; e.g.

a. If $-|\theta_{cr}| < \theta < |\theta_{cr}|$ then "subsonic" solution applies. Go to Step 14.

b. If $-90 \leq \theta < |\theta_{cr}|$ or $|\theta_{cr}| < \theta \leq 90$ then "supersonic" solution applies. Go to Step 29.

14. Compute β as follows

$$\beta \equiv \sqrt{1 - \bar{U}^2} \tag{109}$$

where

$$\bar{U} \equiv U/a \tag{110}$$

$$U = \frac{1}{m} \tilde{W}_A \sin \sigma \ . \tag{111}$$

15. Compute β_w as follows

$$\beta_w \equiv \sqrt{1 - \bar{W}^2} \tag{112}$$

where

$$\bar{W} = \bar{U}/\cos \phi \ . \tag{113}$$

16. Compute C, D, E and F as follows

$$C = \left[\frac{\gamma-1}{\gamma+1} + \frac{3-\gamma}{\gamma+1} m\right] \tan \phi - \left[(m-1)^2 + \frac{2(m-1)}{\gamma+1}\right] \sin \phi \cos \phi \tag{114}$$

$$D = \frac{\beta_w}{\beta^2} (m-1) [1 + (m-1) \cos^2 \phi] \tag{115}$$

$$D' = \frac{\beta^2}{\beta_w} D \tag{116}$$

$$E = 2\left[1 - \frac{\gamma-1}{\gamma+1} m\right] + 2(m-1)\frac{\beta_w^2 \cos^2 \phi}{\beta^2} \tag{117}$$

$$F = \frac{\beta_w}{\beta^2}[2\ (m-1) \sin \phi \cos \phi] \tag{118}$$

$$F' = \frac{\beta^2}{\beta_w} F \tag{119}$$

17. Compute $\tilde{a}$, $\tilde{b}$, $\tilde{c}$ and $\tilde{d}$ as follows

$$\tilde{a} = m \frac{CE + DF}{C^2 + D^2} \tag{120}$$

$$\tilde{b} = m \frac{CF - DE}{C^2 + D^2} \tag{121}$$

$$\tilde{c} = \frac{\tilde{a}}{m} D' - F' \tag{122}$$

$$\tilde{d} = \frac{\tilde{b}}{m} D' \tag{123}$$

18. Compute A and B as follows

$$A = \sec \phi + 2(m-1) \cos \phi + \frac{\tilde{a}}{m}(m-1)^2 \sin \phi \tag{124}$$

$$B = \frac{\tilde{b}}{m}(m-1)^2 \sin \phi \tag{125}$$

19. Compute ϕ', δ_s and δ_p as follows

$$\phi' = -\tan^{-1}\left[\frac{\bar{U}^2 \tan \phi}{\beta^2}\right] \tag{126}$$

$$\delta_s = \tan^{-1}\left[\frac{-B}{A}\right] \tag{127}$$

$$\delta_p = \tan^{-1}\left[\frac{\tilde{c}\,\beta_w - \tilde{d} \tan \phi}{\tilde{d}\,\beta_w + \tilde{c} \tan \phi}\right] \tag{128}$$

20. Compute S^* as follows

$$S^* = \frac{1}{m}\sqrt{A^2 + B^2} \tag{129}$$

21. Compute Π_o^* (the subscript zero indicates that Π^* is being evaluated at $x = \tilde{x} = 0$) as follows

$$\Pi_o^* = \frac{1}{m\beta}\sqrt{\tilde{c}^2 + \tilde{d}^2} \tag{130}$$

22. Compute the ratio of the refracted shear wave velocity amplitude to the incident shear wave velocity amplitude; i.e.

$$\frac{[|\tilde{w}_s^2 + \tilde{w}_s'^2|]^{1/2}}{|\tilde{w}_A|} = S^* \sin\sigma \quad . \tag{131}$$

22. Compute the ratio of the generated pressure wave velocity amplitude at $\tilde{x} = 0$ to the incident shear wave velocity amplitude; i.e.

$$\frac{[|\tilde{w}_p^2 + \tilde{w}_p'^2|]^{1/2}}{|\tilde{w}_A|} = \Pi_o^* \sin\sigma \quad . \tag{132}$$

23. Compute the rms pressure just after the shock by using equations (102) and (130); i.e.

$$(\delta p)_{rms} = \varepsilon \frac{\sqrt{2}\ \gamma\ m\ |\sec\phi|}{(\gamma+1)\ m - (\gamma-1)}|\Pi_o^*|\ p \tag{133}$$

where

$$\frac{p}{p_A} = \frac{2\gamma}{\gamma+1}\bar{U}_A^2 - \frac{\gamma-1}{\gamma+1} \quad \text{(reference 8 or Equation (64))} \tag{134}$$

$$p_A = 1 \text{ atm} = 14.696 \text{ psia} \tag{135}$$

24. Compute the sound pressure level just behind the shock, i.e. at $\tilde{x} = 0$, using equation (103) as follows

$$SPL_o = 20 \log_{10} \frac{(\delta p)_{rms}}{p_{ref}} \tag{136}$$

where

$$p_{ref} = 0.29 \times 10^{-8} \text{ psi.} \tag{137}$$

25. Compute the surface wave number k_{sur} for the pressure waves by using equation (96) as follows

$$k_{sur} = \frac{\cos(\sigma + \phi' - \delta) \cos\theta}{\cos\phi'} k \; . \tag{96}$$

26. Compute the pressure wave frequency f from equation (99) as follows

$$f = \frac{\tilde{M}_A \, k \, a_A}{2\pi} \cos(\sigma + \theta) \tag{138}$$

27. Compute the ratio of surface pressure wave velocity to the local speed of sound from equation (101) as follows

$$\frac{V_{p_{sur}}}{a} = \frac{\cos\phi' \cos(\sigma + \theta)}{\cos\theta \cos(\sigma + \phi' - \delta)} \tilde{M}_A \frac{a_A}{a} \; . \tag{101}$$

28. Compute the shock front displacement amplitude $|\delta\tilde{x}|$ and phase δ_{shock} as follows

$$|\delta\tilde{x}| = \frac{\varepsilon}{\bar{k}\cos\theta} \sqrt{\tilde{a}^2 + \tilde{b}^2} \tag{139}$$

and

$$\delta_{shock} = \tan^{-1}(\tilde{a}/\tilde{b}). \tag{140}$$

The steps that follow are for the "supersonic" solution and they correspond to the foregoing Steps (14) through (28).

29. Compute β as follows

$$\beta = \sqrt{1 - \bar{U}^2} \; . \tag{109}$$

30. Compute β_w as follows

$$\beta_w = \sqrt{\bar{W}^2 - 1} \tag{141}$$

where

$$\bar{W} = \bar{U}/\cos \phi \; . \tag{113}$$

31. Compute C', D', E', F' and G as follows

$$C' = 2 \, \frac{\gamma-1}{\gamma+1} \, m - 2 \, [1 + (m-1) \cos^2 \phi] \tag{142}$$

$$D' = (m-1) \, [1 + (m-1) \cos^2 \phi] \tag{143}$$

$$E' = (m-1)^2 \sin \phi \cos \phi - \left[1 + \frac{3-\gamma}{\gamma+1} \, m \right] \tan \phi \tag{144}$$

$$F' = 2 \, (m-1) \sin \phi \cos \phi \tag{145}$$

$$G' = \tan \, (\mu - \phi) \tag{146}$$

where

$$\mu = \tan^{-1} \, (1/\beta_w) \; . \tag{147}$$

32. Compute $\tilde{a}$ and $\tilde{c}$ as follows

$$\tilde{a} = m \, \frac{C' + G'F'}{E' + G'D'} \tag{148}$$

$$\tilde{c} = \frac{\tilde{a}}{m} \, D' - F' \; . \tag{149}$$

33. Compute A as follows

$$A = \sec \phi + 2\,(m-1)\cos \varphi + \frac{\tilde{a}}{m}\,(m-1)^2 \sin \phi . \qquad (150)$$

34. Compute ϕ' as follows

$$\phi' = |[|\phi| - \mu]| \text{ with sign of } \phi$$

or

$$\phi' = \frac{\phi}{|\phi|}\,|[|\phi| - \mu]| \qquad (151)$$

35. Compute S^{**} as follows

$$S^{**} = A/m \qquad (152)$$

36. Compute Π^{**} as follows

$$\Pi^{**} = \frac{\tilde{c}}{m}\,\frac{\sin \mu}{\cos\,(\phi-\mu)} \qquad (153)$$

37. From equations (91) compute the ratio of the refracted shear wave velocity amplitude to the incident shear wave velocity amplitude; i.e.

$$\frac{[|\tilde{w}_s^2 + \tilde{w}_s'^2|]^{1/2}}{|\tilde{w}_A|} = S^{**} \sin \sigma . \qquad (154)$$

38. From equations (91) compute the ratio of the generated pressure wave velocity amplitude to the incident shear wave velocity amplitude, i.e.

$$\frac{[|\tilde{w}_p^2 + \tilde{w}_p'^2|]^{1/2}}{|\tilde{w}_A|} = \Pi^{**} \sin \sigma . \qquad (155)$$

39. Compute the rms pressure by using equations (102) and (153); i.e.

$$(\delta p)_{rms} = \varepsilon \frac{\sqrt{2}\ \ \gamma\ m\ \sec\ \phi}{(\gamma+1)\ m\ -\ (\gamma-1)}\ \Pi^{**}\ p \tag{156}$$

where p is given by equation (134).

40. Compute the sound pressure level by using equation (103) as follows

$$SPL = 20\ \log_{10}\ \frac{(\delta p)_{rms}}{p_{ref}} \tag{157}$$

where

$$p_{ref} = 0.29 \times 10^{-8}\ psi. \tag{137}$$

41. Compute the surface wave number k_{sur} for the pressure waves by equation (96) as follows

$$k_{sur} = \frac{\cos\ (\sigma+\phi' - \delta)\ \cos\ \theta}{\cos\ \phi'}\ k\ \ . \tag{96}$$

42. Compute the pressure wave frequency f from equation (99) as follows

$$f = \frac{\tilde{M}_A\ k\ a_A}{2\pi}\ \cos\ (\sigma+\theta)\ . \tag{138}$$

43. Compute the ratio of surface pressure wave velocity to the local speed of sound from equation (101) as follows

$$\frac{V_{p_{sur}}}{a} = \frac{\cos\ \phi'\ \ \cos\ (\sigma+\theta)}{\cos\ \theta\ \cos\ (\sigma+\varphi' - \delta)}\ \tilde{M}_A\ \frac{a_A}{a}\ . \tag{101}$$

44. Compute the shock wave displacement amplitude $|\delta\tilde{x}|$ as follows

$$|\delta\tilde{x}| = \frac{\varepsilon\ \tilde{a}}{k \cos\theta} \quad . \tag{158}$$

A FORTRAN IV program to make these computations is given in Appendix C.

Results

The shear wave-shock front interaction will be illustrated for the same two Saturn V interstage flare angles, namely, $\delta = 8^\circ\ 58'$ and $\delta = 16^\circ\ 44'$.

Appendix D contains computed data for the following cases:

$\tilde{M}_A$	1.50	2.00	2.50	3.00	1.75	2.00	2.50	3.00
δ	8.98	8.96	8.96	8.97	16.73	16.73	16.74	16.75

The data column headings are defined as:

THETA - , the shear wave incidence angle, in degrees

PHI-PR - ϕ', equation (126) or (151)

WS/WA - shear wave amplitude ratio, equation (131) or (154)

DEL S - δ_S, equation (127)

WP/WA - pressure wave amplitude ratio, equation (132) or (155)

DEL P - δ_p, equation (128)

(DP)RMS - as defined by equation (133) or (156)

KSUR/K - k_{sur}/k, equation (96)

VSUR/A - $V_{p_{sur}}/a$, equation (101)

ADX/EL - as defined by equation (139) or (158)

DEL SH - δ_{shock}, equation (140)

It should be noted that there is at least one shear-wave incidence angle for each case considered that produces shock front resonance.

CHAPTER III

EXPERIMENTAL INVESTIGATIONS

A model experiment was designed to study the interaction of sound waves and an oblique shock front. From the analysis of this phenomenon presented in Chapter 2 it is clear that the sound field after the shock will depend on the initial Mach number, the turning angle (oblique shock angle) and the angle of incidence of the plane sound waves. The experimental system to be described used a fixed Mach number, $M_1 \approx 1.6$, fixed incidence angle, $\theta = 90 - \sigma$, and a variable turning angle, δ. The sound pressure level difference across the shock front for these conditions is shown in Figure 16 .

Instrumentation and Equipment

Model Wind Tunnel

The low speed supersonic wind tunnel shown schematically in Figure 17 was built for these tests. Atmospheric air entered the tunnel by flowing around the horn, down a 24-inch long calming section and then through a 16-to-1 smooth contraction. After passing through the tunnel the air entered a vacuum chamber. The area ratio at the wedge (model) was 1.531 but the wall boundary layers reduced this to an effective area ratio of 1.250 with a corresponding Mach number of 1.6.

Wedge

The wedge was mounted on a circular holder with the wedge leading edge at the holder's axis of rotation (see Figure 17). A half-degree incremented protractor coupled with a pointer on the holder indicated the wedge angle-flow turning angle δ-to within a quarter of a degree.

A static pressure tap 0.0135-inch in diameter was provided 0.2-inch from the leading edge.

Static Pressure Probe

A circular probe holder formed the tunnel wall below the wedge (see Figure 17) and its axis of rotation was also at the wedge leading edge. As shown in Figure 18 , the static pressure tap was located 0.265-inch off center and, therefore, it was possible to measure the static pressure along a 180-degree circular arc. A 0-50 psi Heise Bourdon gauge was used as a pressure transducer.

Acoustic Pressure Probes

Two acoustic pressure probes were used. The one shown in Figure 17 consisted of a one-inch long 0.5 mm (0.009-inch I.D.) Brüel and Kjaer Type DB 0240 probe mounted on a B&K Type 4134 condenser microphone cartridge. A vacuum tight extension was built to couple the microphone cartridge and a B&K Type 2615 cathode follower. A B&K Type 2107 frequency analyzer was used to determine the root-mean-square sound pressure level.

The probe tip mated with a 0.009-inch hole cast into the probe holder thereby producing a smooth surface at the sensing port. The port, as shown in Figure 18, was located 0.345-inch off the center of rotation, and 20.5 degrees behind the static pressure tap. The acoustic pressure, therefore, could be measured along 180 degrees of a circular arc. This path intersected the oblique shock front at right angles.

It should be noted that both the static pressure and the acoustic pressure are sensed at ports that are normal to the flow direction and beneath a viscous boundary layer. Since there is a subsonic region next to the wall, the increase in time-mean pressure due to the shock is felt upstream of the shock front. In an attempt to circumvent the boundary-layer effects a second probe was developed.

As shown in Figure 19 this probe extended from the calming chamber to the vacuum chamber. It was a B&K Type DB 0241 (1 mm O.D.) probe that was modified by plugging the tip, drilling a 0.0135-inch hole in the side of the tip and adding a length of tubing to the other end of the plug. The probe could traverse a one-inch path in the flow direction and its axial position was set to within 0.001-inch with a micrometer. The boundary layer above this port was much thinner and the acoustic pressure so determined is believed to be much more indicative of that in the flow.

The same microphone cartridge and cathode follower were used with this probe but a different extension was required.

Sound Generator

The sound field was generated by an Altec 802D driver loudspeaker in conjunction with the conical horn - cutoff frequency of 450 Hz - shown in Figure 17 . A Hewlett-Packard Model 206A audio signal generator acted as the electrical power source. A Marantz Model 9 power amplifier was required to increase the power output to levels up to 30 watts. The power to the driver was monitored by a Fluke Model 102R VAW meter and the frequency was measured with a Hewlett-Packard Model 5212A electronic counter.

Regulated 60-Hz, 117-volt power was supplied for all electronic systems by a Sorensen Model 2501 A.C. line voltage regulator.

Experimental Procedure

The following is a synopsis of the experimental procedure used for taking all of the data:

1. The electronic systems were turned on and allowed to stabilize for at least eight hours. They were calibrated just before making a data run.
2. The vacuum system was started and run for at least 30 minutes before taking data.
3. The pressure gauge zero was checked against a high vacuum.
4. The desired turning angle was set by rotating the wedge holder.

5. The acoustic pressure port was positioned upstream of the shock front.

6. Power was supplied to the driver at the desired frequency. (The system could be tuned to obtain higher SPL's by making slight changes in the horn's axial location and in the driving frequency.)

7. The power was varied until the desired SPL was obtained. (Since the flow noise level was quite high the impressed sound pressure was "viewed" in an eight percent band about the driver frequency by operating the B&K 2107 in the frequency analysis mode.)

8. The driver frequency, current, voltage and power were measured.

9. The flow field was traversed by either rotating the probe holder or inserting the linear motion acoustic pressure probe.

10. Sound pressure levels were recorded for each angular or axial position by time averaging the output from the driver frequency band with a B&K Type 2417 random signal voltmeter. (Averaging times of up to 100 seconds were required when the level was close to the random amplitude background noise.)

11. Static pressure was recorded at each angular position of the probe holder.

12. Finally, background SPL's in the same frequency band were recorded. (The field was probed without power to the driver.)

Results

Fluctuating pressure data were taken for stationary oblique shock fronts irradiated with sound waves. Since two different probes were used to obtain these data typical results will now be presented for each probe.

Tunnel Wall Tap Data

Figure 20 shows a typical fluctuating pressure distribution with and without an impressed sound field. Assuming that the background pressure field and the impressed sound pressure field are not correlated, the sound pressure distribution is easily obtained. It is shown in Figure 21 together with the static pressure distribution.

It should be noted that the static pressure starts its rise some 30 degrees before the predicted inviscid shock front position. This rather steep adverse pressure gradient undoubtedly thickens the boundary layer before the shock which in turn gives rise to a possible separated flow below the primary shock and curved oblique shocks at the corners formed by the intersection of the primary shock front and the upper and lower tunnel walls. Thus the unsteady pressure component was sensed beneath a very complex flow region and a reasonable comparison with the predicted acoustic pressure level distribution is not to be expected.

The dip in the sound pressure curve prior to the primary shock front position was characteristic of all data taken. As shown in Figure 16 attenuation of the sound pressure by shock interaction was predicted and this premature dip may be due to, at least in part, an interaction of the sound waves and the corner shocks.

The rise in the pressure level near the shock front is to be expected since the shock is oscillating relative to the pressure transducer with the same frequency as the impressed sound waves. However the level was expected to decrease away from the shock and be approximately 9 dB less than the sound pressure level before the shock. As shown in Figure 21, this did not occur and it can only be said that there was no appreciable change in level.

In an attempt to measure the acoustic pressure through a much thinner and hopefully less complex boundary layer the side tap needle probe was installed and the following data were obtained.

Needle Probe Data

Figure 22 is a composite of the pressure data obtained with the needle probe. The parameter is the power supplied to the acoustic driver. The premature dip is evident for the high power run but it is apparently absent for the low power run. The increase in sound pressure level as the shock front is approached is much more evident with this probe. Increases of 17.5 to 23.0 dB from the initial level were obtained. A characteristic not found with the wall tap probe was the sharp drop in level after the maximum, a subsequent rise again, and then a gradual decrease in sound pressure level.

This second dip is felt to be due to the relative position of the oscillating shock and the acoustic pressure tap. If the peak-to-peak amplitude of the shock displacement is less than the pressure tap diameter then the apparent acoustic pressure should drop to a relative minimum when the shock's mean position is in the center of the tap.

Finally, it should be noted that the sound pressure level downstream of the shock did not go below its initial level and for the low-powered and non-powered cases the minimum levels were at least five decibles higher than their initial levels.

Since a large increase in the pressure level at the shock front was found for the case of natural pressure fluctuations at a frequency of 1818 Hz, a frequency analysis was performed to determine the effect of the shock front interaction with these fluctuations at other frequencies. To perform this analysis the pressure, as detected by the uncalibrated probe, was tape recorded for two cases: (1) probe at the shock front and (2) probe in the same position but with no shock present (the model was removed). Figure 23 shows the results and, for clarity, the difference of the two spectra is shown in Figure 24.

CHAPTER IV

DISCUSSION OF RESULTS

Since there are two different phenomena treated in this study the discussion is divided into a section on sound wave-shock front interaction and one on shear wave-shock front interaction. Finally, an appraisal of the status of each of the theoretical analyses is presented.

Sound Wave-Shock Front Interaction

Analytical Study

The first part of this discussion is based on the results given in Appendix B. Figures 8 and 9 will be helpful for visualizing the orientation of the incident sound wave--as given by θ (THETA), the refracted sound wave--as given by ϕ' (PHIP), and the generated entropy-vorticy wave--as given by β (BETA). In looking at these data note in particular the behavior of the ratio of the amplitude of the acoustic pressures in Regions 1 and 2 (PP2/PP1).

Although the analysis was for a plane sound wave it will be more instructive to think of the oblique shock front being simultaneously irradiated with equal amplitude plane sound waves with orientations from $\theta = -90°$ to $\theta = 90°$. Since the governing equation is linear these fields will superpose. Look at the sound field downstream of the shock front. For the case of $M_1 = 1.50$ and $\delta = 8.98°$, the sound pressure is amplified by the shock when $-90° \leq \theta < -40°$, attenuated when $-35° < \theta < 70°$, and amplified again when $75° < \theta < 90°$. Contrast this with the case of $M_1 = 3.00$

and $\delta = 16.75°$ where there is amplification for all orientations but $-5° < \theta < 20°$ and where shock resonance occurs at $\theta \approx 53°$.

Since shock resonance was predicted for all but one of the cases considered, it is interesting to compare the incident sound wave angle which produces resonance, θ_r, with the angle of the flow before the shock, $\theta_f = 90 - \sigma$.

δ	M_1	θ_f	θ_r	δ	M_1	θ_f	θ_r
8.98	1.50	35.6	--	16.74	1.75	32.5	82
8.96	2.00	51.8	82	16.73	2.00	42.2	74
8.97	2.50	59.1	68	16.74	2.50	51.1	63
8.98	3.00	63.5	57	16.75	3.00	55.9	53

For relatively low Mach numbers the sound ray is almost parallel to the shock front and moving leftward; however, at higher Mach numbers the sound ray aligns with the flow. Thus plane sound waves traveling in the flow direction would be strongly amplified for the case of $M_1 = 3.00$ and $\delta = 16.75°$.

Although the change in acoustic pressure across the shock front is independent of frequency, the peak-to-peak shock front displacement, $|2\alpha|$, is inversely proportional to frequency since

$$|2\alpha| = |PPAMPL| \frac{U_{0_1}}{\omega_1} \quad .$$

Experimental Study

The experimental study highlighted the difficulty of interpreting fluctuating pressure data from a supersonic flow. It can be said with certainty that the impressed sound field interacted with the oblique shock and caused significantly amplified pressure fluctuations near the shock front. However, the shock process in this miniature system was too complex to permit a comparison of predicted and measured sound pressure levels. A decrease of about nine decibels was predicted but no appreciable change was found except in the vicinity of the shock front.

The most interesting data to come from this study was that which showed strong amplification of the natural pressure fluctuations in the flow at the shock front. Figure 24 shows an amplification of about 26 dB for frequencies from 20 to 2000 Hz and definitely indicates that the shock motion contains all the frequencies present in the shockless flow.

This points up a clear need for the accurate determination of supersonic-tunnel sound fields if vehicle surface pressure data are to be properly interpreted. The analyst must be able to separate tunnel sound effects from vehicle self noise effects.

Shear Wave-Shock Front Interaction

The results given in Appendix D show an erratic behavior for most of the computed properties. In particular, the transition from the "supersonic" to the "subsonic" solution looks suspicious for ϕ' and δ_p.

Since the results are in doubt it will only be noted that shock resonance is predicted for all eight cases and that the results for positive θ are similar to those of Ribner.

Status of the Analytical Studies

The analysis of plane sound wave interaction with oblique shock fronts has been independently performed by two of the authors. Although the resulting forms of the solution differed slightly the predicted data agreed. Thus it is felt that this solution is reliable.

The shear wave analysis is not ready for application. There were two functional differences between Ribner's development and the one presented herein that have not been resolved. Further, an independent check of this analysis has not been obtained.

CHAPTER V

CONCLUSIONS AND RECOMMENDATIONS

From the plane sound wave-oblique shock front interaction study it is concluded that:

1. There exists, under suitable conditions, a sound wave incidence angle such that shock wave resonance will occur.

2. The amplification of plane sound waves by the excited shock is independent of the frequency of the sound.

3. The amplitude of the shock front displacement is inversely proportional to the sound frequency and directly proportional to the magnitude of the sound particle velocity.

4. The analysis appears to be reliable enough for application.

5. Oblique shock fronts may be excited by an impressed sound field and/or by a natural sound field.

From the shear wave-oblique shock front interaction analysis it is concluded that:

1. There appears to be a shear wave incidence angle such that shock front resonance is produced.

2. The predicted results seem to be erratic in behavior and are, at this stage of development, suspect.

3. The analysis is not reliable enough for application.

As a logical extension of the sound wave-shock front study it is recommended that:

1. The analysis should be applied to a multiple shock field of finite

extent with the objective being the prediction of the far sound field associated with specific sound wave irradiation.

2. An experiment should be designed to confirm the prediction of shock resonance.

To put the shear wave-shock front analysis on a firm base it is recommended that:

1. The study should be repeated by another analyst.

2. An experiment should be designed to confirm the predicted downstream velocity and pressure field.

APPENDICES

APPENDIX A

FORTRAN IV PROGRAM FOR SOUND WAVE - SHOCK FRONT INTERACTION

```
              PROGRAM MAIN(INPUT,OUTPUT,TAPE5=INPUT,TAPE6=OUTPUT)
      C            THE EFFECT OF PLANE SOUND WAVES ON A STATIONARY OBLIQUE SHOCK
      C            T1 IS THE ABSOLUTE TEMPERATURE IN REGION 1 IN DEGREES RANKINE
003           0    T1=518.7
      C            SS1 IS THE SPEED OF SOUND IN REGION 1
004           0    PLF=((1.4*53.35)*32.174)*T1
010           0    SS1=SQRT(PLF)
      C            THE WORKING FLUID IS DRY AIR
      C            G IS THE RATIO OF SPECIFIC HEATS
012           0    G=1.4
014           0    SHR=(G+1.0)/(G-1.0)
017           0    PI=3.1415926536
      C            S1 IS THE MACH NUMBER IN REGION 1
      C            SIGD IS THE OBLIQUE SHOCK ANGLE IN DEGREES
      C            DELTAD IS THE FLARE (TURNING) ANGLE IN DEGREES
021       100 0    READ(5,101) S1,SIGD,DELTAD
033       101 0    FORMAT(3F10.3)
033           0    SIGR=SIGD*PI/180.0
035           0    A=S1*S1*(SIN(SIGR))*(SIN(SIGR))
      C            RR21 = (DENSITY 2)/(DENSITY 1)
043           0    RR21=((G+1.0)*A)/(2.0+(G-1.0)*A)
      C            PP21 = (PRESSURE 2)/(PRESSURE 1)
052           0    PP21=1.0+G*A*(1.0-(1.0/RR21))
057           0    DELTAR=SIGR-ATAN((SIN(SIGR)/COS(SIGR))/RR21)
071           0    DELTAD=DELTAR*180.0/PI
      C            T2 IS THE ABSOLUTE TEMPERATURE IN REGION 2 IN DEGREES RANKINE
073           0    T2=T1*(PP21/RR21)
      C            SS2 IS THE SPEED OF SOUND IN REGION 2
076           0    SJF=((T2*1.4)*53.35)*32.174
101           0    SS2=SQRT(SJF)
      C            S2 IS THE MACH NUMBER IN REGION 2
103           0    S2= S1*(COS(SIGR)/COS(SIGR-DELTAR))*(SS1/SS2)
      C            PHIR IS THE ANGLE PHI IN RADIANS
116           0    PHIR=PI/2.0+DELTAR-SIGR
      C            THE FOLLOWING ARE CONVENIENT ABBREVIATIONS
122           0    R = RR21
123           0    AX=S1*SIN(SIGR)
126           0    AXX=AX*AX
127           0    SX=SS2/SS1
131           0    SXX=SX*SX
132           0    WRITE(6,108) S1,DELTAD,SIGD,S2
146       108 0    FORMAT(1H1///20X,4HM1 =,F6.2,2X,7HDELTA =,F6.2,2X,7HSIGMA =,
              1           F6.2,2X,4HM2 =,F5.2,2X,9HTHETACP =,9X,
              2           9HTHETACN =/)
146           0    WRITE(6,109)
152       109 0    FORMAT(20X,90(1H-)/20X,5HTHETA,3X,4HBETA,5X,4HPHIP,5X,
              1           7HPP2/PP1,4X,6HSPL2/1,3X,7HU02/U01,3X,5HUEVW2,4X,
              2           5HSPRCU,4X,6HAT/UP1,3X,6HPPAMPL/20X,90(1H-))
      C            THD IS THETA, ANGLE OF INCIDENT SOUND WAVE IN DEGREES
152           0    THD=-95.0
154       110 0    THD=THD+5.0
156           0    IF(THD.GT.90.0) GO TO 100
161           0    THR=THD*PI/180.0
162           0    BETAR=ATAN((S1*SIN(THR)*COS(SIGR)*COS(PHIR))/((SIN(PHIR))*(1.0
              1         +S1*SIN(SIGR)*COS(THR))))
211           0    BETAD=BETAR*180.0/PI
      C            SUB-ROUTINE FOR FINDING PHI-PRIME
214           0    TRAN=(SS2/SS1)*SIN(THR)/(1.0+S1*SIN(SIGR+THR))
```

```
230         0      DFLP=20.0*PI/180.0
233         0      N=0
234         0      IF(THD)111,112,113
236     111 0      PHIPR=2.0*BETAR
240         0      DFLPR=-1.0*PI/180.0
243         0      GO TO 114
243     112 0      BETAR=0.0
244         0      PHIPR=0.0
245         0      GO TO 115
245     113 0      PHIPR=2.0*BETAR
247         0      DELPR=1.0*PI/180.0
252         0      GO TO 114
252     114 0      N=N+1
254         0      TEST=DELP
255         0      PHIPR=PHIPR+DELPR
257         0      GAMR=TRAN*(1.0+S2*COS(PHIR-PHIPR))/COS(PHIPR)
271         0      PHIPP=ATAN(GAMR)
273         0      DELP=ABS((PHIPR-PHIPP)/PHIPR)
277         0      IF(DELP.LT.0.0001) GO TO 115
302         0      IF(N.GT.200) GO TO 115
305         0      IF(DELP.LT.TEST) GO TO 114
307         0      PHIPR=PHIPR-2.0*DELPR
311         0      DELPR=DELPR/2.0
312         0      DELP=DELP+1.0
314         0      GO TO 114
314     115 0      PHIPD=PHIPR*180.0/PI
      C            END PHI-PRIME SUB-ROUTINE
316         0      A1=(2.0*R/SHR-1.0)*COS(THR)/SIN(SIGR)+(G-1.0-R*(G-1.0)/SHR)*
            1         S1
337         0      B1=-(2.0*R/SHR-1.0)*COS(SIGR)/SIN(SIGR)
351         0      C1=-(2.0*R/SHR-1.0)/SIN(SIGR)
360         0      A2=SIN(THR)*SIN(PHIR)+SIN(SIGR)*COS(PHIR)*A1/R
375         0      B2=SIN(SIGR)*SIN(PHIR)+SIN(SIGR)*COS(PHIR)*B1/R
412         0      C2=SIN(SIGR)*COS(PHIR)*C1/R
421         0      A3=SIN(THR)*COS(PHIR)-COS(SIGR)*COS(PHIR)*A1
435         0      B3=SIN(SIGR)*COS(PHIR)-COS(SIGR)/SIN(PHIR)-COS(SIGR)*COS(PHIR)
            1         *B1
457         0      C3=-COS(SIGR)*COS(PHIR)*C1
466         0      A4=(2.0*G*AXX-G*(G-1.0))/(2.0*G*AXX-(G-1.0))+
            1         4.0*G*AX*COS(THR)/(2.0*G*AXX-(G-1.0))
507         0      B4=-4.0*G*AXX*COS(SIGR)/(SIN(SIGR)*(2.0*G*AXX-(G-1.0)))
524         0      C4=-4.0*G*AXX/(SIN(SIGR)*(2.0*G*AXX-(G-1.0)))
536         0      A5=1.0-2.0*((COS(THR)/AX)+0.5*(G-1.0))*((R/SHR)-1.0)
552         0      B5=-2.0*((R/SHR)-1.0)
556         0      C5=B5/SIN(SIGR)
561         0      BX=S1*SIN(SIGR+THR)
566         0      CX=S1*SIN(THR)
571         0      A11=(1.0+BX)*C2-CX*B2
576         0      A12=1.0
577         0      A13=COS(PHIR-PHIPR)
603         0      A14=0.0
604         0      A21=(1.0+BX)*C3-CX*B3
611         0      A22=1.0*COS(PHIR-BETAR)/SIN(PHIR-BETAR)
623         0      A23=-SIN(PHIR-PHIPR)
630         0      A24=0.0
631         0      A31=(1.0+BX)*C4-CX*B4
636         0      A32=0.0
636         0      A33=G*SS1*S1/SS2
642         0      A34=0.0
642         0      A41=(1.0+BX)*C5-CX*B5
```

```
      0    A42=0.0
      0    A43=S1/SX
      0    A44=1.0
      0    D1=A2
      0    D2=A3
      0    D3=A4*S1
      0    D4=A5*S1
      0    DET=A11*A22*A33+A12*A23*A31+A13*A21*A32 -
      1        A31*A22*A13-A11*A32*A23-A33*A21*A12
      0    ESTAR=(D1*A22*A33+D2*A32*A13+D3*A23*A12-
      1             D1*A23*A32-D2*A12*A33-D3*A22*A13)/DET
      0    FSTAR=(D1*A23*A31+D2*A11*A33+D3*A13*A21-
      1             D1*A21*A33-D2*A31*A13-D3*A11*A23)/DET
      0    USTAR=(D1*A32*A21+D2*A12*A31+D3*A11*A22-
      1             D1*A31*A22-D2*A11*A32-D3*A21*A12)/DET
      0    HSTAR=(-D1*(A21*A32*A43+A31*A42*A23+A41*A33*A22-
      1              A41*A32*A23-A31*A22*A43-A21*A33*A42)+
      2              D2*(A11*A32*A43+A12*A33*A41+A13*A42*A31-
      3              A41*A32*A13-A31*A12*A43-A11*A33*A42)-
      4              D3*(A11*A22*A43+A12*A23*A41+A31*A42*A21-
      5              A41*A22*A13-A21*A12*A43-A11*A23*A42)+D4*DET)/DET
C          PPP21 IS THE RATIO OF THE PERTURBED PRESSURE IN REGION 2 TO
C          THAT IN REGION 1 EVALUATED AT THE SHOCK FRONT
      0    PPP21=USTAR*PP21/SX
      0    RPPP2=ABS(PPP21)
C          SPL21 = SPL2 - SPL1
      0    SPL21=20.0*ALOG10(RPPP2)
C          U0201 IS THE RATIO OF THE SOUND PARTICLE VELOCITY IN
C          REGION2 TO THAT IN REGION 1 EVALUATED AT THE SHOCK FRONT
      0    U0201=USTAR
C          UEVW2 IS THE RATIO OF THE RMS OF THE E-V VELOCITY TO THE
C          PRODUCT OF THE UNPERTURBED VELOCITY IN REGION 2, I.E. W2, AND
C          THE ACOUSTIC MACH NUMBER IN REGION 1
      0    UEVW2=(SIN(PHIR)*FSTAR)/(SQRT(2.0)*S1*COS(SIGR)*
      1              SIN(SIGR-BETAR))
C          SPRCU IS THE RATIO OF THE AMPLITUDE OF THE ENTROPY
C          PERTURBATION IN REGION 2 TO THE PRODUCT OF THE CONSTANT
C          PRESSURE SPECIFIC HEAT AND THE ACOUSTIC PARTICLE VELOCITY
C          IN REGION 1
      0    SPRCU=-HSTAR
C          ATUP1 IS THE RATIO OF THE SHOCK FRONT VELOCITY TO THE
C          SOUND PARTICLE VELOCITY IN REGION 1 EVALUATED AT THE
C          SHOCK FRONT
      0    ATUP1=-ESTAR*(1.0+BX)
C          PAMPL IS THE RATIO OF THE PRODUCT OF THE PEAK-TO-PEAK
C          AMPLITUDE OF THE SHOCK FRONT MOTION AND THE CIRCULAR
C          FREQUENCY IN REGION 1 TO THE SOUND PARTICLE VELOCITY IN
C          REGION 1
      0    PAMPL=2.0*ESTAR
      0    WRITE(6,116) THD,BETAD,PHIPD,PPP21,SPL21,U0201,UEVW2,
      1                   SPRCU,ATUP1,PAMPL
  116 0    FORMAT(20X,F5.1,F9.3,F9.3,F10.4,F10.3,F10.4,4F9.3)
      0    GO TO 110
  117 0    N=N
         END

SED COMPILER SPACE
300
```

APPENDIX B

SOUND WAVE SHOCK FRONT DATA

M1 = 1.50 DELTA = 8.98 SIGMA = 54.44 M2 = 1.16 THETACP = THETACN =

THETA	BETA	PHIP	PP2/PP1	SPL2/1	U02/U01	UEVW2	SPRCU	AT/UP1	PPAMPL
-90.0	-41.551	-89.977	1.5481	3.796	1.0528	-.019	.111	-.030	.466
-85.0	-38.592	-87.309	1.5561	3.841	1.0583	.011	-.268	-.032	.271
-80.0	-35.763	-80.525	1.4896	3.461	1.0131	.004	-.794	-.009	.051
-75.0	-33.049	-74.130	1.4286	3.098	.9716	-.007	-1.289	.030	-.128
-70.0	-30.439	-68.066	1.3704	2.737	.9320	-.020	-1.759	.083	-.277
-65.0	-27.922	-62.274	1.3129	2.364	.8929	-.034	-2.207	.146	-.403
-60.0	-25.488	-56.726	1.2553	1.975	.8537	-.047	-2.635	.218	-.510
-55.0	-23.127	-51.380	1.1970	1.562	.8141	-.059	-3.041	.297	-.604
-50.0	-20.832	-46.211	1.1378	1.121	.7738	-.069	-3.425	.382	-.685
-45.0	-18.595	-41.189	1.0776	.649	.7329	-.076	-3.785	.472	-.757
-40.0	-16.408	-36.308	1.0167	.144	.6915	-.080	-4.121	.564	-.821
-35.0	-14.265	-31.537	.9554	-.397	.6497	-.081	-4.430	.658	-.878
-30.0	-12.159	-26.862	.8939	-.974	.6079	-.078	-4.711	.752	-.928
-25.0	-10.086	-22.269	.8327	-1.590	.5663	-.073	-4.961	.846	-.973
-20.0	-8.038	-17.740	.7723	-2.244	.5252	-.064	-5.180	.937	-1.014
-15.0	-6.011	-13.260	.7133	-2.935	.4851	-.052	-5.366	1.025	-1.050
-10.0	-3.999	-8.820	.6562	-3.659	.4463	-.037	-5.518	1.108	-1.081
-5.0	-1.997	-4.403	.6017	-4.412	.4092	-.020	-5.634	1.186	-1.109
0.0	0.000	0.000	.5505	-5.185	.3744	.000	-5.713	1.257	-1.133
5.0	1.997	4.403	.5032	-5.965	.3422	.021	-5.755	1.321	-1.153
10.0	3.999	8.820	.4607	-6.732	.3133	.044	-5.758	1.375	-1.169
15.0	6.011	13.260	.4238	-7.457	.2882	.067	-5.722	1.419	-1.180
20.0	8.038	17.740	.3934	-8.104	.2675	.091	-5.647	1.452	-1.187
25.0	10.086	22.269	.3705	-8.625	.2520	.114	-5.532	1.472	-1.189
30.0	12.159	26.866	.3563	-8.963	.2423	.135	-5.377	1.477	-1.185
35.0	14.265	31.537	.3523	-9. 61	.2396	.154	-5.180	1.468	-1.174
40.0	16.408	36.308	.3602	-8.868	.2450	.170	-4.941	1.441	-1.155
45.0	18.595	41.189	.3824	-8.351	.2600	.181	-4.659	1.394	-1.124
50.0	20.832	46.211	.4218	-7.498	.2868	.186	-4.330	1.324	-1.080
55.0	23.127	51.380	.4829	-6.323	.3284	.184	-3.951	1.228	-1.017
60.0	25.488	56.726	.5723	-4.848	.3892	.173	-3.513	1.097	-.928
65.0	27.922	62.282	.7008	-3.088	.4766	.150	-3.003	.922	-.800
70.0	30.439	68.066	.8867	-1.044	.6031	.112	-2.396	.685	-.613
75.0	33.049	74.098	1.1649	1.325	.7922	.056	-1.642	.351	-.326
80.0	35.763	80.525	1.6160	4.169	1.0990	-.025	-.622	-.159	.153
85.0	38.592	87.184	2.4376	7.739	1.6578	-.134	.960	-1.041	1.054
90.0	41.551	89.852	3.3588	10.524	2.2843	-.162	2.634	-2.104	2.247

M1 = 2.00 DELTA = 8.96 SIGMA = 38.20 M2 = 1.68 THETACP = THETACN =

THETA	BETA	PHIP	PP2/PP1	SPL2/1	U02/U01	UEVW2	SPRCU	AT/UP1	PPAMPL
-90.0	-41.343	-89.999	1.4736	3.367	.977[illegible]	-.045	-.500	.101	.354
-85.0	-38.352	-87.454	1.5280	3.683	1.0131	-.011	-.738	.048	.210
-80.0	-35.500	-80.594	1.5159	3.614	1.0050	-.000	-1.126	.007	-.040
-75.0	-32.773	-74.077	1.4989	3.515	.9937	.004	-1.531	-.010	-.105
-70.0	-30.157	-67.935	1.4768	3.386	.9791	.003	-1.949	-.006	-.229
-65.0	-27.640	-62.091	1.4486	3.219	.9604	-.001	-2.380	.017	-.338
-60.0	-25.211	-56.505	1.4139	3.008	.9374	-.008	-2.818	.056	-.435
-55.0	-22.861	-51.140	1.3726	2.751	.9100	-.017	-3.263	.110	-.521
-50.0	-20.580	-45.961	1.3245	2.441	.8781	-.026	-3.709	.177	-.599
-45.0	-18.360	-40.947	1.2700	2.076	.8420	-.034	-4.154	.256	-.671
-40.0	-16.193	-36.074	1.2092	1.650	.8017	-.042	-4.594	.345	-.736
-35.0	-14.073	-31.321	1.1426	1.158	.7575	-.048	-5.026	.443	-.797
-30.0	-11.992	-26.667	1.0706	.592	.7098	-.052	-5.447	.549	-.854
-25.0	-9.944	-22.098	.9937	-.055	.6588	-.054	-5.852	.661	-.907
-20.0	-7.923	-17.600	.9124	-.796	.6049	-.052	-6.238	.777	-.957
-15.0	-5.924	-13.154	.8276	-1.644	.5487	-.046	-6.603	.898	-1.004
-10.0	-3.940	-8.748	.7398	-2.617	.4905	-.035	-6.942	1.020	-1.049
-5.0	-1.968	-4.367	.6499	-3.743	.4309	-.020	-7.254	1.144	-1.092
0.0	0.000	0.000	.5585	-5.059	.3703	.000	-7.535	1.267	-1.133
5.0	1.968	4.367	.4666	-6.621	.3094	.026	-7.782	1.388	-1.171
10.0	3.940	8.748	.3751	-8.518	.2487	.058	-7.994	1.505	-1.209
15.0	5.924	13.152	.2848	-10.909	.1888	.096	-8.167	1.618	-1.244
20.0	7.923	17.600	.1968	-14.120	.1305	.141	-8.299	1.725	-1.278
25.0	9.944	22.098	.1121	-19.006	.0743	.193	-8.388	1.825	-1.310
30.0	11.992	26.671	.0320	-29.900	.0212	.253	-8.432	1.915	-1.340
35.0	14.073	31.317	-.0422	-27.486	-.0280	.323	-8.429	1.994	-1.368
40.0	16.193	36.074	-.1089	-19.257	-.0722	.402	-8.374	2.060	-1.393
45.0	18.360	40.955	-.1660	-15.600	-.1100	.494	-8.264	2.111	-1.414
50.0	20.580	45.973	-.2104	-13.541	-.1395	.600	-8.093	2.143	-1.429
55.0	22.861	51.129	-.2374	-12.492	-.1574	.724	-7.850	2.150	-1.435
60.0	25.211	56.485	-.2387	-12.441	-.1583	.873	-7.513	2.123	-1.425
65.0	27.640	62.093	-.1973	-14.099	-.1308	1.053	-7.038	2.044	-1.387
70.0	30.157	67.939	-.0670	-23.473	-.0444	1.264	-6.300	1.859	-1.282
75.0	32.773	74.046	.3276	-9.693	.2172	1.367	-4.814	1.371	-.966
80.0	35.500	80.500	2.9763	9.474	1.9732	-3.268	2.941	-1.666	1.206
85.0	38.352	87.704	-2.9341	9.350	-1.9453	-168.830	-13.052	4.942	-3.697
90.0	41.343	89.937	-2.2993	7.232	-1.5244	-6.139	-10.917	4.251	-3.306

M1 = 2.50 DELTA = 8.97 SIGMA = 30.89 M2 = 2.13 THETACP = THETACN =

THETA	BETA	PHIP	PP2/PP1	SPL2/1	U02/U01	UEVW2	SPRCU	AT/UP1	PPAMPL
-90.0	-40.802	-89.978	1.5191	3.632	.9405	-.049	-1.029	.168	.293
-85.0	-37.720	-88.439	1.6116	4.145	.9978	-.015	-1.143	.095	.184
-80.0	-34.807	-80.738	1.6195	4.188	1.0026	-.001	-1.436	.014	.032
-75.0	-32.043	-73.930	1.6250	4.217	1.0061	.008	-1.765	-.035	-.094
-70.0	-29.411	-67.588	1.6228	4.205	1.0047	.012	-2.131	-.059	-.204
-65.0	-26.896	-61.604	1.6115	4.145	.9977	.012	-2.532	-.061	-.302
-60.0	-24.483	-55.923	1.5905	4.031	.9847	.008	-2.963	-.042	-.390
-55.0	-22.161	-50.504	1.5595	3.860	.9655	.003	-3.421	-.005	-.470
-50.0	-19.918	-45.308	1.5184	3.628	.9401	-.004	-3.902	.049	-.544
-45.0	-17.745	-40.302	1.4671	3.329	.9083	-.012	-4.401	.120	-.613
-40.0	-15.632	-35.454	1.4056	2.957	.8702	-.020	-4.915	.205	-.678
-35.0	-13.570	-30.746	1.3341	2.504	.8259	-.028	-5.441	.304	-.740
-30.0	-11.553	-26.153	1.2529	1.958	.7757	-.034	-5.974	.415	-.799
-25.0	-9.573	-21.654	1.1622	1.306	.7195	-.038	-6.511	.538	-.857
-20.0	-7.623	-17.234	1.0625	.527	.6578	-.039	-7.048	.672	-.913
-15.0	-5.697	-12.874	.9540	-.409	.5906	-.037	-7.583	.815	-.968
-10.0	-3.788	-8.558	.8372	-1.543	.5183	-.030	-8.113	.967	-1.022
-5.0	-1.891	-4.272	.7124	-2.945	.4411	-.018	-8.634	1.126	-1.077
0.0	0.000	0.000	.5799	-4.733	.3590	.000	-9.145	1.293	-1.132
5.0	1.891	4.272	.4399	-7.133	.2723	.026	-9.645	1.465	-1.189
10.0	3.788	8.559	.2924	-10.681	.1810	.061	-10.133	1.644	-1.247
15.0	5.697	12.874	.1371	-17.261	.0849	.108	-10.611	1.829	-1.309
20.0	7.623	17.234	-.0267	-31.467	-.0165	.169	-11.081	2.020	-1.374
25.0	9.573	21.654	-.2004	-13.961	-.1241	.247	-11.549	2.219	-1.446
30.0	11.553	26.153	-.3867	-8.253	-.2394	.350	-12.025	2.429	-1.526
35.0	13.570	30.750	-.5902	-4.580	-.3654	.487	-12.527	2.654	-1.617
40.0	15.632	35.451	-.8194	-1.730	-.5073	.673	-13.087	2.904	-1.727
45.0	17.745	40.302	-1.0907	.754	-.6753	.942	-13.765	3.197	-1.867
50.0	19.918	45.305	-1.4378	3.154	-.8902	1.359	-14.683	3.571	-2.059
55.0	22.161	50.510	-1.9433	5.771	-1.2031	2.098	-16.136	4.117	-2.357
60.0	24.483	55.904	-2.8613	9.131	-1.7715	3.741	-19.032	5.119	-2.926
65.0	26.896	61.604	-5.6084	14.977	-3.4722	9.958	-28.412	8.157	-4.679
70.0	29.411	67.572	43.2358	32.717	26.7676	-157.589	145.780	-46.360	26.836
75.0	32.043	73.961	3.3314	10.453	2.0625	8.336	4.235	-1.878	1.103
80.0	34.807	80.613	1.3357	2.514	.8270	-.391	-2.419	.308	-.185
85.0	37.720	87.439	.5923	-4.549	.3667	-.803	-4.607	1.093	-.673
90.0	40.802	89.853	.2087	-13.610	.1292	-.726	-5.499	1.466	-.932

M1 = 3.00 DELTA = 8.98 SIGMA = 26.47 M2 = 2.56 THETACP = THETACN =

THETA	BETA	PHIP	PP2/PP1	SPL2/1	U02/U01	UEVW2	SPRCU	AT/UP1	PPAMPL
-90.0	-40.235	-89.969	1.5989	4.076	.9185	-.047	-1.527	.209	.248
-85.0	-37.050	-89.099	1.7194	4.707	.9874	-.016	-1.545	.127	.162
-80.0	-34.068	-80.887	1.7459	4.840	1.0026	-.000	-1.733	.018	.026
-75.0	-31.265	-73.779	1.7693	4.956	1.0160	.010	-1.980	-.054	-.087
-70.0	-28.616	-67.201	1.7829	5.023	1.0238	.016	-2.286	-.099	-.186
-65.0	-26.103	-61.066	1.7855	5.035	1.0254	.018	-2.645	-.119	-.275
-60.0	-23.709	-55.293	1.7762	4.990	1.0200	.017	-3.054	-.117	-.356
-55.0	-21.418	-49.817	1.7543	4.882	1.0074	.013	-3.508	-.093	-.430
-50.0	-19.217	-44.603	1.7194	4.708	.9874	.008	-4.004	-.049	-.500
-45.0	-17.094	-39.604	1.6711	4.460	.9597	.001	-4.537	.013	-.566
-40.0	-15.039	-34.791	1.6093	4.133	.9241	-.006	-5.106	.094	-.630
-35.0	-13.041	-30.133	1.5336	3.714	.8807	-.014	-5.705	.192	-.692
-30.0	-11.092	-25.602	1.4440	3.192	.8293	-.021	-6.334	.307	-.752
-25.0	-9.184	-21.180	1.3405	2.545	.7698	-.026	-6.989	.437	-.812
-20.0	-7.308	-16.845	1.2227	1.746	.7021	-.029	-7.668	.584	-.873
-15.0	-5.459	-12.576	1.0906	.753	.6263	-.029	-8.371	.746	-.934
-10.0	-3.629	-8.357	.9436	-.504	.5419	-.026	-9.096	.923	-.997
-5.0	-1.811	-4.170	.7814	-2.143	.4487	-.016	-9.846	1.115	-1.063
0.0	0.000	0.000	.6027	-4.398	.3461	.000	-10.621	1.323	-1.132
5.0	1.811	4.170	.4062	-7.825	.2333	.025	-11.430	1.549	-1.207
10.0	3.629	8.357	.1893	-14.457	.1087	.062	-12.280	1.794	-1.289
15.0	5.459	12.576	-.0519	-25.694	-.0298	.115	-13.188	2.063	-1.382
20.0	7.308	16.843	-.3238	-9.794	-.1860	.190	-14.180	2.362	-1.488
25.0	9.184	21.180	-.6370	-3.917	-.3658	.296	-15.300	2.702	-1.615
30.0	11.092	25.606	-1.0100	.086	-.5800	.452	-16.625	3.103	-1.773
35.0	13.041	30.129	-1.4769	3.387	-.8481	.689	-18.295	3.602	-1.981
40.0	15.039	34.797	-2.1084	6.479	-1.2107	1.078	-20.599	4.272	-2.278
45.0	17.094	39.595	-3.0715	9.747	-1.7638	1.797	-24.220	5.294	-2.754
50.0	19.217	44.591	-4.8871	13.781	-2.8065	3.451	-31.284	7.224	-3.689
55.0	21.418	49.805	-10.3353	20.286	-5.9351	9.616	-53.125	13.033	-6.571
60.0	23.709	55.293	118.9562	41.508	68.3111	-180.013	474.254	-125.173	62.676
65.0	26.103	61.082	8.3402	18.424	4.7894	-80.149	23.808	-6.966	3.484
70.0	28.616	67.232	4.0282	12.102	2.3132	-4.852	6.671	-2.382	1.197
75.0	31.265	73.779	2.4509	7.787	1.4074	.691	.701	-.724	.367
80.0	34.068	80.887	1.6001	4.083	.9189	-.083	-2.295	.155	-.080
85.0	37.050	88.099	1.0637	.536	.6108	-.295	-3.992	.691	-.365
90.0	40.235	89.969	.7366	-2.655	.4230	-.331	-4.775	.970	-.526

M1 = 1.75 DELTA = 16.74 SIGMA = 57.50 M2 = 1.09 THETACP = THETACN =

THETA	BETA	PHIP	PP2/PP1	SPL2/1	U02/U01	UEVW2	SPRCU	AT/UP1	PPAMPL
-90.0	-39.028	-89.994	2.2632	7.094	1.0884	-.057	.064	-.015	.500
-85.0	-35.583	-89.916	2.3261	7.333	1.1186	.008	-.209	-.032	.334
-80.0	-32.433	-81.523	2.1390	6.604	1.0287	.013	-.888	-.007	.041
-75.0	-29.534	-73.521	1.9885	5.970	.9563	.005	-1.474	.041	-.175
-70.0	-26.848	-66.368	1.8693	5.434	.8990	-.007	-1.981	.104	-.335
-65.0	-24.344	-59.844	1.7667	4.943	.8496	-.020	-2.437	.178	-.461
-60.0	-21.995	-53.841	1.6736	4.473	.8049	-.032	-2.855	.260	-.564
-55.0	-19.778	-48.252	1.5856	4.004	.7625	-.043	-3.242	.349	-.649
-50.0	-17.674	-42.997	1.4999	3.522	.7213	-.051	-3.600	.443	-.722
-45.0	-15.667	-38.030	1.4154	3.017	.6807	-.058	-3.933	.541	-.785
-40.0	-13.742	-33.296	1.3310	2.483	.6401	-.062	-4.240	.641	-.840
-35.0	-11.886	-28.756	1.2462	1.912	.5993	-.063	-4.521	.743	-.890
-30.0	-10.088	-24.374	1.1610	1.297	.5583	-.061	-4.777	.845	-.934
-25.0	-8.337	-20.124	1.0754	.632	.5172	-.057	-5.006	.946	-.975
-20.0	-6.625	-15.981	.9896	-.091	.4759	-.051	-5.208	1.045	-1.012
-15.0	-4.943	-11.916	.9039	-.878	.4347	-.041	-5.382	1.141	-1.046
-10.0	-3.284	-7.913	.8187	-1.738	.3937	-.030	-5.528	1.234	-1.078
-5.0	-1.638	-3.946	.7344	-2.681	.3532	-.016	-5.644	1.322	-1.107
0.0	0.000	0.000	.6516	-3.721	.3133	.000	-5.730	1.405	-1.135
5.0	1.638	3.946	.5708	-4.870	.2745	.018	-5.787	1.482	-1.161
10.0	3.284	7.913	.4926	-6.150	.2369	.037	-5.813	1.552	-1.186
15.0	4.943	11.916	.4177	-7.582	.2009	.057	-5.809	1.613	-1.209
20.0	6.625	15.981	.3468	-9.199	.1668	.078	-5.774	1.667	-1.231
25.0	8.337	20.124	.2805	-11.041	.1349	.100	-5.710	1.711	-1.251
30.0	10.088	24.374	.2198	-13.161	.1057	.122	-5.615	1.745	-1.270
35.0	11.886	28.756	.1655	-15.625	.0796	.143	-5.491	1.769	-1.288
40.0	13.742	33.296	.1189	-18.500	.0572	.164	-5.337	1.782	-1.303
45.0	15.667	38.030	.0814	-21.790	.0391	.183	-5.154	1.782	-1.316
50.0	17.674	43.005	.0553	-25.150	.0266	.200	-4.941	1.768	-1.324
55.0	19.778	48.244	.0440	-27.124	.0212	.215	-4.696	1.737	-1.328
60.0	21.995	53.833	.0541	-25.332	.0260	.225	-4.414	1.686	-1.321
65.0	24.344	59.844	.0993	-20.057	.0478	.228	-4.081	1.605	-1.296
70.0	26.848	66.384	.2173	-13.257	.1045	.219	-3.658	1.466	-1.228
75.0	29.534	73.568	.5635	-4.982	.2710	.179	-2.973	1.160	-1.013
80.0	32.433	81.616	3.6647	11.281	1.7624	-.194	.795	-1.122	1.028
85.0	35.583	89.166	-1.9669	5.876	-.9459	.455	-5.187	2.849	-2.759
90.0	39.028	89.932	-1.5364	3.730	-.7389	.360	-4.363	2.512	-2.590

M1 = 2.00 DELTA = 16.73 SIGMA = 47.80 M2 = 1.37 THETACP = THETACN =

THETA	BETA	PHIP	PP2/PP1	SPL2/1	U02/U01	UEVW2	SPRCU	AT/UP1	PPAMPL
-90.0	-38.986	-89.988	2.1540	6.665	1.0289	-.060	-.332	.068	.398
-85.0	-35.530	-89.936	2.2530	7.055	1.0762	-.006	-.518	.028	.269
-80.0	-32.374	-81.537	2.1435	6.622	1.0239	.009	-1.047	.001	.034
-75.0	-29.471	-73.512	2.0467	6.221	.9776	.011	-1.544	.006	-.149
-70.0	-26.784	-66.333	1.9651	5.867	.9386	.006	-2.004	.036	-.291
-65.0	-24.280	-59.802	1.8897	5.528	.9026	-.001	-2.438	.083	-.407
-60.0	-21.933	-53.787	1.8159	5.182	.8674	-.010	-2.855	.145	-.503
-55.0	-19.719	-48.195	1.7408	4.815	.8315	-.019	-3.257	.220	-.586
-50.0	-17.619	-42.940	1.6627	4.416	.7942	-.028	-3.644	.304	-.658
-45.0	-15.616	-37.974	1.5808	3.977	.7551	-.036	-4.017	.397	-.723
-40.0	-13.695	-33.242	1.4944	3.490	.7138	-.042	-4.375	.497	-.781
-35.0	-11.844	-28.704	1.4035	2.944	.6704	-.046	-4.716	.602	-.835
-30.0	-10.052	-24.330	1.3080	2.332	.6248	-.047	-5.040	.713	-.884
-25.0	-8.307	-20.086	1.2080	1.641	.5770	-.047	-5.344	.826	-.931
-20.0	-6.601	-15.948	1.1038	.858	.5273	-.043	-5.628	.942	-.975
-15.0	-4.925	-11.893	.9959	-.036	.4757	-.037	-5.889	1.059	-1.017
-10.0	-3.271	-7.896	.8845	-1.066	.4225	-.028	-6.127	1.177	-1.057
-5.0	-1.632	-3.938	.7701	-2.269	.3679	-.015	-6.341	1.293	-1.097
0.0	0.000	0.000	.6533	-3.698	.3120	.000	-6.529	1.409	-1.135
5.0	1.632	3.938	.5342	-5.445	.2552	.019	-6.692	1.522	-1.174
10.0	3.271	7.896	.4135	-7.671	.1975	.040	-6.828	1.632	-1.212
15.0	4.925	11.893	.2912	-10.715	.1391	.065	-6.937	1.739	-1.252
20.0	6.601	15.948	.1676	-15.513	.0801	.094	-7.020	1.842	-1.292
25.0	8.307	20.086	.0425	-27.424	.0203	.125	-7.079	1.941	-1.334
30.0	10.052	24.330	-.0845	-21.459	-.0404	.161	-7.114	2.037	-1.378
35.0	11.844	28.704	-.2148	-13.361	-.1026	.200	-7.129	2.129	-1.427
40.0	13.695	33.242	-.3504	-9.109	-.1674	.244	-7.129	2.221	-1.481
45.0	15.616	37.966	-.4957	-6.096	-.2368	.293	-7.121	2.315	-1.544
50.0	17.619	42.940	-.6590	-3.622	-.3148	.350	-7.121	2.417	-1.622
55.0	19.719	48.187	-.8577	-1.333	-.4097	.418	-7.156	2.543	-1.724
60.0	21.933	53.803	-1.1348	1.098	-.5420	.508	-7.295	2.724	-1.876
65.0	24.280	59.810	-1.6209	4.195	-.7742	.648	-7.737	3.064	-2.155
70.0	26.784	66.318	-3.0154	9.587	-1.4403	.990	-9.551	4.110	-2.969
75.0	29.471	73.567	29.6579	29.443	14.1663	-6.011	40.511	-21.469	16.015
80.0	32.374	81.498	1.7268	4.745	.8248	.082	-1.686	.303	-.235
85.0	35.530	89.061	.6640	-3.556	.3172	.401	-2.975	1.074	-.871
90.0	38.986	89.972	.3197	-9.904	.1527	.622	-3.168	1.274	-1.088

M1 = 2.50 DELTA = 16.74 SIGMA = 38.90 M2 = 1.80 THETACP = THETACN =

THETA	BETA	PHIP	PP2/PP1	SPL2/1	U02/U01	UEVW2	SPRCU	AT/UP1	PPAMPL
-90.0	-38.395	-89.977	2.2795	7.157	.9838	-.056	-.867	.142	.299
-85.0	-34.776	-89.802	2.4165	7.664	1.0430	-.013	-.961	.081	.202
-80.0	-31.517	-82.034	2.3815	7.537	1.0279	.010	-1.320	.008	.024
-75.0	-28.558	-73.428	2.3195	7.308	1.0011	.018	-1.730	-.032	-.133
-70.0	-25.849	-65.894	2.2662	7.106	.9781	.019	-2.132	-.037	-.257
-65.0	-23.351	-59.147	2.2130	6.900	.9552	.017	-2.535	-.018	-.359
-60.0	-21.030	-53.005	2.1553	6.670	.9302	.011	-2.941	.022	-.446
-55.0	-18.857	-47.344	2.0904	6.405	.9022	.004	-3.351	.080	-.522
-50.0	-16.811	-42.075	2.0167	6.093	.8704	-.003	-3.765	.153	-.591
-45.0	-14.871	-37.125	1.9332	5.725	.8344	-.010	-4.180	.240	-.654
-40.0	-13.020	-32.439	1.8391	5.292	.7938	-.017	-4.597	.339	-.712
-35.0	-11.245	-27.970	1.7341	4.781	.7484	-.023	-5.013	.449	-.768
-30.0	-9.532	-23.676	1.6179	4.179	.6983	-.027	-5.427	.570	-.821
-25.0	-7.869	-19.526	1.4903	3.466	.6432	-.029	-5.837	.699	-.873
-20.0	-6.248	-15.491	1.3513	2.615	.5832	-.029	-6.242	.837	-.925
-15.0	-4.659	-11.543	1.2006	1.588	.5182	-.027	-6.641	.983	-.976
-10.0	-3.093	-7.661	1.0381	.325	.4481	-.021	-7.034	1.136	-1.029
-5.0	-1.543	-3.820	.8634	-1.276	.3727	-.012	-7.420	1.296	-1.082
0.0	0.000	0.000	.6758	-3.404	.2917	.000	-7.800	1.463	-1.139
5.0	1.543	3.820	.4741	-6.483	.2046	.017	-8.176	1.638	-1.198
10.0	3.093	7.661	.2566	-11.816	.1107	.038	-8.551	1.821	-1.263
15.0	4.659	11.545	.0202	-33.876	.0087	.066	-8.932	2.016	-1.335
20.0	6.248	15.489	-.2395	-12.413	-.1034	.100	-9.327	2.224	-1.416
25.0	7.869	19.528	-.5304	-5.508	-.2289	.143	-9.752	2.451	-1.511
30.0	9.532	23.673	-.8652	-1.258	-.3734	.198	-10.232	2.709	-1.626
35.0	11.245	27.966	-1.2666	2.053	-.5467	.268	-10.811	3.013	-1.771
40.0	13.020	32.439	-1.7780	4.998	-.7674	.364	-11.572	3.397	-1.967
45.0	14.871	37.133	-2.4918	7.930	-1.0755	.502	-12.694	3.933	-2.256
50.0	16.811	42.075	-3.6426	11.228	-1.5722	.729	-14.622	4.801	-2.744
55.0	18.857	47.340	-6.0503	15.636	-2.6114	1.198	-18.914	6.632	-3.796
60.0	21.030	52.997	-15.8699	24.011	-6.8496	3.073	-37.251	14.163	-8.163
65.0	23.351	59.140	24.7208	27.861	10.6697	-4.537	40.071	-17.103	9.982
70.0	25.849	65.886	6.5397	16.311	2.8226	-1.057	5.900	-3.144	1.868
75.0	28.558	73.366	3.5309	10.958	1.5240	-.401	.527	-.862	.525
80.0	31.517	82.034	2.2433	7.018	.9682	.006	-1.574	.095	-.059
85.0	34.776	89.552	1.5811	3.979	.6824	.542	-2.476	.553	-.359
90.0	38.395	89.914	1.2606	2.011	.5441	6.390	-2.710	.706	-.479

M1 = 3.00 DELTA = 16.75 SIGMA = 34.10 M2 = 2.16 THETACP = THETACN =

THETA	BETA	PHIP	PP2/PP1	SPL2/1	U02/U01	UEVW2	SPRCU	AT/UP1	PPAMPL
-90.0	-37.805	-89.985	2.5187	8.024	.9665	-.047	-1.302	.174	.235
-85.0	-33.982	-89.965	2.6922	8.602	1.0331	-.012	-1.324	.107	.160
-80.0	-30.598	-82.695	2.7065	8.648	1.0386	.013	-1.561	.009	.016
-75.0	-27.570	-73.390	2.6624	8.505	1.0217	.023	-1.901	-.061	-.126
-70.0	-24.836	-65.437	2.6259	8.385	1.0077	.027	-2.253	-.090	-.237
-65.0	-22.343	-58.437	2.5866	8.255	.9926	.026	-2.621	-.089	-.329
-60.0	-20.051	-52.143	2.5392	8.[illegible]94	.9744	.023	-3.007	-.063	-.408
-55.0	-17.926	-46.411	2.4805	7.891	.9519	.017	-3.411	-.017	-.478
-50.0	-15.939	-41.123	2.4085	7.635	.9242	.011	-3.832	.048	-.543
-45.0	-14.068	-36.195	2.3216	7.316	.8909	.005	-4.269	.130	-.603
-40.0	-12.294	-31.561	2.2186	6.922	.8514	-.002	-4.722	.228	-.661
-35.0	-10.601	-27.163	2.0988	6.439	.8054	-.008	-5.189	.341	-.716
-30.0	-8.974	-22.961	1.9611	5.850	.7526	-.013	-5.669	.468	-.772
-25.0	-7.401	-18.915	1.8047	5.128	.6925	-.016	-6.163	.610	-.827
-20.0	-5.871	-14.993	1.6287	4.237	.6250	-.018	-6.670	.765	-.884
-15.0	-4.375	-11.165	1.4317	3.117	.5494	-.018	-7.191	.934	-.942
-10.0	-2.904	-7.406	1.2121	1.671	.4651	-.015	-7.730	1.117	-1.004
-5.0	-1.448	-3.692	.9675	-.287	.3713	-.009	-8.289	1.316	-1.071
0.0	0.000	0.000	.6945	-3.167	.2665	.000	-8.875	1.534	-1.144
5.0	1.448	3.692	.3880	-8.223	.1489	.014	-9.498	1.772	-1.225
10.0	2.904	7.405	.0402	-27.911	.0154	.033	-10.174	2.036	-1.319
15.0	4.375	11.165	-.3610	-8.849	-.1385	.060	-10.927	2.336	-1.430
20.0	5.871	14.993	-.8357	-1.559	-.3207	.097	-11.799	2.684	-1.565
25.0	7.401	18.915	-1.4184	3.036	-.5443	.148	-12.861	3.106	-1.738
30.0	8.974	22.963	-2.1734	6.743	-.8340	.220	-14.245	3.648	-1.973
35.0	10.601	27.163	-3.2340	10.195	-1.2410	.330	-16.222	4.405	-2.317
40.0	12.294	31.557	-4.9264	13.851	-1.8905	.515	-19.460	5.612	-2.889
45.0	14.068	36.199	-8.3096	18.392	-3.1887	.899	-26.114	8.027	-4.068
50.0	15.939	41.128	-19.7930	25.930	-7.5954	2.223	-49.237	16.247	-8.156
55.0	17.926	46.414	77.2502	37.758	29.6441	-9.003	148.609	-53.353	26.679
60.0	20.051	52.133	13.4153	22.552	5.1480	-1.614	18.944	-7.601	3.808
65.0	22.343	58.437	7.2400	17.195	2.7783	-.887	6.683	-3.194	1.612
70.0	24.836	65.422	4.8277	13.675	1.8526	-.581	2.096	-1.487	.761
75.0	27.570	73.390	3.4950	10.869	1.3412	-.369	-.284	-.552	.288
80.0	30.598	82.695	2.6265	8.388	1.0079	-.095	-1.713	.052	-.028
85.0	33.982	89.965	2.0858	6.385	.8004	10.209	-2.449	.393	-.217
90.0	37.805	89.860	1.7865	5.040	.6856	-.559	-2.647	.502	-.288

APPENDIX C

FORTRAN II-D PROGRAM FOR SHEAR WAVE - SHOCK FRONT INTERACTION

*LIST PRINTER


```
C           THE EFFECT OF SHEAR WAVES ON A STATIONARY OBLIQUE  SHOCK
C           T1 IS THE ABSOLUTE TEMPERATURE IN REGION 1 IN DEGREES RANKINE
      0     T1=518.7
C           SS1 IS THE SPEED OF SOUND IN REGION 1
      0     SS1=SQRTF(1.4*53.35*32.174*T1)
C           THE WORKING FLUID IS DRY AIR
C           G IS THE RATIO OF SPECIFIC HEATS
      0     G=1.4
            SHR=(G-1.)/(G+1.)
            PI=3.1415926536
C           S1 IS THE MACH NUMBER IN REGION 1
C           SIGD IS THE OBLIQUE SHOCK ANGLE IN DEGREES
C           DELTAD IS THE FLARE (TURNING) ANGLE IN DEGREES
 100  0     READ 101, S1, SIGD, DELTAD
 101        FORMAT(3F10.3)
            SIGR=SIGD*PI/180.
            AX=S1*SINF(SIGR)
            AXX=AX*AX
C           RR21=(DENSITY 2)/(DENSITY 1)
      0     RR21=((G+1.)*AXX)/(2.+(G-1.)*AXX)
C           PP21=(PRESSURE 2)/(PRESSURE 1)
      0     PP21=1.+G*AXX*(1.-(1./RR21))
            DELTAR=SIGR-ATANF((SINF(SIGR)/COS(SIGR))/RR21)
            DELTAD=DELTAR*180./PI
C           T2 IS THE ABSOLUTE TEMPERATURE IN REGION 2
      0     T2=T1*(PP21/RR21)
C           SS2 IS THE SPEED OF SOUND IN REGION 2
      0     SS2=SQRTF(1.4*53.35*32.174*T2)
C           S2 IS THE MACH NUMBER IN REGION 2
      0     S2=S1*(COSF(SIGR)/COSF(SIGR-DELTAR))*(SS1/SS2)
C           R=(DENSITY 2)/(DENSITY 1)=M
      0     R=RR21
C           THECR IS THE CRITICAL VALUE OF THETA
      0     THECR=ATANF(SQRTF(((G+1.)*(R-1.))/(2.*R*R)))
            THECD=THECR*180./PI
            PRINT 102, S1,DELTAD,SIGD,S2,THECD
 102        FORMAT(1H1,1H0,1H ,10X,4HMA =,F6.2,2X,7HDELTA =,F6.2,2X,
      1            7HSIGMA =,F6.2,2X,3HM =,F5.2,2X,10HTHETA CR =,F8.2/)
            PRINT 103
 103        FORMAT(10X,88(1H-)/11X,5HTHETA,2X,6HPHI-PR,3X,5HWS/WA,2X,
      1           5HDEL S,3X,5HWP/WA,2X,5HDEL P,4X,7H(DP)RMS,2X,6HKSUR/K,
      2           2X,6HVSUR/A,2X,6HADX/EL,1X,6HDEL SH/10X,88(1H-))
            THDN=-THECD
            THDP=+THECD
C           THD IS THETA, ANGLE OF INCIDENT SHEAR WAVES IN DEGREES
      0     THD=-90.
 104        THD=THD+5.
            THR=THD*PI/180.
C           PHIR IS THE ANGLE PHI IN RADIANS
      0     PHIR=ATANF(R*SINF(THR)/COSF(THR))
            TEST1=THD-85.
            TEST2=THD-THDN
            TEST3=THD-THDP
            IF(TEST1) 105,105,100
 105        IF(TEST2) 108,108,106
 106        IF(TEST3) 107,108,108
C           THE FOLLOWING IS THE SUBSONIC SOLUTION
 107  0     UBL=(AX*SS1)/(R*SS2)
```

```
      BETAL=SQRTF(1.-UBL*UBL)
      WBL=UBL/COSF(PHIR)
      BETWL=SQRTF(1.-WBL*WBL)
      CL=(1.0*SHR+((3.-G)/(G+1.))*R)*(SINF(PHIR)/COSF(PHIR))-
     1   ((R-1.)*(R-1.)+2.*(R-1.)/(G+1.))*SINF(PHIR)*COSF(PHIR)
      DL=(BETWL*(R-1.)/(BETAL*BETAL))*(1.+(R-1.)*COSF(PHIR)*
     1   COSF(PHIR))
      DPL=(BETAL*BETAL/BETWL)*DL
      EL=2.*(1.-R*SHR)+2.*(R-1.)*(BETWL*COSF(PHIR)/BETAL)*
     1   (BETWL*COSF(PHIR)/BETAL)
      FL=(BETWL/(BETAL*BETAL))*(2.*(R-1.)*SINF(PHIR)* COSF(PHIR))
      FPL=(BETAL*BETAL/BETWL)*FL
      AWL=R*(CL*EL+DL*FL)/(CL*CL+DL*DL)
      BWL=R*(CL*FL-DL*EL)/(CL*CL+DL*DL)
      CWL=AWL*DPL/R-FPL
      DWL=BWL*DPL/R
      AL=1./COSF(PHIR)+2.*(R-1.)*COSF(PHIR)+AWL*(R-1.)*(R-1.)*
     1   SINF(PHIR)/R
      BL=BWL*(R-1.)*(R-1.)*SINF(PHIR)/R
C     PHIPL IS THE ANGLE PHI-PRIME IN RADIANS
     0PHIPL=-ATANF((UBL*UBL*SINF(PHIR))/(BETAL*BETAL*COSF(PHIR)))
C     DSRL IS THE SHEAR WAVE PHASE
     0DSRL=ATANF(-BL/AL)
C     DPRL IS THE PRESSURE WAVE PHASE
     0DPRL=ATANF((CWL*BETWL-DWL*SINF(PHIR)/COSF(PHIR))/(DWL*BETWL+
     1      CWL*SINF(PHIR)/COSF(PHIR)))
      STARL=SQRTF(AL*AL+BL*BL)/R
      PISTL=SQRTF(CWL*CWL+DWL*DWL)/(R*BETAL)
C     WSRWL IS THE SHEAR WAVE AMPLITUDE RATIO
     0WSRWL=STARL*SINF(SIGR)
C     WPRWL IS THE PRESSURE WAVE AMPLITUDE RATIO
     0WPRWL=PISTL*SINF(SIGR)
C     DPRML IS THE RATIO OF THE RMS OF THE PERTURBATION PRESSURE
C     TO EPSILON - IN PSI (PRESSURE IN REGION 1 ASSUMED TO BE 1 ATM,
C     I.E. P1=14.696 PSIA
     0DPRML=SQRTF(2.)*G*R*ABSF(PISTL)*PP21*14.696/
     1       (ABSF(COSF(PHIR))*((G+1.)*R-(G-1.)))
C     SSURL IS THE RATIO OF THE SURFACE WAVE NUMBER TO THAT OF THE
C     INCIDENT SHEAR WAVE
     0SSURL=COSF(SIGR+PHIPL-DELTAR)*COSF(THR)/COSF(PHIPL)
C     VSURL IS THE RATIO OF THE SURFACE PRESSURE WAVE VELOCITY TO
C     THE LOCAL SPEED OF SOUND
     0VSURL=COSF(PHIPL)*COSF(SIGR+THR)*S1*SS1/(COSF(THR)*
     1       COSF(SIGR+PHIPL-DELTAR)*SS2)
C     DXWPL IS THE RATIO OF THE SHOCK FRONT DISPLACEMENT AMPLITUDE
C     TO EPSILON TIMES THE WAVELENGTH OF THE INCIDENT SHEAR WAVE
     0DXWPL=SQRTF(AWL*AWL+BWL*BWL)/(2.*PI*COSF(THR))
C     DSHRL IS THE SHOCK WAVE PHASE
     0DSHRL=ATANF(AWL/BWL)
      RD=180./PI
      PHIDL=PHIPL*RD
      DSDL=DSRL*RD
      DPDL=DPRL*RD
      DSHDL=DSHRL*RD
      PRINT 109, THD,PHIDL,WSRWL,DSDL,WPRWL,DPDL,DPRML,SSURL,VSURL,
     1           DXWPL,DSHDL
  109 FORMAT(10X,F6.1,F8.2,F8.3,F7.2,F8.3,F7.2,E11.4,4F8.3)
      GO TO 104
C     THE FOLLOWING IS THE SUPERSONIC SOLUTION
```

```
 108 0     UBG=(AX*SS1)/(R*SS2)
           BETAG=SQRTF(1.-UBG*UBG)
           WBG=UBG/COSF(PHIR)
           BETWG=SQRTF(WBG*WBG-1.)
           CPG=2.*R*SHR-2.*(1.+(R-1.)*COSF(PHIR)*COSF(PHIR))
           DPG=(R-1.)*(1.+(R-1.)*COSF(PHIR)*COSF(PHIR))
           EPG=(R-1.)*(R-1.)*SINF(PHIR)*COSF(PHIR)-(1.+
     1        (3.-G)*R/(1.+G))*SINF(PHIR)/COSF(PHIR)
           FPG=2.*(R-1.)*SINF(PHIR)*COSF(PHIR)
           SUR IS THE MACH ANGLE IN RADIANS
     0     SUR=ATANF(1./BETWG)
           GPG=SINF(SUR-PHIR)/COSF(SUR-PHIR)
           AWG=R*(CPG+GPG*FPG)/(EPG+GPG*DPG)
           CWG=AWG*DPG/R-FPG
           AG=1./COSF(PHIR)+2.*(R-1.)*COSF(PHIR)+AWG*(R-1.)*(R-1.)*
              SINF(PHIR)/R
           PHIPG=(PHIR/ABSF(PHIR))*ABSF(ABSF(PHIR)-SUR)
           PHIDG=PHIPG*180./PI
           STARG=AG/R
           PISTG=CWG*SINF(SUR)/(R*COSF(PHIR-SUR))
           WSRWG=STARG*SINF(SIGR)
           DSDG=0.0
           WPRWG=PISTG*SINF(SIGR)
           DPDG=0.0
           DPRMG=SQRTF(2.)*G*R*ABSF(PISTG)*PP21*14.696/
     1           (ABSF(COSF(PHIR))*((G+1.)*R-(G-1.)))
           SSURG=COSF(SIGR+PHIPG-DELTAR)*COSF(THR)/COSF(PHIPG)
           VSURG=COSF(PHIPG)*COSF(SIGR+THR)*S1*SS1/
     1           (COSF(THR)*COSF(SIGR+PHIPG-DELTAR)*SS2)
           DXWPG=ABSF(AWG)/(2.*PI*COSF(THR))
           DSHDG=-90.*(THR/ABSF(THR))
           PRINT 109, THD,PHIDG,WSRWG,DSDG,WPRWG,DPDG,DPRMG,SSURG,VSURG,
     1                DXWPG,DSHDG
           GO TO 104
 110       N=1
       CALL EXIT
        END
00009 51870000-3
00019 14000000-1
00029 53350000-2
00039 32174000-2
00049 10000000-1
00059 31415926-1
00069 18000000-3
00079 20000000-1
00089 90000000-2
00099 50000000-1
00109 85000000-2
00119 30000000-1
00129 14696000-2
00139 00000000RR
00143 0001
 00153     T1       00163    SS1       00173      G       00183     SHR
 00213   SIGD       00223 DELTAD       00233   SIGR       00243      AX
 00273   PP21       00283 DELTAR       00293     T2       00303     SS2
 00333  THECR       00343  THECD       00353   THDN       00363    THDP
 00393   PHIR       00403  TEST1       00413  TEST2       00423   TEST3
 00453    WBL       00463  BETWL       00473     CL       00483      DL
 00513     FL       00523    FPL       00533    AWL       00543     BWL
```

APPENDIX D

SHEAR WAVE - SHOCK FRONT DATA

MA = 1.50 DELTA = 8.98 SIGMA = 54.43 M = 1.16 THETA CR = 26.03

THETA	PHI-PR	WS/WA	DEL S	WP/WA	DEL P	(DP)RMS	KSUR/K	VSUR/A	ADX/EL	DEL SH
-85.0	-81.98	9.200	0.00	-2.420	0.00	1.0163E+03	.502	2.408	4.338	90.000
-80.0	-73.89	4.397	0.00	-5.186	0.00	1.0871E+03	.550	2.301	4.705	90.000
-75.0	-65.67	2.643	0.00	-8.901	0.00	1.2406E+03	.589	2.230	5.497	90.000
-70.0	-57.25	1.503	0.00	-15.251	0.00	1.5889E+03	.618	2.186	7.284	90.000
-65.0	-48.54	-.022	0.00	-32.881	0.00	2.7292E+03	.637	2.165	13.100	90.000
-60.0	-39.47	33.790	0.00	518.270	0.00	3.5685E+04	.644	2.169	181.836	90.000
-55.0	-29.92	3.160	0.00	26.140	0.00	1.5354E+03	.637	2.202	8.457	90.000
-50.0	-19.79	2.092	0.00	11.030	0.00	5.6438E+02	.615	2.273	3.455	90.000
-45.0	-8.92	1.607	0.00	4.707	0.00	2.1328E+02	.575	2.408	1.554	90.000
-40.0	-2.94	1.215	0.00	-.549	0.00	2.2369E+01	.565	2.405	.094	90.000
-35.0	-16.22	-1.064	0.00	-36.638	0.00	1.3551E+03	.744	1.778	10.137	90.000
-30.0	-32.13	1.527	0.00	5.797	0.00	1.9719E+02	.995	1.284	2.056	90.000
-25.0	54.84	1.200	-2.23	1.134	-41.95	3.5901E+01	-.281	-4.345	.701	69.082
-20.0	47.94	1.129	-3.74	1.197	85.04	3.5656E+01	-.083	-13.937	.625	42.908
-15.0	39.21	1.085	-3.44	1.260	56.87	3.5787E+01	.115	9.361	.583	28.899
-10.0	28.23	1.057	-2.55	1.312	35.54	3.5950E+01	.313	3.194	.558	18.148
-5.0	14.91	1.041	-1.35	1.344	17.17	3.6063E+01	.509	1.791	.545	8.792
0.0	0.00	1.036	0.00	1.355	0.00	3.6102E+01	.701	1.164	.540	0.000
5.0	-14.91	1.041	1.35	1.344	-17.17	3.6063E+01	.887	.804	.545	-8.792
10.0	-28.23	1.057	2.55	1.312	-35.54	3.5950E+01	1.067	.567	.558	-18.148
15.0	-39.21	1.085	3.44	1.260	-56.87	3.5787E+01	1.239	.398	.583	-28.899
20.0	-47.94	1.129	3.74	1.197	-85.04	3.5656E+01	1.401	.268	.625	-42.908
25.0	-54.84	1.200	2.23	1.134	41.95	3.5901E+01	1.552	.165	.701	-69.082
30.0	32.13	1.182	0.00	.223	0.00	7.5914E-00	.219	.619	.385	-90.000
35.0	16.22	1.205	0.00	.064	0.00	2.4038E-00	.404	.034	.295	-90.000
40.0	2.94	1.249	0.00	.003	0.00	1.3976E-01	.509	-.213	.248	-90.000
45.0	8.92	1.314	0.00	-.024	0.00	1.1258E-00	.416	-.552	.218	-90.000
50.0	19.79	1.408	0.00	-.037	0.00	1.9194E-00	.285	-1.224	.196	-90.000
55.0	29.92	1.540	0.00	-.041	0.00	2.4509E-00	.167	-2.798	.181	-90.000
60.0	39.47	1.729	0.00	-.040	0.00	2.8213E-00	.057	-10.141	.169	-90.000
65.0	48.54	2.009	0.00	-.037	0.00	3.0849E-00	-.044	15.499	.160	-90.000
70.0	57.25	2.445	0.00	-.031	0.00	3.2732E-00	-.139	5.710	.154	-90.000
75.0	65.67	3.192	0.00	-.024	0.00	3.4051E-00	-.226	3.938	.149	-90.000
80.0	73.89	4.717	0.00	-.016	0.00	3.4925E-00	-.306	3.204	.145	-90.000
85.0	81.98	9.349	0.00	-.008	0.00	3.5423E-00	-.379	2.809	.144	-90.000

MA = 2.00 DELTA = 8.96 SIGMA = 38.20 M = 1.67 THETA CR = 26.39

THETA	PHI-PR	WS/WA	DEL S	WP/WA	DEL P	(DP)RMS	KSUR/K	VSUR/A	ADX/EL	DEL SH
-85.0	-82.09	6.991	0.00	-1.679	0.00	9.7343E+02	.382	3.334	4.032	90.000
-80.0	-74.12	3.336	0.00	-3.590	0.00	1.0384E+03	.449	3.090	4.362	90.000
-75.0	-66.01	1.999	0.00	-6.129	0.00	1.1782E+03	.509	2.927	5.068	90.000
-70.0	-57.68	1.134	0.00	-10.369	0.00	1.4889E+03	.562	2.816	6.628	90.000
-65.0	-49.07	.025	0.00	-21.435	0.00	2.4503E+03	.606	2.741	11.423	90.000
-60.0	-40.07	-53.291	0.00	-777.005	0.00	7.3610E+04	.641	2.696	364.472	90.000
-55.0	-30.58	2.612	0.00	20.403	0.00	1.6470E+03	.666	2.679	8.820	90.000
-50.0	-20.48	1.663	0.00	8.322	0.00	5.8442E+02	.678	2.690	3.480	90.000
-45.0	-9.59	1.260	0.00	3.599	0.00	2.2346E+02	.675	2.740	1.580	90.000
-40.0	-2.33	.949	0.00	-.126	0.00	7.0656E-00	.683	2.725	.200	90.000
-35.0	-15.79	-.482	0.00	-20.009	0.00	1.0105E+03	.827	2.247	7.280	90.000
-30.0	-32.16	1.187	0.00	4.092	0.00	1.8970E+02	1.021	1.805	1.946	90.000
-25.0	53.39	.925	-2.80	.855	-48.99	3.6799E+01	.194	9.314	.682	65.606
-20.0	46.41	.870	-4.15	.904	82.27	3.6582E+01	.337	5.244	.608	41.594
-15.0	37.72	.835	-3.78	.955	55.18	3.6744E+01	.477	3.585	.566	28.119
-10.0	26.97	.813	-2.79	.995	34.53	3.6929E+01	.614	2.673	.542	17.686
-5.0	14.17	.801	-1.47	1.021	16.69	3.7054E+01	.746	2.089	.529	8.575
0.0	0.00	.796	0.00	1.030	0.00	3.7097E+01	.872	1.678	.525	0.000
5.0	-14.17	.801	1.47	1.021	-16.69	3.7054E+01	.992	1.369	.529	-8.575
10.0	-26.97	.813	2.79	.995	-34.53	3.6929E+01	1.104	1.125	.542	-17.686
15.0	-37.72	.835	3.78	.955	-55.18	3.6744E+01	1.207	.924	.566	-28.119
20.0	-46.41	.870	4.15	.904	-82.27	3.6582E+01	1.302	.754	.608	-41.594
25.0	-53.39	.925	2.80	.855	48.99	3.6799E+01	1.386	.605	.682	-65.606
30.0	32.16	.912	0.00	.179	0.00	8.3179E-00	.489	1.413	.389	-90.000
35.0	15.79	.926	0.00	.049	0.00	2.5104E-00	.601	.895	.296	-90.000
40.0	2.33	.958	0.00	0.000	0.00	5.0358E-02	.653	.583	.247	-90.000
45.0	9.59	1.006	0.00	-.021	0.00	1.3103E-00	.558	.394	.217	-90.000
50.0	20.48	1.076	0.00	-.030	0.00	2.1589E-00	.443	.131	.195	-90.000
55.0	30.58	1.175	0.00	-.033	0.00	2.7254E-00	.334	-.311	.180	-90.000
60.0	40.07	1.318	0.00	-.032	0.00	3.1193E-00	.230	-1.152	.168	-90.000
65.0	49.07	1.530	0.00	-.029	0.00	3.3993E-00	.130	-3.258	.159	-90.000
70.0	57.68	1.861	0.00	-.025	0.00	3.5990E-00	.034	-16.995	.152	-90.000
75.0	66.01	2.428	0.00	-.019	0.00	3.7389E-00	-.058	12.601	.148	-90.000
80.0	74.12	3.587	0.00	-.013	0.00	3.8315E-00	-.146	6.005	.144	-90.000
85.0	82.09	7.108	0.00	-.006	0.00	3.8843E-00	-.230	4.427	.143	-90.000

MA = 2.50 DELTA = 8.96 SIGMA = 30.88 M = 2.12 THETA CR = 27.20

THETA	PHI-PR	WS/WA	DEL S	WP/WA	DEL P	(DP)RMS	KSUR/K	VSUR/A	ADX/EL	DEL SH
-85.0	-82.39	5.795	0.00	-1.112	0.00	8.8393E+02	.324	4.157	3.376	90.000
-80.0	-74.71	2.754	0.00	-2.363	0.00	9.3677E+02	.398	3.782	3.629	90.000
-75.0	-66.88	1.640	0.00	-3.982	0.00	1.0480E+03	.466	3.541	4.159	90.000
-70.0	-58.82	.925	0.00	-6.542	0.00	1.2842E+03	.528	3.379	5.277	90.000
-65.0	-50.45	.096	0.00	-12.369	0.00	1.9291E+03	.583	3.266	8.307	90.000
-60.0	-41.67	-4.574	0.00	-59.411	0.00	7.6605E+03	.629	3.191	35.068	90.000
-55.0	-32.35	2.832	0.00	19.287	0.00	2.1128E+03	.667	3.145	10.473	90.000
-50.0	-22.34	1.570	0.00	6.928	0.00	6.5796E+02	.694	3.128	3.630	90.000
-45.0	-11.45	1.143	0.00	3.048	0.00	2.5497E+02	.709	3.145	1.662	90.000
-40.0	-.64	.850	0.00	.389	0.00	2.9058E+01	.713	3.182	.427	90.000
-35.0	-14.52	.020	0.00	-8.022	0.00	5.4055E+02	.839	2.734	3.478	90.000
-30.0	-32.10	1.045	0.00	2.854	0.00	1.7557E+02	1.006	2.286	1.717	90.000
-25.0	49.88	.796	-4.20	.692	-62.00	3.9335E+01	.439	5.211	.640	59.259
-20.0	42.81	.746	-5.27	.738	76.26	3.9208E+01	.546	4.132	.569	38.800
-15.0	34.29	.715	-4.70	.785	51.44	3.9466E+01	.650	3.403	.530	26.427
-10.0	24.17	.695	-3.46	.823	32.26	3.9717E+01	.748	2.871	.508	16.677
-5.0	12.55	.684	-1.82	.847	15.61	3.9880E+01	.841	2.460	.495	8.098
0.0	0.00	.681	0.00	.855	0.00	3.9935E+01	.927	2.128	.492	0.000
5.0	-12.55	.684	1.82	.847	-15.61	3.9880E+01	1.007	1.851	.495	-8.098
10.0	-24.17	.695	3.46	.823	-32.26	3.9717E+01	1.078	1.612	.508	-16.677
15.0	-34.29	.715	4.70	.785	-51.44	3.9466E+01	1.142	1.402	.530	-26.427
20.0	-42.81	.746	5.27	.738	-76.26	3.9208E+01	1.196	1.212	.569	-38.800
25.0	-49.88	.796	4.20	.692	62.00	3.9335E+01	1.242	1.038	.640	-59.259
30.0	32.10	.788	0.00	.168	0.00	1.0383E+01	.600	1.864	.401	-90.000
35.0	14.52	.791	0.00	.040	0.00	2.7172E-00	.680	1.381	.296	-90.000
40.0	.64	.813	0.00	-.003	0.00	2.8176E-01	.707	1.064	.245	-90.000
45.0	11.45	.849	0.00	-.022	0.00	1.8980E-00	.602	.931	.214	-90.000
50.0	22.34	.904	0.00	-.030	0.00	2.8929E-00	.497	.732	.192	-90.000
55.0	32.35	.985	0.00	-.032	0.00	3.5520E-00	.396	.416	.177	-90.000
60.0	41.67	1.102	0.00	-.031	0.00	4.0081E-00	.297	-.119	.165	-90.000
65.0	50.45	1.276	0.00	-.027	0.00	4.3312E-00	.200	-1.174	.156	-90.000
70.0	58.82	1.549	0.00	-.023	0.00	4.5610E-00	.106	-4.090	.150	-90.000
75.0	66.88	2.019	0.00	-.017	0.00	4.7218E-00	.013	-45.677	.145	-90.000
80.0	74.71	2.979	0.00	-.012	0.00	4.8281E-00	-.076	10.790	.142	-90.000
85.0	82.39	5.901	0.00	-.006	0.00	4.8887E-00	-.162	6.174	.140	-90.000

MA = 3.00 DELTA = 8.97 SIGMA = 26.46 M = 2.55 THETA CR = 27.83

THETA	PHI-PR	WS/WA	DEL S	WP/WA	DEL P	(DP)RMS	KSUR/K	VSUR/A	ADX/EL	DEL SH
-85.0	-82.70	5.026	0.00	-.773	0.00	8.1665E+02	.287	4.940	2.850	90.000
-80.0	-75.32	2.381	0.00	-1.634	0.00	8.5999E+02	.364	4.433	3.044	90.000
-75.0	-67.80	1.409	0.00	-2.720	0.00	9.4958E+02	.437	4.121	3.444	90.000
-70.0	-60.03	.794	0.00	-4.353	0.00	1.1317E+03	.504	3.912	4.252	90.000
-65.0	-51.92	.136	0.00	-7.666	0.00	1.5806E+03	.565	3.767	6.227	90.000
-60.0	-43.38	-1.916	0.00	-22.553	0.00	3.8352E+03	.618	3.666	16.076	90.000
-55.0	-34.25	3.707	0.00	22.214	0.00	3.1999E+03	.664	3.599	14.537	90.000
-50.0	-24.38	1.600	0.00	6.263	0.00	7.7940E+02	.700	3.562	3.943	90.000
-45.0	-13.53	1.102	0.00	2.732	0.00	2.9821E+02	.725	3.557	1.773	90.000
-40.0	-1.32	.807	0.00	.663	0.00	6.4323E+01	.735	3.596	.615	90.000
-35.0	-12.94	.245	0.00	-3.582	0.00	3.1180E+02	.837	3.213	1.718	90.000
-30.0	-31.80	.966	0.00	2.130	0.00	1.6831E+02	.987	2.751	1.554	90.000
-25.0	46.62	.717	-5.65	.584	-71.24	4.2341E+01	.576	4.723	.605	54.859
-20.0	39.55	.669	-6.52	.628	71.32	4.2340E+01	.663	4.079	.536	36.602
-15.0	31.30	.640	-5.76	.674	48.28	4.2724E+01	.744	3.582	.499	25.068
-10.0	21.81	.622	-4.22	.710	30.33	4.3062E+01	.820	3.180	.478	15.859
-5.0	11.23	.612	-2.22	.734	14.68	4.3275E+01	.890	2.844	.466	7.710
0.0	0.00	.609	0.00	.742	0.00	4.3346E+01	.953	2.555	.462	0.000
5.0	-11.23	.612	2.22	.734	-14.68	4.3275E+01	1.009	2.299	.466	-7.710
10.0	-21.81	.622	4.22	.710	-30.33	4.3062E+01	1.057	2.069	.478	-15.859
15.0	-31.30	.640	5.76	.674	-48.28	4.2724E+01	1.097	1.858	.499	-25.068
20.0	-39.55	.669	6.52	.628	-71.32	4.2340E+01	1.129	1.660	.536	-36.602
25.0	-46.62	.717	5.65	.584	71.24	4.2341E+01	1.152	1.471	.605	-54.859
30.0	31.80	.714	0.00	.161	0.00	1.2769E+01	.664	2.262	.412	-90.000
35.0	12.94	.707	0.00	.031	0.00	2.7772E-00	.724	1.794	.295	-90.000
40.0	1.32	.721	0.00	-.008	0.00	8.2032E-01	.725	1.498	.242	-90.000
45.0	13.53	.750	0.00	-.024	0.00	2.7133E-00	.623	1.388	.210	-90.000
50.0	24.38	.795	0.00	-.031	0.00	3.8651E-00	.525	1.212	.189	-90.000
55.0	34.25	.863	0.00	-.032	0.00	4.6231E-00	.429	.940	.173	-90.000
60.0	43.38	.962	0.00	-.030	0.00	5.1453E-00	.334	.500	.161	-90.000
65.0	51.92	1.112	0.00	-.026	0.00	5.5141E-00	.240	-.289	.153	-90.000
70.0	60.03	1.348	0.00	-.022	0.00	5.7760E-00	.147	-2.072	.146	-90.000
75.0	67.80	1.755	0.00	-.017	0.00	5.9589E-00	.056	-9.617	.142	-90.000
80.0	75.32	2.588	0.00	-.011	0.00	6.0797E-00	-.033	22.908	.138	-90.000
85.0	82.70	5.124	0.00	-.005	0.00	6.1486E-00	-.121	8.207	.137	-90.000

MA = 1.75 DELTA = 16.73 SIGMA = 57.50 M = 1.08 THETA CR = 28.59

THETA	PHI-PR	WS/WA	DEL S	WP/WA	DEL P	(DP)RMS	KSUR/K	VSUR/A	AUX/EL	DEL SH
-85.0	-83.37	9.494	0.00	-.935	0.00	7.3278E+02	.555	2.445	2.056	90.000
-80.0	-76.66	4.474	0.00	-1.956	0.00	7.6269E+02	.609	2.321	2.171	90.000
-75.0	-69.79	2.630	0.00	-3.185	0.00	8.2223E+02	.655	2.230	2.400	90.000
-70.0	-62.66	1.490	0.00	-4.875	0.00	9.3461E+02	.691	2.164	2.827	90.000
-65.0	-55.17	.418	0.00	-7.724	0.00	1.1699E+03	.716	2.119	3.713	90.000
-60.0	-47.20	-1.456	0.00	-14.924	0.00	1.8553E+03	.731	2.093	6.271	90.000
-55.0	-38.58	-32.856	0.00	-155.549	0.00	1.6284E+04	.733	2.087	59.705	90.000
-50.0	-29.12	5.017	0.00	15.592	0.00	1.3999E+03	.720	2.108	5.714	90.000
-45.0	-18.51	2.777	0.00	5.852	0.00	4.5680E+02	.690	2.167	2.171	90.000
-40.0	-6.29	1.915	0.00	2.171	0.00	1.4898E+02	.635	2.299	.945	90.000
-35.0	-8.51	1.082	0.00	-1.483	0.00	9.0353E+01	.700	2.021	.197	90.000
-30.0	-29.74	2.166	0.00	3.404	0.00	1.8558E+02	.979	1.388	1.436	90.000
-25.0	40.76	1.467	-8.85	1.023	-83.83	5.0448E+01	.176	7.329	.547	49.261
-20.0	33.93	1.357	-9.52	1.129	63.65	5.0901E+01	.298	4.067	.482	33.534
-15.0	26.35	1.292	-8.35	1.236	43.18	5.1709E+01	.419	2.695	.448	23.131
-10.0	18.05	1.252	-6.15	1.325	27.15	5.2328E+01	.536	1.930	.428	14.682
-5.0	9.18	1.230	-3.25	1.384	13.15	5.2698E+01	.649	1.436	.417	7.149
0.0	0.00	1.223	0.00	1.405	0.00	5.2819E+01	.757	1.087	.414	0.000
5.0	-9.18	1.230	3.25	1.384	-13.15	5.2698E+01	.859	.823	.417	-7.149
10.0	-18.05	1.252	6.15	1.325	-27.15	5.2328E+01	.955	.613	.428	-14.682
15.0	-26.35	1.292	8.35	1.236	-43.18	5.1709E+01	1.044	.441	.448	-23.131
20.0	-33.93	1.357	9.52	1.129	-63.65	5.0901E+01	1.124	.294	.482	-33.534
25.0	-40.76	1.467	8.85	1.023	83.83	5.0448E+01	1.196	.167	.547	-49.261
30.0	29.74	1.483	0.00	.327	0.00	1.7864E+01	.332	.200	.425	-90.000
35.0	8.51	1.419	0.00	.032	0.00	1.9686E-00	.540	-.123	.287	-90.000
40.0	6.29	1.423	0.00	-.043	0.00	2.9696E-00	.524	-.380	.233	-90.000
45.0	18.51	1.462	0.00	-.070	0.00	5.4759E-00	.380	-.870	.201	-90.000
50.0	29.12	1.538	0.00	-.077	0.00	6.9752E-00	.253	-1.821	.180	-90.000
55.0	38.58	1.658	0.00	-.075	0.00	7.9522E-00	.135	-4.324	.165	-90.000
60.0	47.20	1.841	0.00	-.069	0.00	8.6212E-00	.026	-27.102	.153	-90.000
65.0	55.17	2.119	0.00	-.060	0.00	9.0916E-00	-.076	10.749	.145	-90.000
70.0	62.66	2.562	0.00	-.049	0.00	9.4248E-00	-.172	5.393	.139	-90.000
75.0	69.79	3.329	0.00	-.037	0.00	9.6569E-00	-.263	3.935	.134	-90.000
80.0	76.66	4.903	0.00	-.025	0.00	9.8101E-00	-.346	3.257	.131	-90.000
85.0	83.37	9.699	0.00	-.012	0.00	9.8973E-00	-.423	2.869	.129	-90.000

MA = 2.00 DELTA = 16.73 SIGMA = 47.80 M = 1.37 THETA CR = 28.60

THETA	PHI-PR	WS/WA	DEL S	WP/WA	DEL P	(DP)RMS	KSUR/K	VSUR/A	ADX/EL	DEL SH
-85.0	-83.39	8.339	0.00	-.809	0.00	7.3098E+02	.463	3.007	2.034	90.000
-80.0	-76.71	3.929	0.00	-1.691	0.00	7.6056E+02	.528	2.801	2.147	90.000
-75.0	-69.86	2.309	0.00	-2.752	0.00	8.1932E+02	.585	2.654	2.371	90.000
-70.0	-62.75	1.309	0.00	-4.206	0.00	9.2996E+02	.635	2.546	2.789	90.000
-65.0	-55.29	.371	0.00	-6.645	0.00	1.1605E+03	.676	2.467	3.653	90.000
-60.0	-47.34	-1.245	0.00	-12.725	0.00	1.8238E+03	.708	2.413	6.113	90.000
-55.0	-38.74	-23.634	0.00	-111.049	0.00	1.3399E+04	.728	2.380	48.718	90.000
-50.0	-29.30	4.517	0.00	13.932	0.00	1.4413E+03	.736	2.371	5.834	90.000
-45.0	-18.70	2.469	0.00	5.172	0.00	4.6515E+02	.729	2.395	2.192	90.000
-40.0	-6.49	1.697	0.00	1.931	0.00	1.5259E+02	.701	2.470	.957	90.000
-35.0	-8.32	.968	0.00	-1.216	0.00	8.5279E+01	.763	2.233	.167	90.000
-30.0	-29.62	1.918	0.00	2.989	0.00	1.8752E+02	.995	1.671	1.439	90.000
-25.0	40.57	1.292	-8.97	.896	-84.16	5.0788E+01	.375	4.290	.546	49.128
-20.0	33.76	1.194	-9.64	.989	63.43	5.1264E+01	.480	3.217	.480	33.458
-15.0	26.20	1.138	-8.45	1.084	43.03	5.2093E+01	.582	2.525	.446	23.082
-10.0	17.94	1.102	-6.23	1.163	27.05	5.2726E+01	.678	2.035	.426	14.652
-5.0	9.12	1.083	-3.30	1.216	13.10	5.3102E+01	.770	1.664	.416	7.134
0.0	0.00	1.076	0.00	1.234	0.00	5.3226E+01	.856	1.371	.413	0.000
5.0	-9.12	1.083	3.30	1.216	-13.10	5.3102E+01	.935	1.129	.416	-7.134
10.0	-17.94	1.102	6.23	1.163	-27.05	5.2726E+01	1.008	.924	.426	-14.652
15.0	-26.20	1.138	8.45	1.084	-43.03	5.2093E+01	1.072	.745	.446	-23.082
20.0	-33.76	1.194	9.64	.989	-63.43	5.1264E+01	1.129	.585	.480	-33.458
25.0	-40.57	1.292	8.97	.896	84.16	5.0788E+01	1.176	.439	.546	-49.128
30.0	29.62	1.307	0.00	.287	0.00	1.8013E+01	.487	.757	.426	-90.000
35.0	8.32	1.249	0.00	.027	0.00	1.9059E-00	.639	.342	.287	-90.000
40.0	6.49	1.251	0.00	-.038	0.00	3.0798E-00	.611	.109	.233	-90.000
45.0	18.70	1.286	0.00	-.062	0.00	5.6081E-00	.482	-.177	.201	-90.000
50.0	29.30	1.352	0.00	-.068	0.00	7.1199E-00	.364	-.651	.179	-90.000
55.0	38.74	1.457	0.00	-.067	0.00	8.1049E-00	.253	-1.526	.164	-90.000
60.0	47.34	1.617	0.00	-.061	0.00	8.7792E-00	.148	-3.606	.153	-90.000
65.0	55.29	1.862	0.00	-.052	0.00	9.2534E-00	.047	-14.386	.145	-90.000
70.0	62.75	2.250	0.00	-.043	0.00	9.5891E-00	-.049	16.355	.138	-90.000
75.0	69.86	2.924	0.00	-.033	0.00	9.8231E-00	-.142	6.644	.134	-90.000
80.0	76.71	4.306	0.00	-.022	0.00	9.9774E-00	-.230	4.646	.131	-90.000
85.0	83.39	8.519	0.00	-.011	0.00	1.0065E+01	-.313	3.786	.129	-90.000

MA = 2.50 DELTA = 16.74 SIGMA = 38.90 M = 1.79 THETA CR = 28.70

THETA	PHI-PR	WS/WA	DEL S	WP/WA	DEL P	(DP)RMS	KSUR/K	VSUR/A	ADX/EL	DEL SH
-85.0	-83.73	7.065	0.00	-.551	0.00	7.1355E+02	.380	3.897	1.747	90.000
-80.0	-77.39	3.323	0.00	-1.146	0.00	7.3861E+02	.453	3.550	1.835	90.000
-75.0	-70.89	1.950	0.00	-1.848	0.00	7.8759E+02	.521	3.312	2.006	90.000
-70.0	-64.12	1.112	0.00	-2.774	0.00	8.7702E+02	.582	3.141	2.315	90.000
-65.0	-56.99	.364	0.00	-4.221	0.00	1.0522E+03	.636	3.014	2.915	90.000
-60.0	-49.37	-.730	0.00	-7.278	0.00	1.4857E+03	.682	2.920	4.384	90.000
-55.0	-41.08	-5.343	0.00	-22.644	0.00	3.8807E+03	.719	2.853	12.420	90.000
-50.0	-31.91	6.096	0.00	16.877	0.00	2.4714E+03	.746	2.811	8.798	90.000
-45.0	-21.54	2.552	0.00	4.908	0.00	6.2214E+02	.760	2.796	2.567	90.000
-40.0	-9.45	1.654	0.00	1.924	0.00	2.1322E+02	.757	2.821	1.130	90.000
-35.0	-5.42	1.022	0.00	-.211	0.00	2.0659E+01	.787	2.706	.181	90.000
-30.0	-27.38	1.889	0.00	2.734	0.00	2.3728E+02	.971	2.174	1.581	90.000
-25.0	38.11	1.138	-10.65	.722	-88.20	5.6182E+01	.571	3.633	.524	47.614
-20.0	31.48	1.047	-11.33	.810	60.59	5.7065E+01	.653	3.096	.459	32.570
-15.0	24.26	.994	-9.99	.900	41.07	5.8248E+01	.730	2.676	.426	22.510
-10.0	16.52	.962	-7.40	.977	25.80	5.9108E+01	.801	2.334	.407	14.300
-5.0	8.37	.944	-3.93	1.028	12.49	5.9609E+01	.867	2.045	.397	6.965
0.0	0.00	.939	0.00	1.046	0.00	5.9772E+01	.926	1.796	.393	0.000
5.0	-8.37	.944	3.93	1.028	-12.49	5.9609E+01	.977	1.575	.397	-6.965
10.0	-16.52	.962	7.40	.977	-25.80	5.9108E+01	1.022	1.374	.407	-14.300
15.0	-24.26	.994	9.99	.900	-41.07	5.8248E+01	1.058	1.189	.426	-22.510
20.0	-31.48	1.047	11.33	.810	-60.59	5.7065E+01	1.087	1.015	.459	-32.570
25.0	-38.11	1.138	10.65	.722	88.20	5.6182E+01	1.107	.849	.524	-47.614
30.0	27.38	1.157	0.00	.225	0.00	1.9545E+01	.632	1.215	.422	-90.000
35.0	5.42	1.086	0.00	.006	0.00	6.3790E-01	.729	.812	.280	-90.000
40.0	9.45	1.079	0.00	-.045	0.00	5.0137E-00	.661	.622	.226	-90.000
45.0	21.54	1.103	0.00	-.061	0.00	7.8562E-00	.549	.413	.195	-90.000
50.0	31.91	1.155	0.00	-.065	0.00	9.5494E-00	.444	.091	.174	-90.000
55.0	41.08	1.242	0.00	-.062	0.00	1.0650E+01	.342	-.425	.159	-90.000
60.0	49.37	1.376	0.00	-.055	0.00	1.1402E+01	.243	-1.360	.148	-90.000
65.0	56.99	1.582	0.00	-.047	0.00	1.1931E+01	.145	-3.520	.140	-90.000
70.0	64.12	1.910	0.00	-.038	0.00	1.2305E+01	.050	-13.657	.134	-90.000
75.0	70.89	2.480	0.00	-.029	0.00	1.2565E+01	-.042	20.565	.130	-90.000
80.0	77.39	3.652	0.00	-.019	0.00	1.2737E+01	-.132	7.817	.127	-90.000
85.0	83.73	7.223	0.00	-.009	0.00	1.2835E+01	-.218	5.446	.125	-90.000

MA = 3.00 DELTA = 16.75 SIGMA = 34.09 M = 2.16 THETA CR = 28.63

THETA	PHI-PR	WS/WA	DEL S	WP/WA	DEL P	(DP)RMS	KSUR/K	VSUR/A	ADX/EL	DEL SH
-85.0	-84.10	6.303	0.00	-.390	0.00	7.1117E+02	.334	4.699	1.497	90.000
-80.0	-78.13	2.961	0.00	-.809	0.00	7.3253E+02	.412	4.214	1.564	90.000
-75.0	-71.99	1.737	0.00	-1.293	0.00	7.7362E+02	.484	3.893	1.694	90.000
-70.0	-65.60	.999	0.00	-1.909	0.00	8.4650E+02	.551	3.666	1.921	90.000
-65.0	-58.83	.369	0.00	-2.812	0.00	9.8173E+02	.611	3.500	2.338	90.000
-60.0	-51.58	-.440	0.00	-4.482	0.00	1.2783E+03	.665	3.374	3.242	90.000
-55.0	-43.65	-2.530	0.00	-9.712	0.00	2.3191E+03	.710	3.280	6.376	90.000
-50.0	-34.82	16.606	0.00	41.191	0.00	8.3749E+03	.746	3.213	25.581	90.000
-45.0	-24.75	3.007	0.00	5.271	0.00	9.2363E+02	.772	3.173	3.256	90.000
-40.0	-12.90	1.756	0.00	2.010	0.00	3.0633E+02	.783	3.167	1.353	90.000
-35.0	-1.86	1.114	0.00	.314	0.00	4.1903E+01	.789	3.158	.447	90.000
-30.0	-23.93	2.377	0.00	3.620	0.00	4.2565E+02	.941	2.644	2.294	90.000
-25.0	35.80	1.060	-12.44	.605	88.70	6.3189E+01	.670	3.676	.506	46.744
-20.0	29.38	.968	-13.25	.692	58.13	6.4733E+01	.739	3.274	.440	32.033
-15.0	22.51	.916	-11.78	.783	39.30	6.6464E+01	.802	2.937	.407	22.156
-10.0	15.25	.885	-8.81	.861	24.66	6.7666E+01	.859	2.648	.389	14.078
-5.0	7.70	.868	-4.72	.914	11.93	6.8351E+01	.910	2.394	.379	6.857
0.0	0.00	.862	0.00	.934	0.00	6.8573E+01	.954	2.164	.376	0.000
5.0	-7.70	.868	4.72	.914	-11.93	6.8351E+01	.991	1.954	.379	-6.857
10.0	-15.25	.885	8.81	.861	-24.66	6.7666E+01	1.020	1.756	.389	-14.078
15.0	-22.51	.916	11.78	.783	-39.30	6.6464E+01	1.041	1.569	.407	-22.156
20.0	-29.38	.968	13.25	.692	-58.13	6.4733E+01	1.054	1.387	.440	-32.033
25.0	-35.80	1.060	12.44	.605	-88.70	6.3189E+01	1.059	1.209	.506	-46.744
30.0	23.93	1.073	0.00	.164	0.00	1.9386E+01	.712	1.531	.408	-90.000
35.0	1.86	.991	0.00	-.012	0.00	1.6858E-00	.773	1.150	.270	-90.000
40.0	12.90	.977	0.00	-.052	0.00	8.0016E-00	.678	1.007	.218	-90.000
45.0	24.75	.993	0.00	-.063	0.00	1.1175E+01	.577	.817	.188	-90.000
50.0	34.82	1.037	0.00	-.064	0.00	1.3064E+01	.480	.534	.168	-90.000
55.0	43.65	1.112	0.00	-.059	0.00	1.4292E+01	.384	.102	.153	-90.000
60.0	51.58	1.230	0.00	-.053	0.00	1.5130E+01	.289	-.615	.143	-90.000
65.0	58.83	1.413	0.00	-.045	0.00	1.5720E+01	.195	-2.022	.135	-90.000
70.0	65.60	1.706	0.00	-.036	0.00	1.6137E+01	.101	-5.974	.129	-90.000
75.0	71.99	2.214	0.00	-.027	0.00	1.6427E+01	.009	-84.303	.125	-90.000
80.0	78.13	3.260	0.00	-.018	0.00	1.6618E+01	-.080	12.646	.122	-90.000
85.0	84.10	6.447	0.00	-.009	0.00	1.6727E+01	-.168	7.202	.120	-90.000

LITERATURE CITED

1. Ribner, H. S., "Convection of a Pattern of Vorticity Through a Shock Wave," NACA TN 2864, 1953.
2. Ribner, H. S., "Shock-Turbulence Interaction and the Generation of Noise," NACA Rep. 1233, 1954.
3. Ram, G. S. and Ribner, H. S., "The Sound Generated by Interaction of a Single Vortex with a Shock Wave," Heat Transfer and Fluid Mechanics Institute (Pasadena, California), 1957.
4. Moore, F. K., "Unsteady Oblique Interaction of a Shock Wave with a Plane Disturbance," NACA Rep. 1165, 1954.
5. Johnson, W. R., "The Interaction of Plane and Cylindrical Sound Waves with a Stationary Shock Wave," University of Michigan Tech. Rep. 2539-8-T ONR Contract Nonr - 1224 (18), 1957.
6. Purdy, K. R., "On the Convection of Plane Sound Waves Through a Stationary Oblique Shock," George C. Marshall Space Flight Center (Aero-Astrodynamics Internal Note to be published).
7. Lowson, M. V., "Pressure Fluctuations Resulting from Shock Interactions," Journal of Sound and Vibration, 7 (3), pp. 380-392, 1968.
8. Shapiro, A. H., Compressible Fluid Flow, I, Ronald Press, New York, 1953.

FIGURES

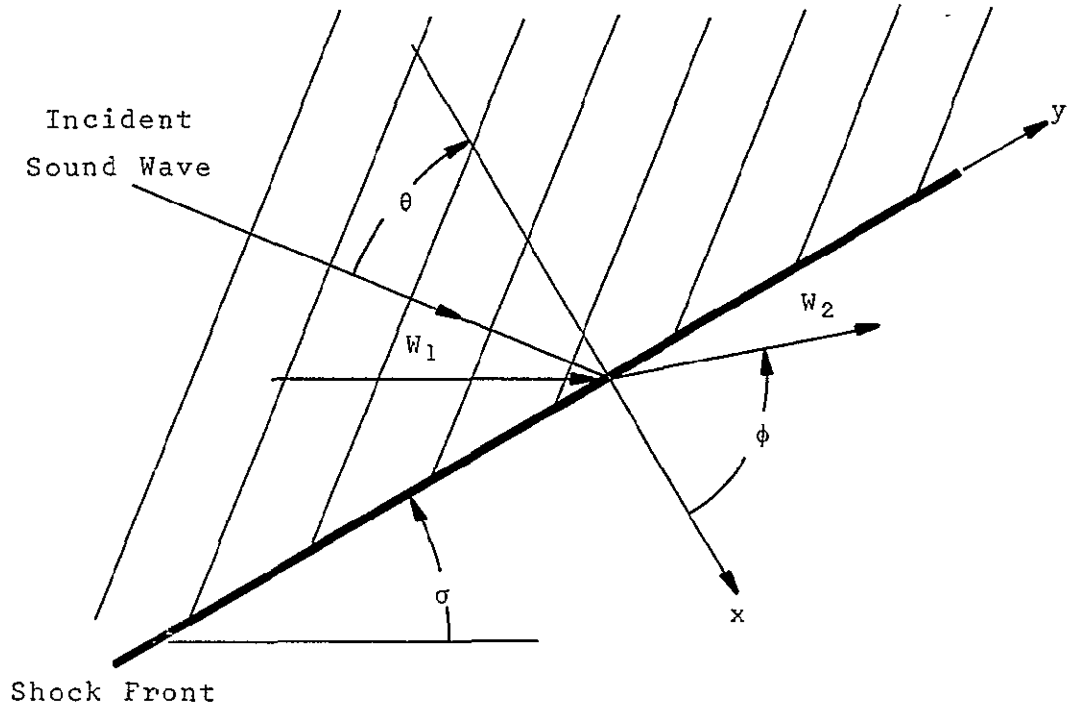

FIGURE 1

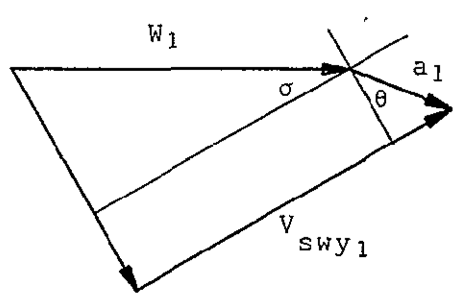

FIGURE 2

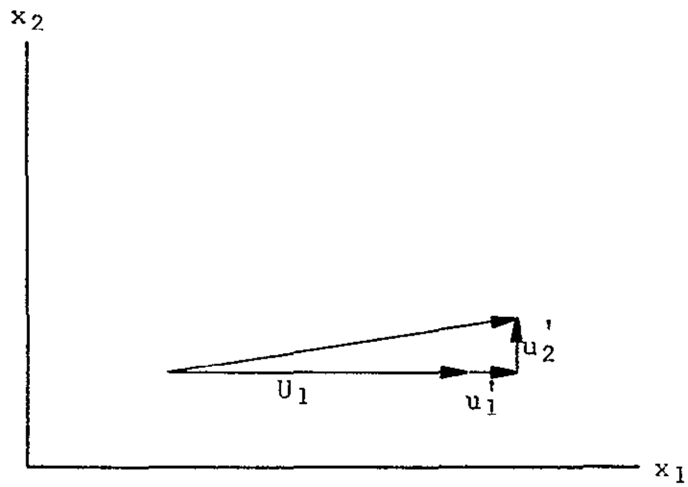

FIGURE 3

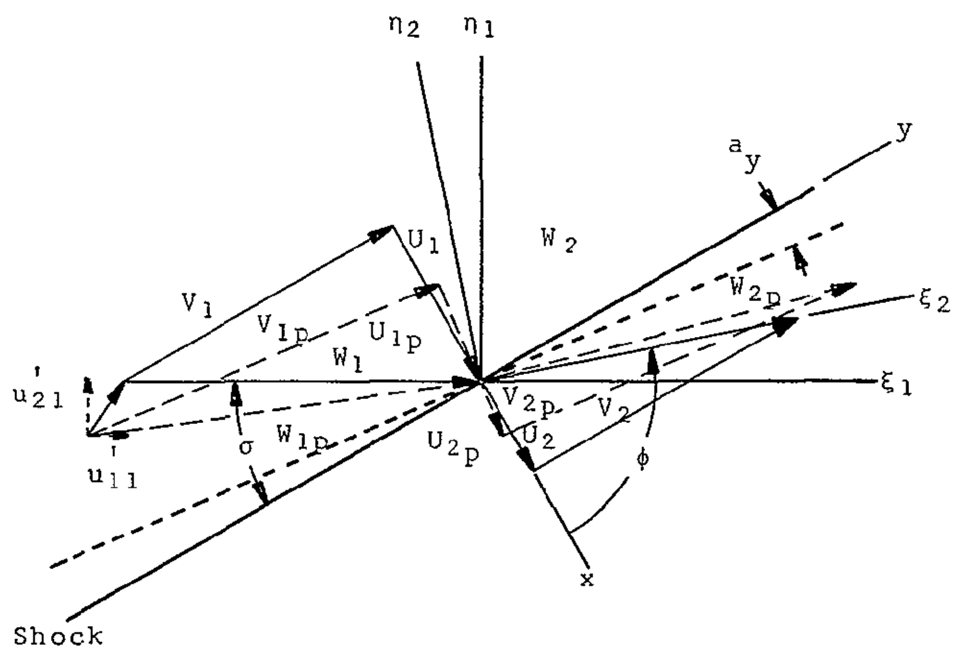

FIGURE 4

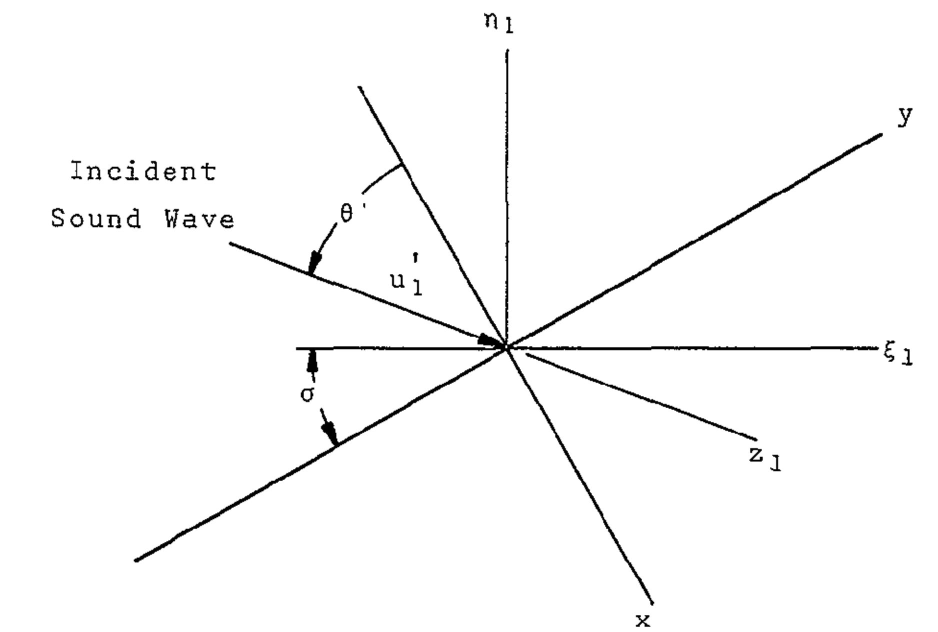

FIGURE 5

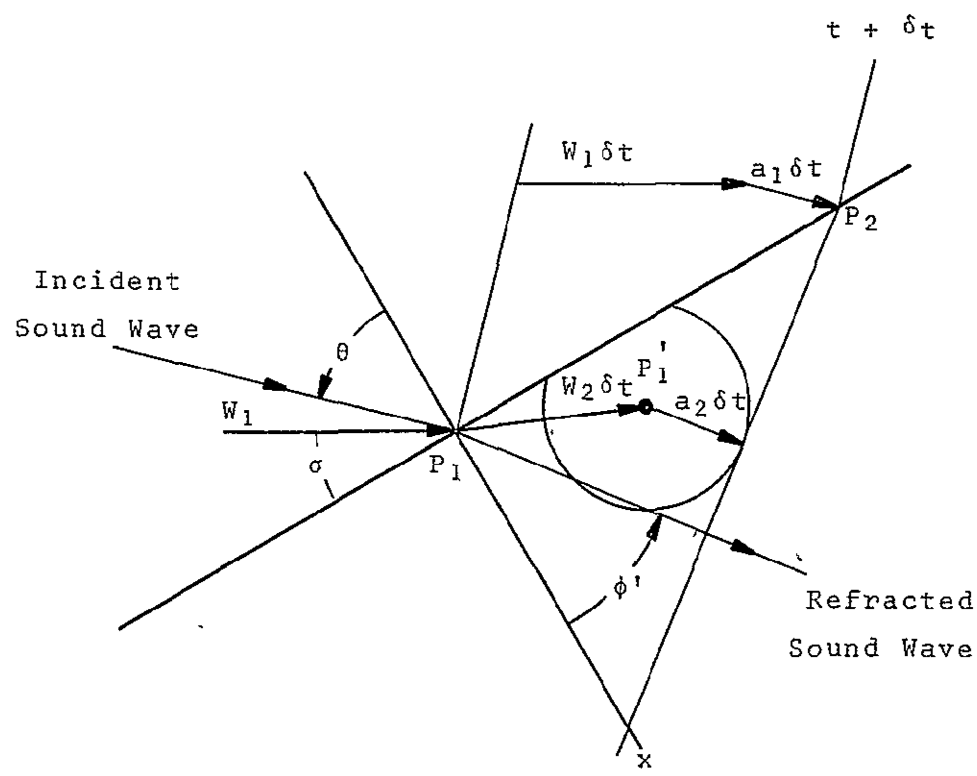

FIGURE 6

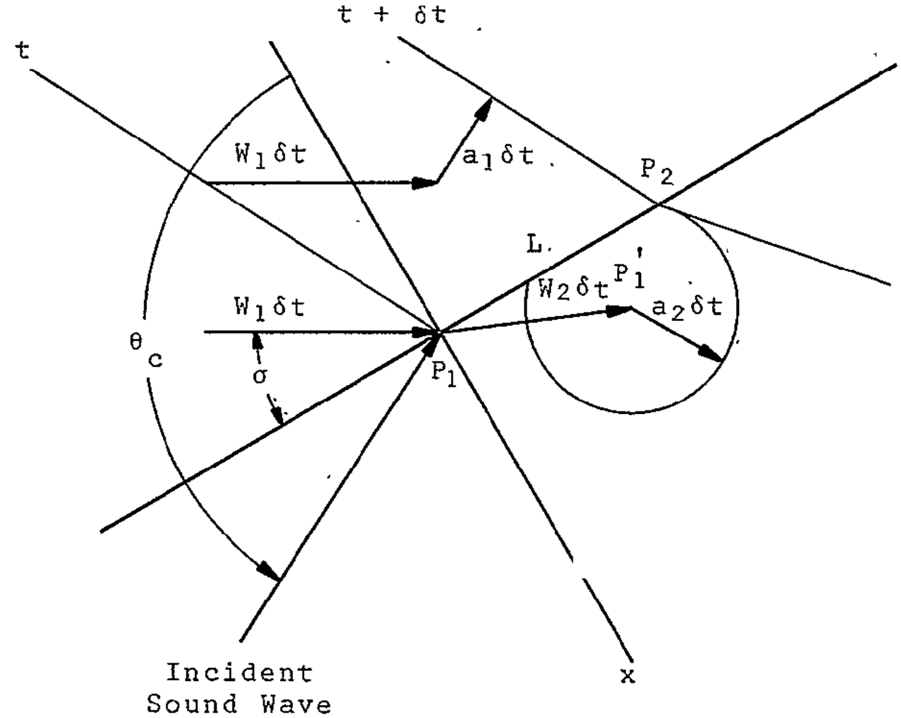

FIGURE 7

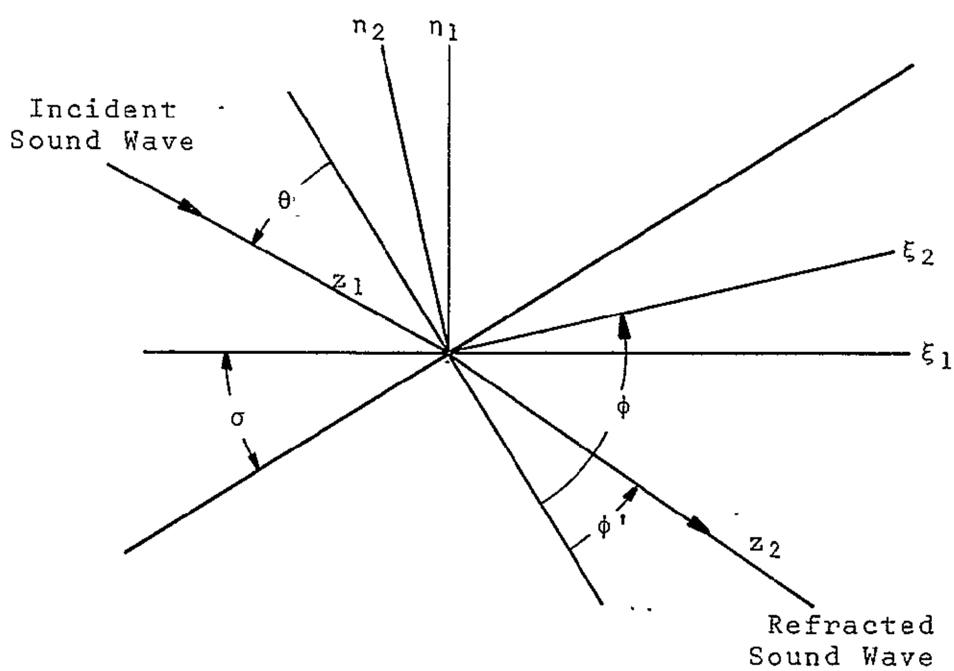

FIGURE 8

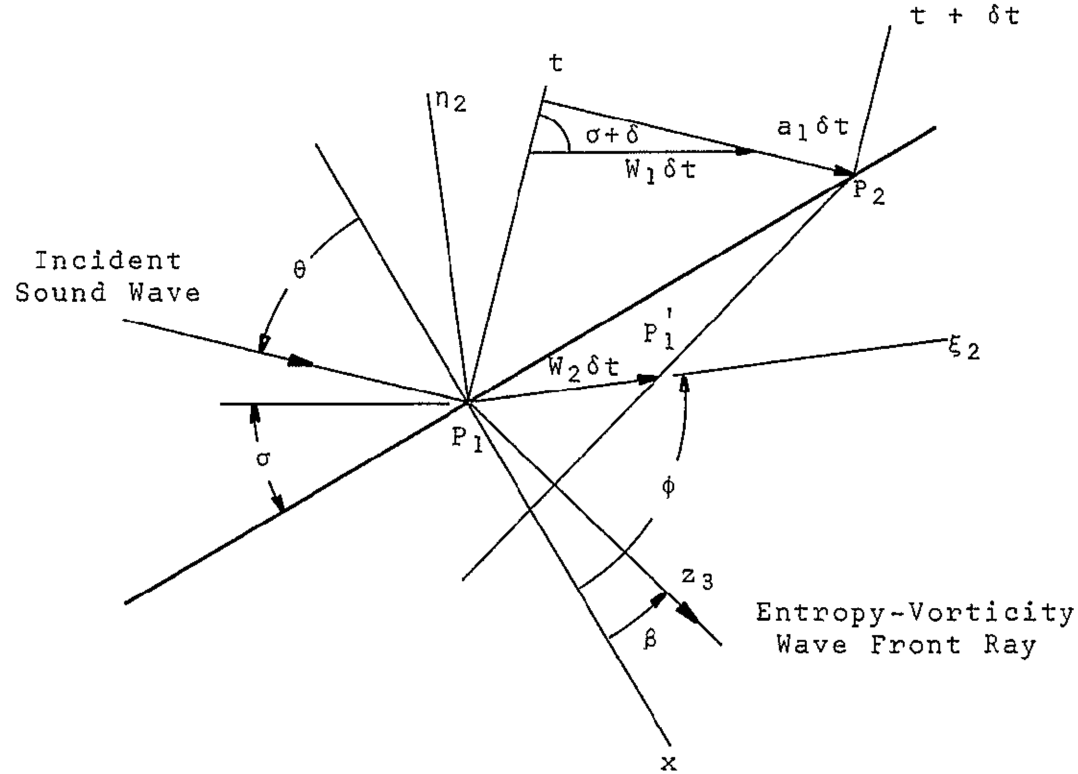
t + δt
t
η_2
σ+δ
$a_1\delta t$
$W_1\delta t$
P_2
θ
Incident
Sound Wave
P_1'
$W_2\delta t$
ξ_2
P_1
σ
φ
z_3
β
Entropy-Vorticity
Wave Front Ray
x

FIGURE 9

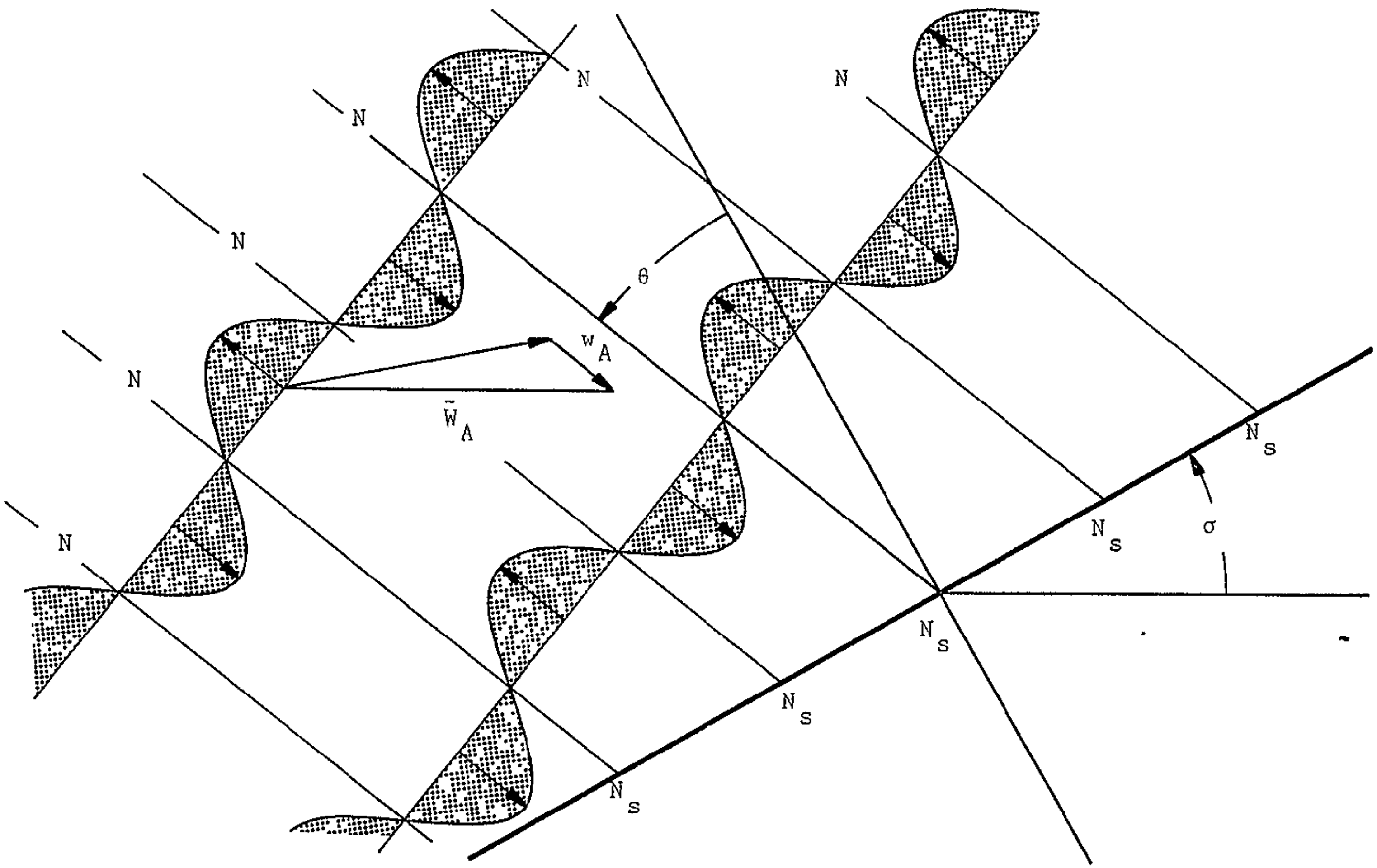

FIGURE 10

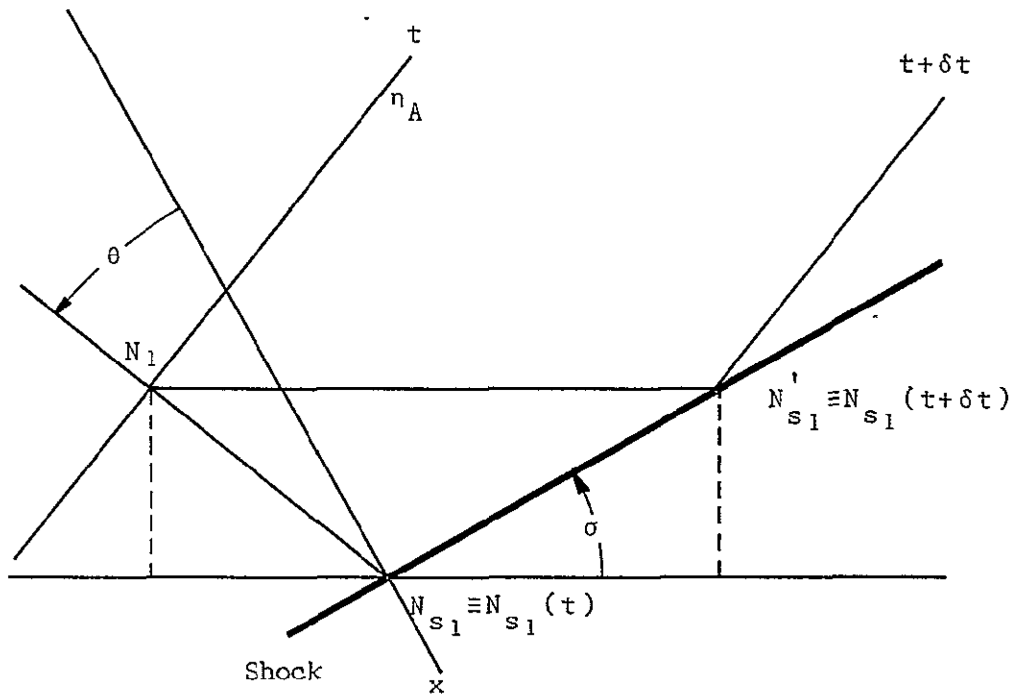

FIGURE 11

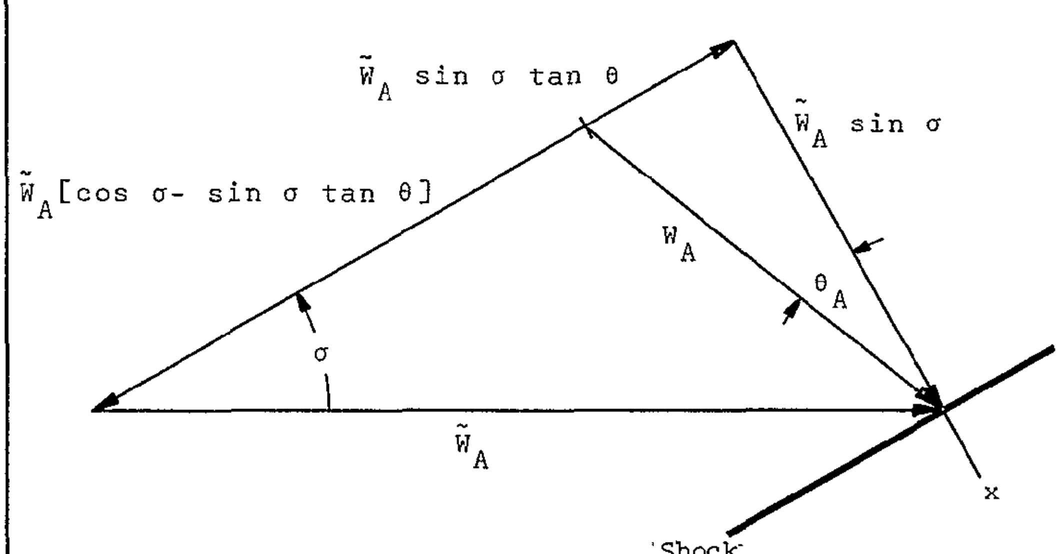

FIGURE 12

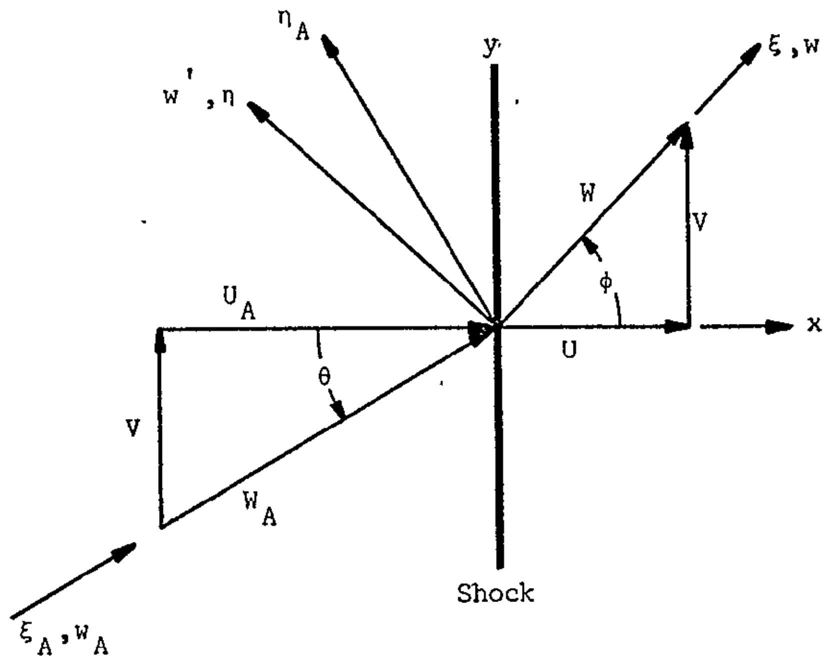

FIGURE 13

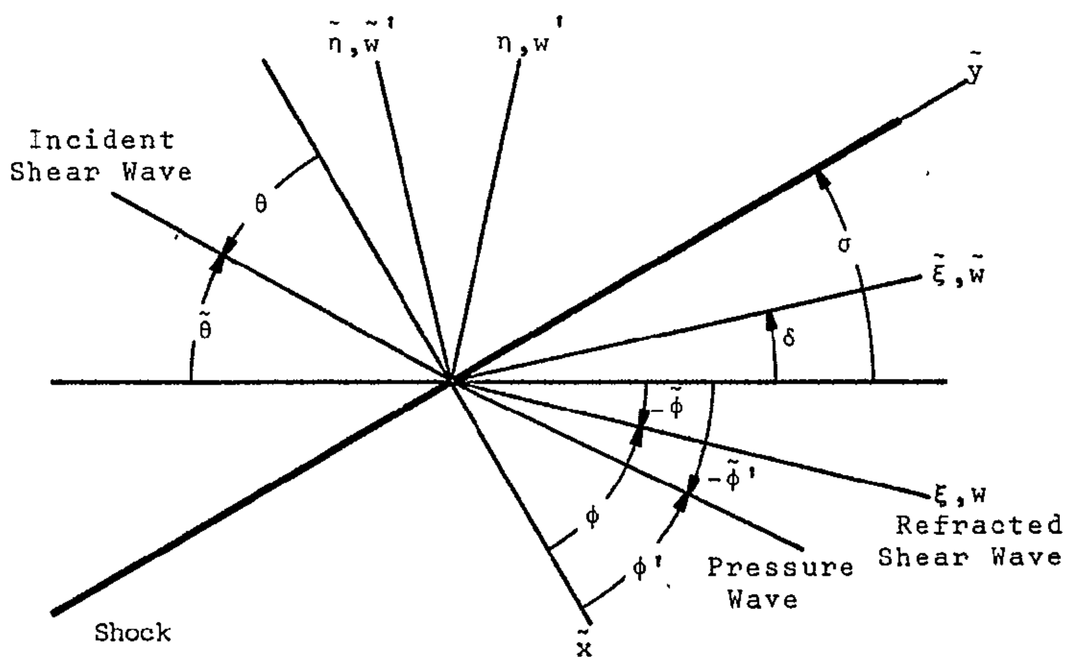

FIGURE 14

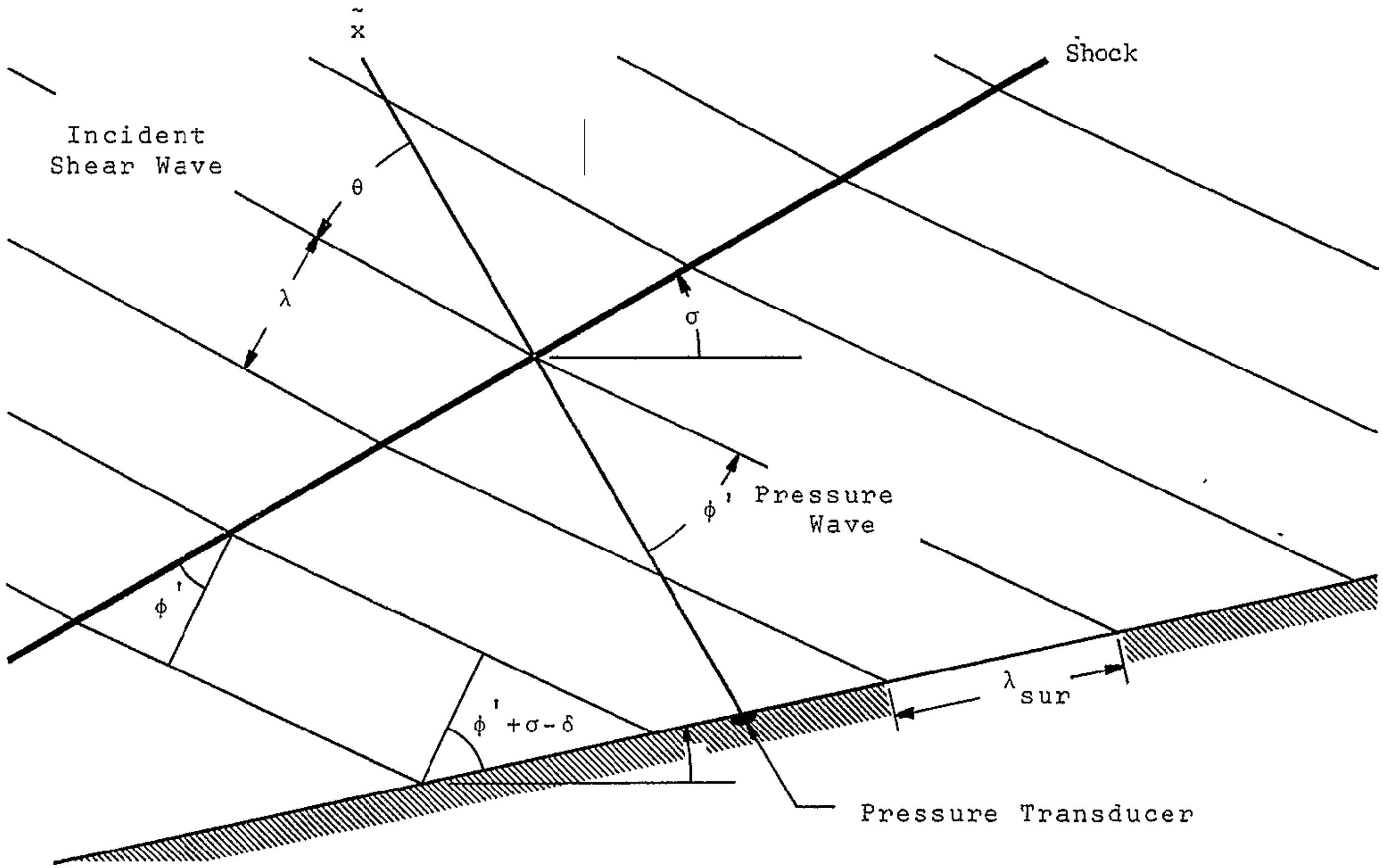
x̃
Shock
Incident
Shear Wave
θ
λ
σ
φ'
Pressure
Wave
φ'
φ' +σ-δ
λ sur
Pressure Transducer

FIGURE 15

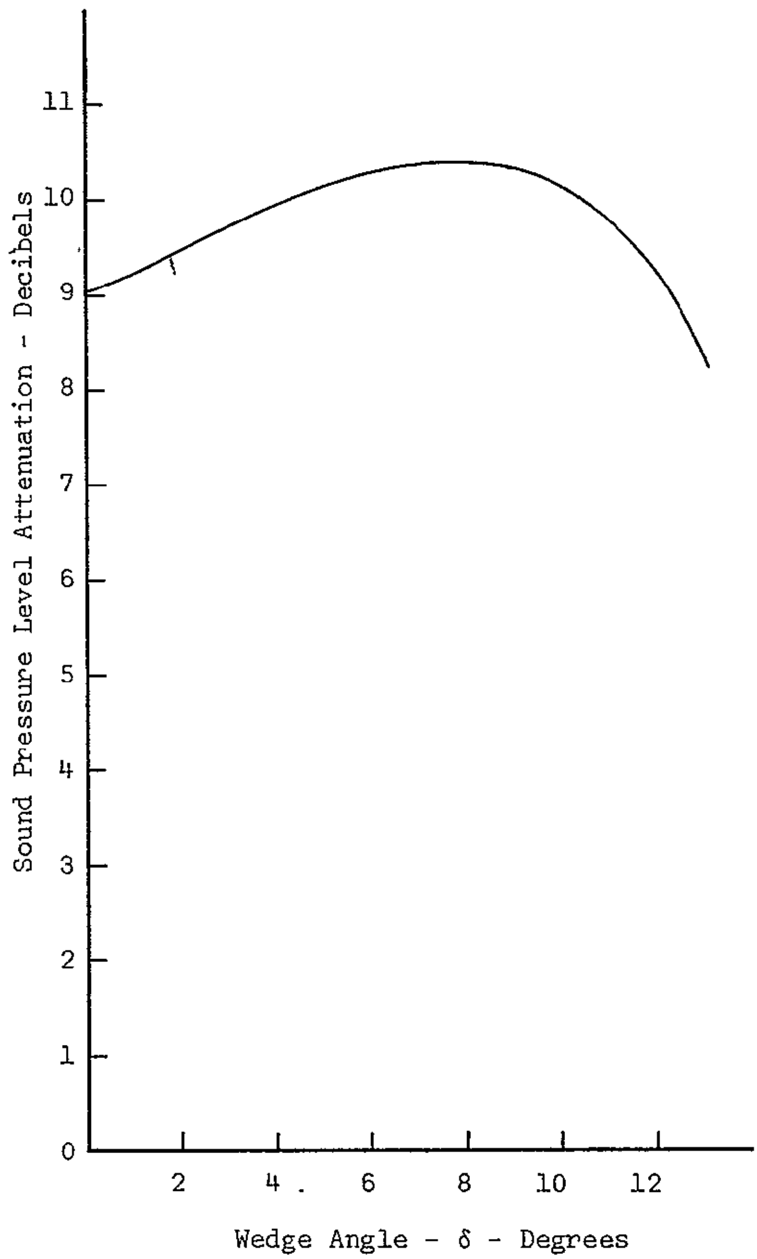
Sound Pressure Level Attenuation - Decibels
11
10
9
8
7
6
5
4
3
2
1
0
2
4
6
8
10
12
Wedge Angle - δ - Degrees

Figure 16

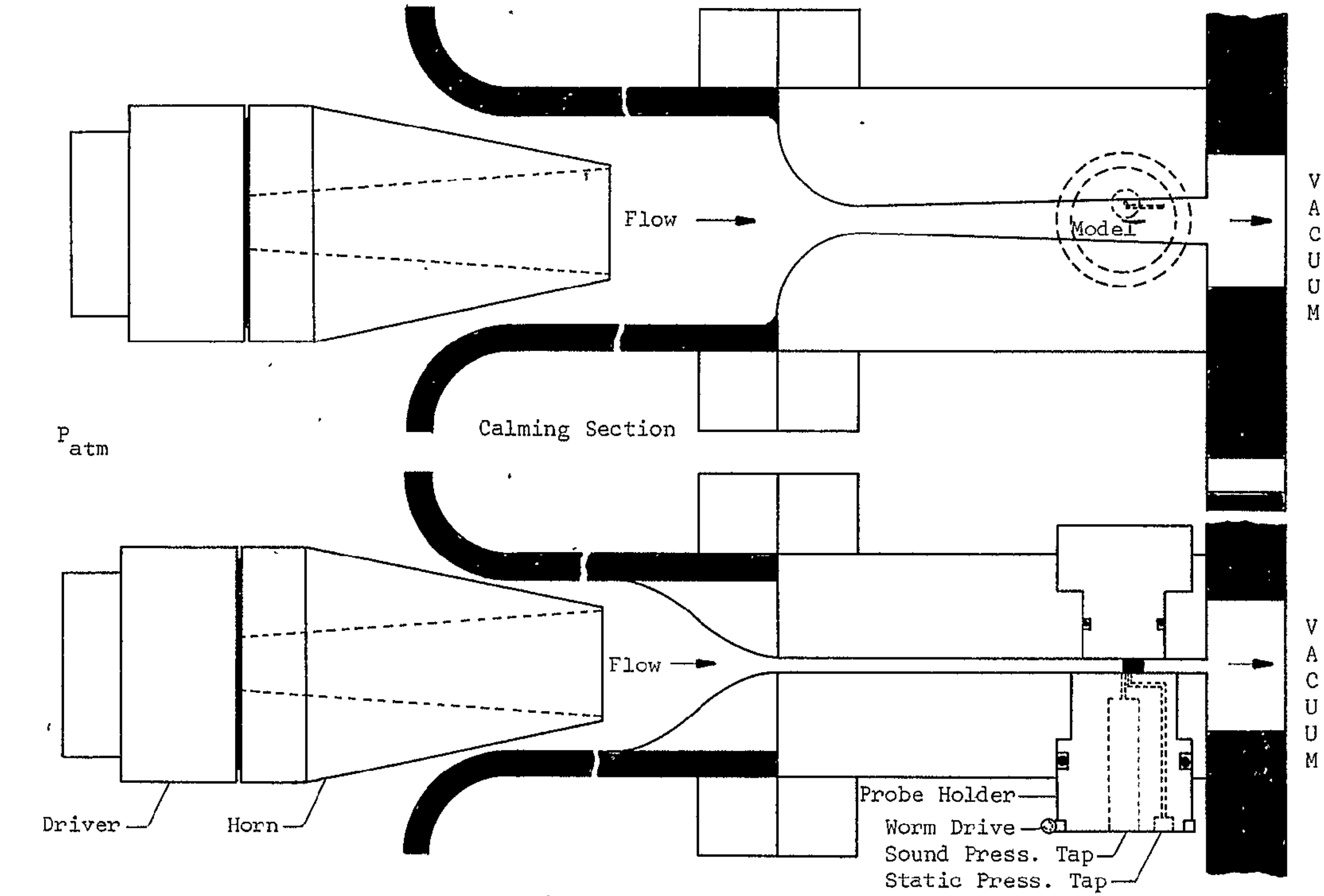
Flow
Model
VACUUM
Patm
Calming Section
Flow
VACUUM
Probe Holder
Worm Drive
Sound Press. Tap
Static Press. Tap
Driver
Horn

Figure 17

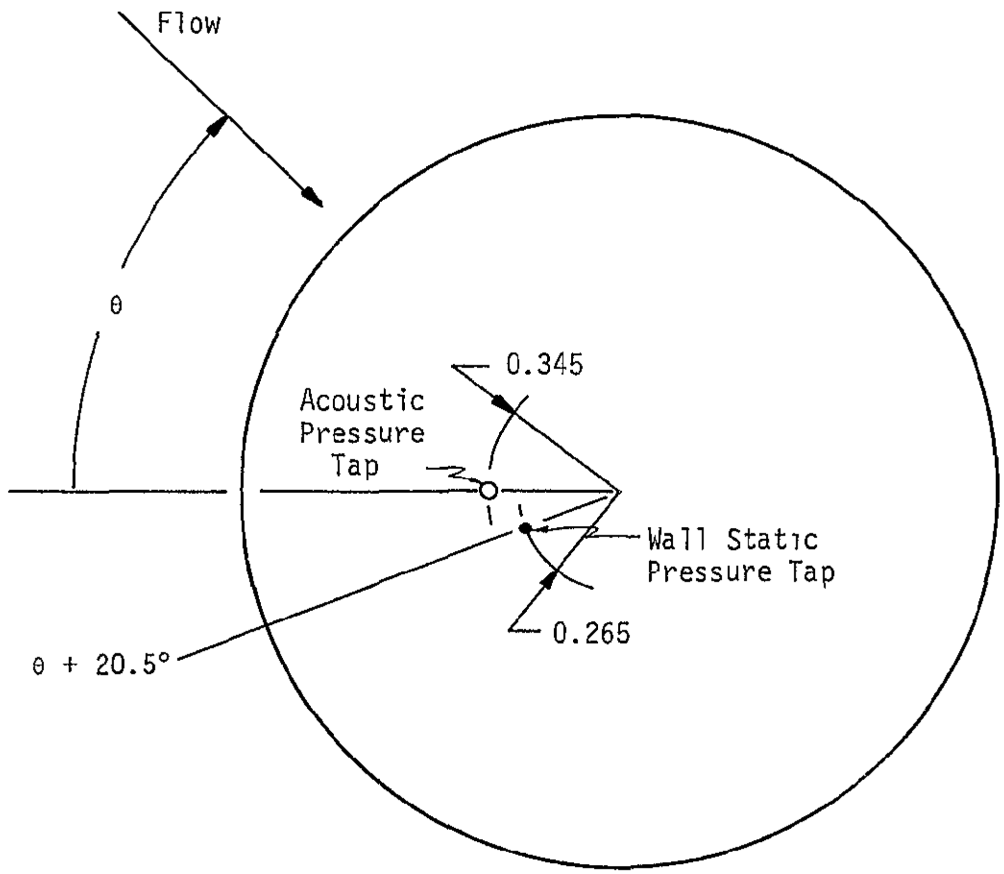
Flow
θ
0.345
Acoustic
Pressure
Tap
Wall Static
Pressure Tap
0.265
θ + 20.5°

FIGURE 18

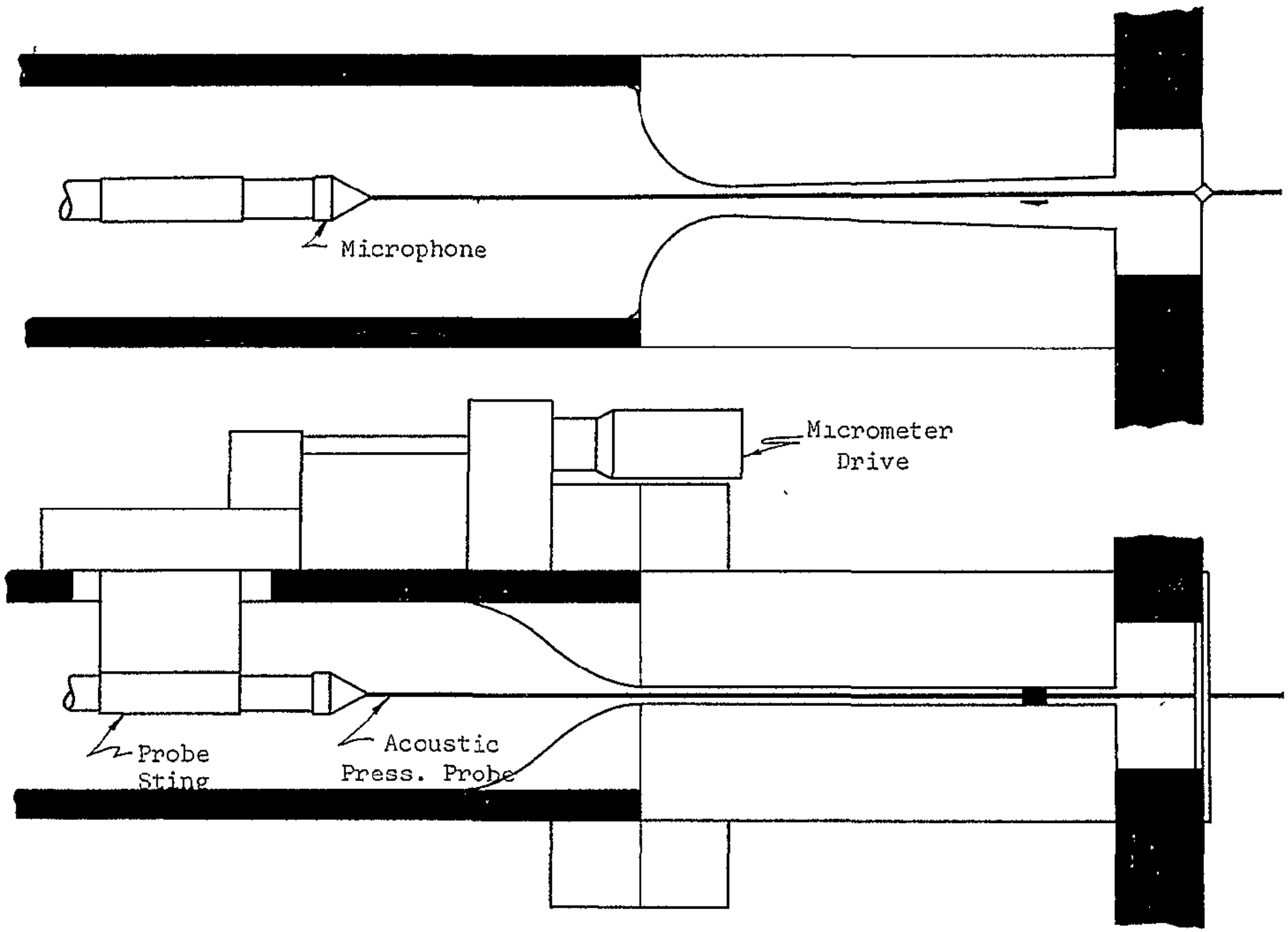

Microphone
Micrometer Drive
Probe Sting
Acoustic Press. Probe

FIGURE 19

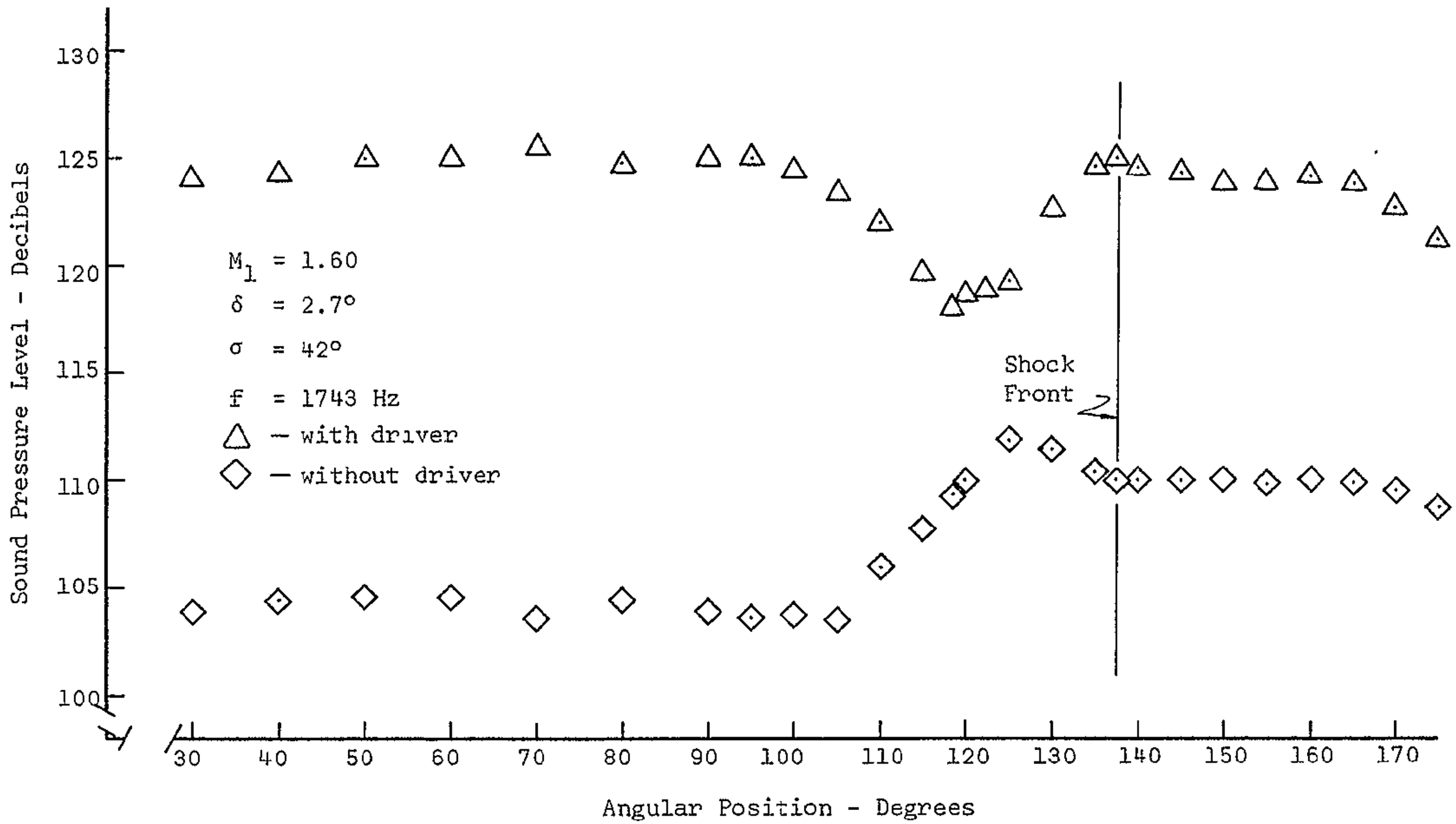
Sound Pressure Level - Decibels
130
125
120
115
110
105
100
30
40
50
60
70
80
90
100
110
120
130
140
150
160
170
Angular Position - Degrees
M_1 = 1.60
δ = 2.7°
σ = 42°
f = 1743 Hz
△ — with driver
◇ — without driver
Shock Front

FIGURE 20

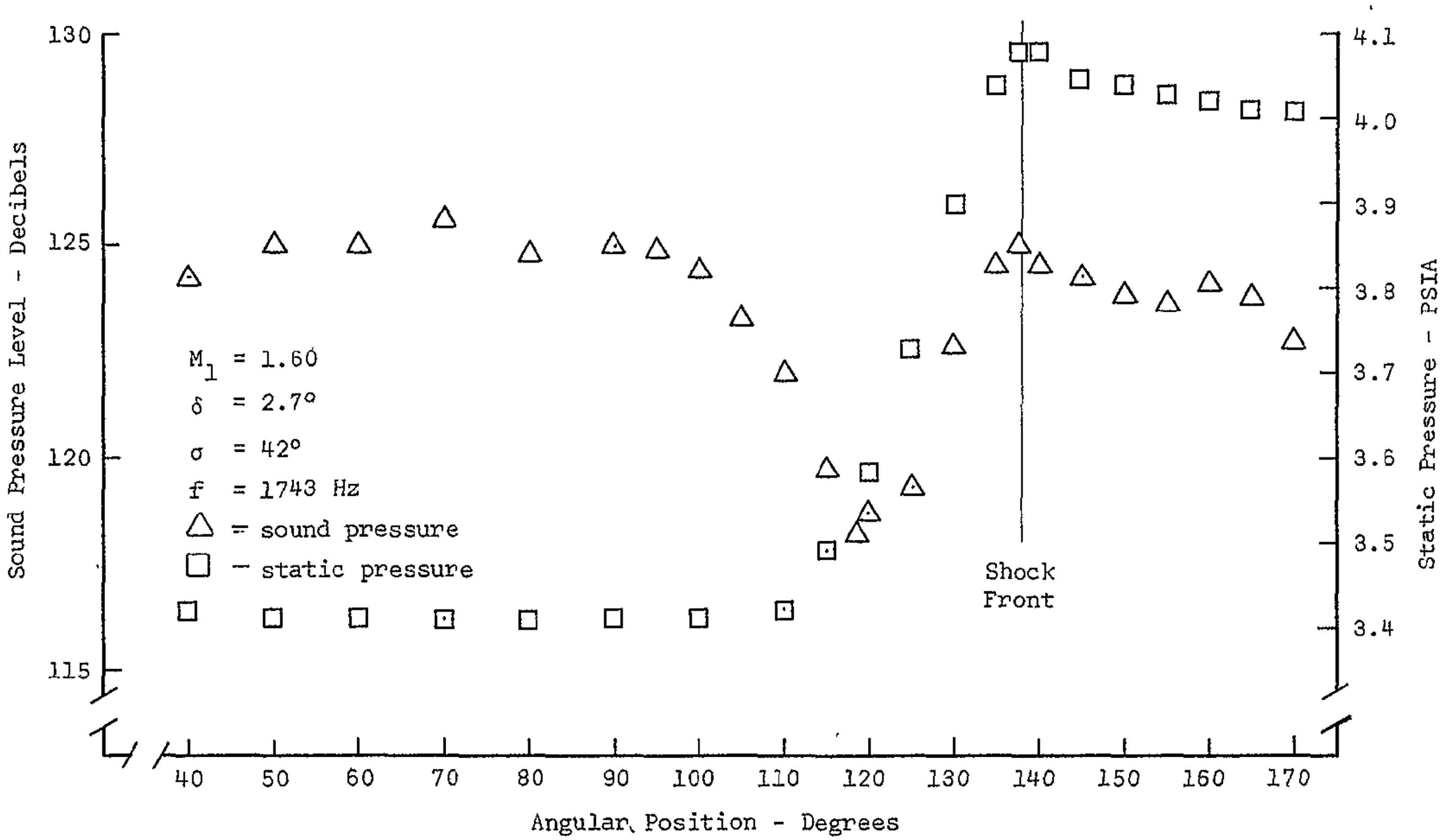

130
125
120
115
Sound Pressure Level - Decibels
4.1
4.0
3.9
3.8
3.7
3.6
3.5
3.4
Static Pressure - PSIA
M_1 = 1.60
δ = 2.7°
σ = 42°
f = 1743 Hz
△ = sound pressure
□ — static pressure
Shock Front
40 50 60 70 80 90 100 110 120 130 140 150 160 170
Angular Position - Degrees

FIGURE 21

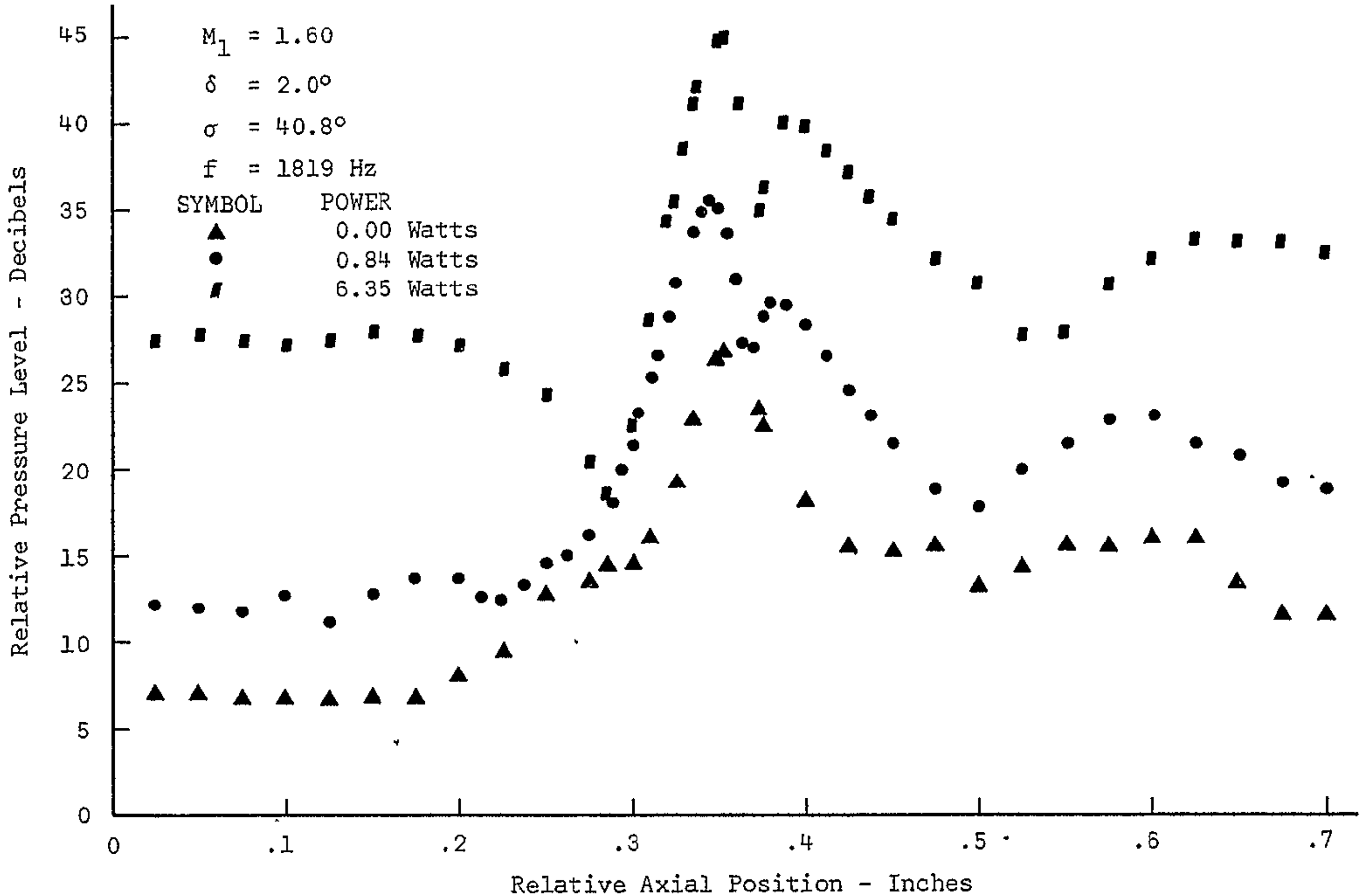

M1 = 1.60
δ = 2.0°
σ = 40.8°
f = 1819 Hz
SYMBOL POWER
0.00 Watts
0.84 Watts
6.35 Watts
Relative Pressure Level - Decibels
0
5
10
15
20
25
30
35
40
45
0
.1
.2
.3
.4
.5
.6
.7
Relative Axial Position - Inches

FIGURE 22

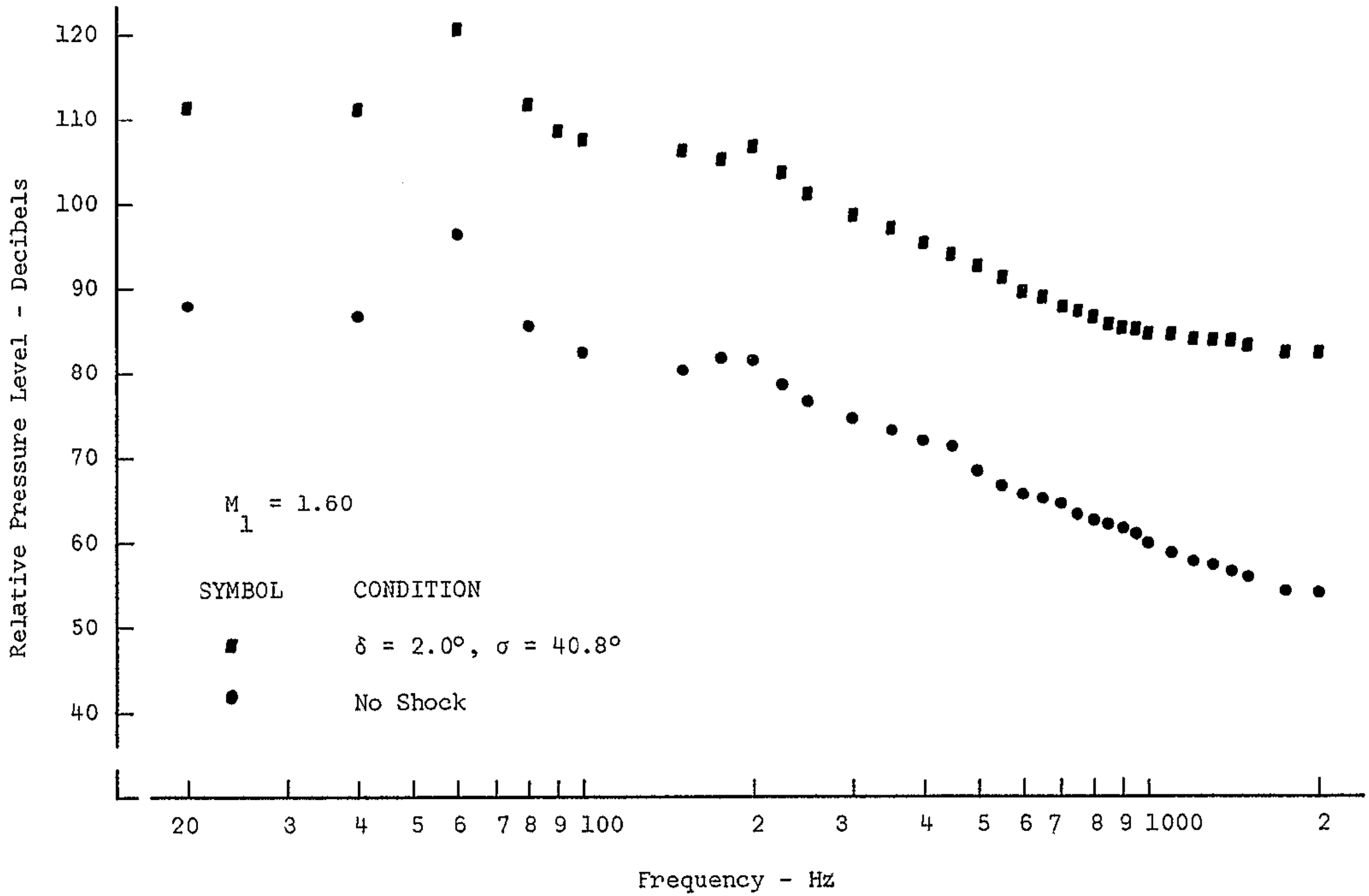
120
110
100
90
80
70
60
50
40
Relative Pressure Level - Decibels
M_1 = 1.60
SYMBOL
CONDITION
δ = 2.0°, σ = 40.8°
No Shock
20
3
4
5
6
7
8
9
100
2
3
4
5
6
7
8
9
1000
2
Frequency - Hz

FIGURE 23

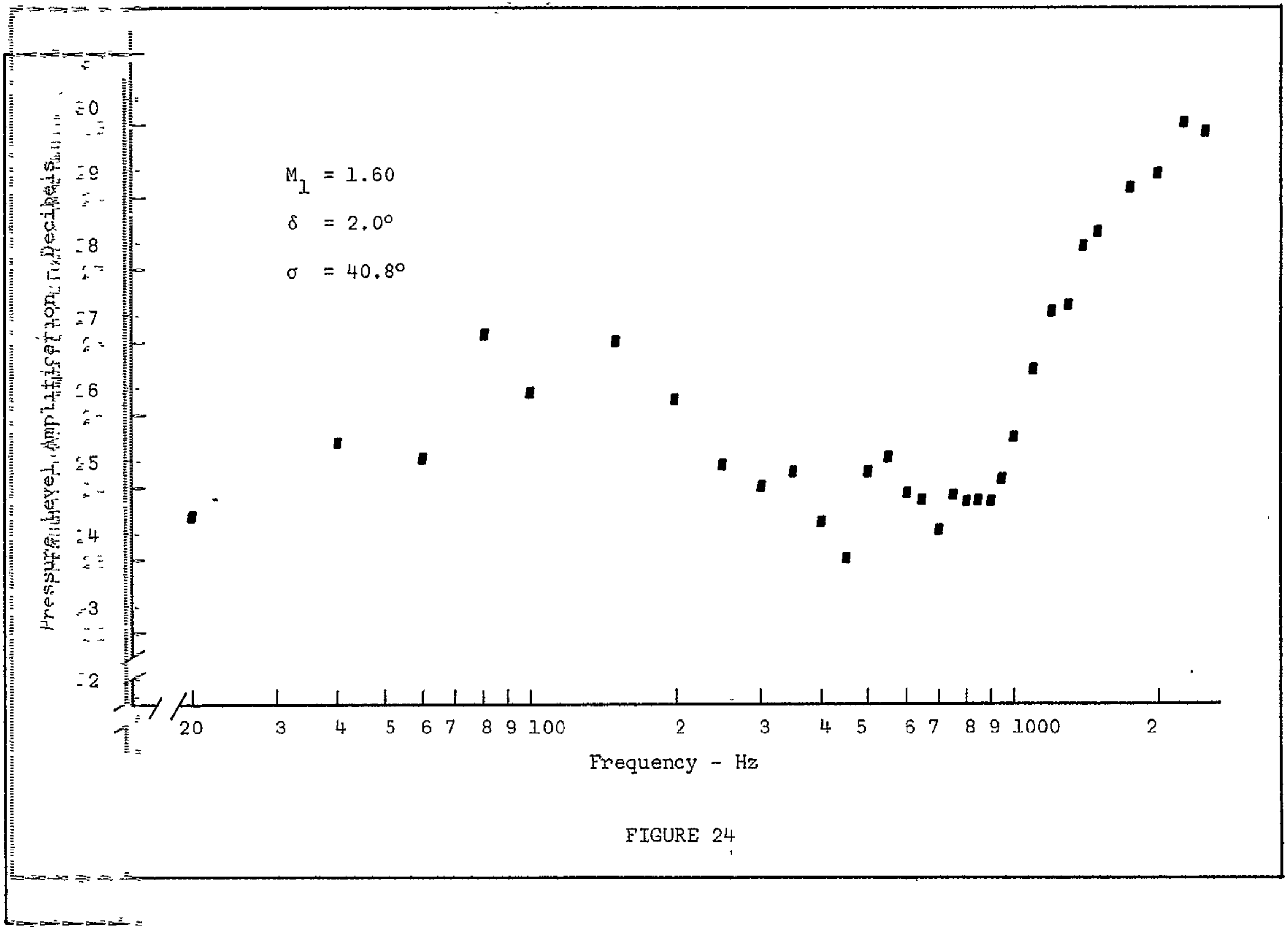

M_1 = 1.60
δ = 2.0°
σ = 40.8°
Pressure Level Amplification, Decibels
20
19
18
17
16
15
14
13
12
20
3
4
5
6
7
8
9
100
2
3
4
5
6
7
8
9
1000
2
Frequency - Hz

FIGURE 24